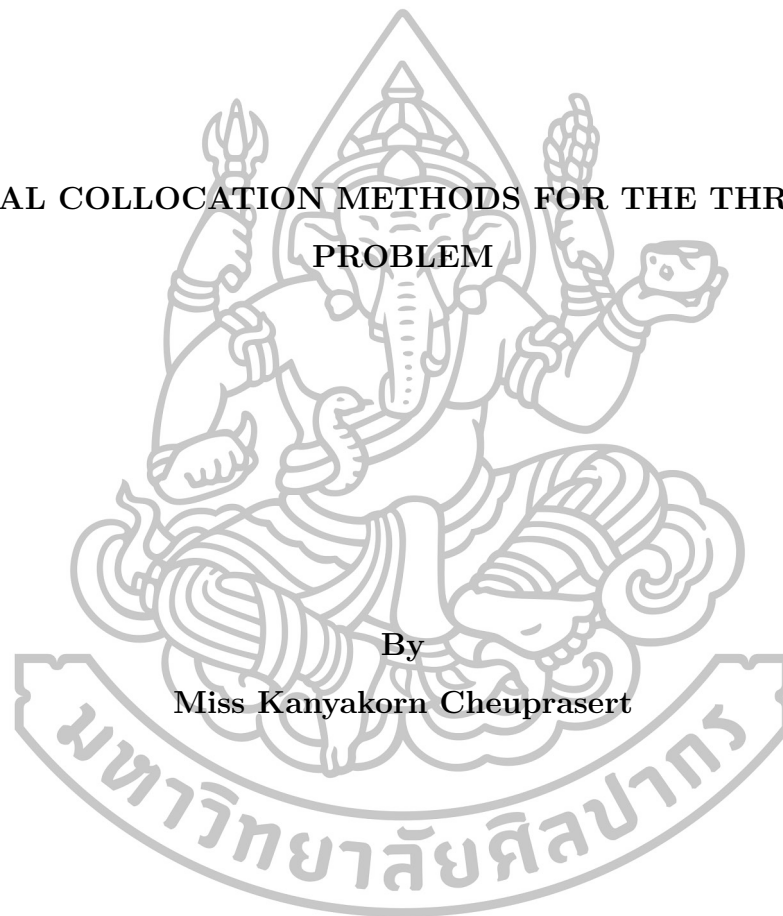




**SPECTRAL COLLOCATION METHODS FOR THE THREE-BODY  
PROBLEM**



By  
Miss Kanyakorn Cheuprasert

A Thesis Submitted in Partial Fulfillment of the Requirements for the  
Degree Master of Science Program in Mathematics  
Department of Mathematics  
Graduate School, Silpakorn University  
Academic Year 2015  
Copyright of Graduate School, Silpakorn University

**SPECTRAL COLLOCATION METHODS FOR THE THREE-BODY  
PROBLEM**



By  
Miss Kanyakorn Cheuprasert

**A Thesis Submitted in Partial Fulfillment of the Requirements for the  
Degree Master of Science Program in Mathematics  
Department of Mathematics  
Graduate School, Silpakorn University  
Academic Year 2015  
Copyright of Graduate School, Silpakorn University**

วิธีการสเปกตรัลคอลโลอิดเซนสำหรับปัญหาสามวัตถุ



โดย  
นางสาวกัลยกร เชื้อประเสริฐ

วิทยานิพนธ์นี้เป็นส่วนหนึ่งของการศึกษาตามหลักสูตรปริญญาวิทยาศาสตรมหาบัณฑิต

สาขาวิชาคณิตศาสตร์ ภาควิชาคณิตศาสตร์

บัณฑิตวิทยาลัย มหาวิทยาลัยศิลปากร ปีการศึกษา 2558

ลิขสิทธิ์ของบัณฑิตวิทยาลัย มหาวิทยาลัยศิลปากร

The Graduate School, Silpakorn University has approved and accredited the Thesis title of "Spectral collocation methods for the three-body problem" submitted by Miss Kanyakorn Cheuprasert as a partial fulfillment of the requirements for the degree of Master of Science in Mathematics

.....  
(Assistant Professor Panjai Tantatsanawong, Ph.D.)

Dean of Graduate School  
...../...../.....

The Thesis Advisor

Dr. Nairat Kanyamee, Ph.D.

The Thesis Examination Committee

..... Chairman

(Dr. Sittisede Polwiang, Ph.D.)

...../...../.....

..... Member

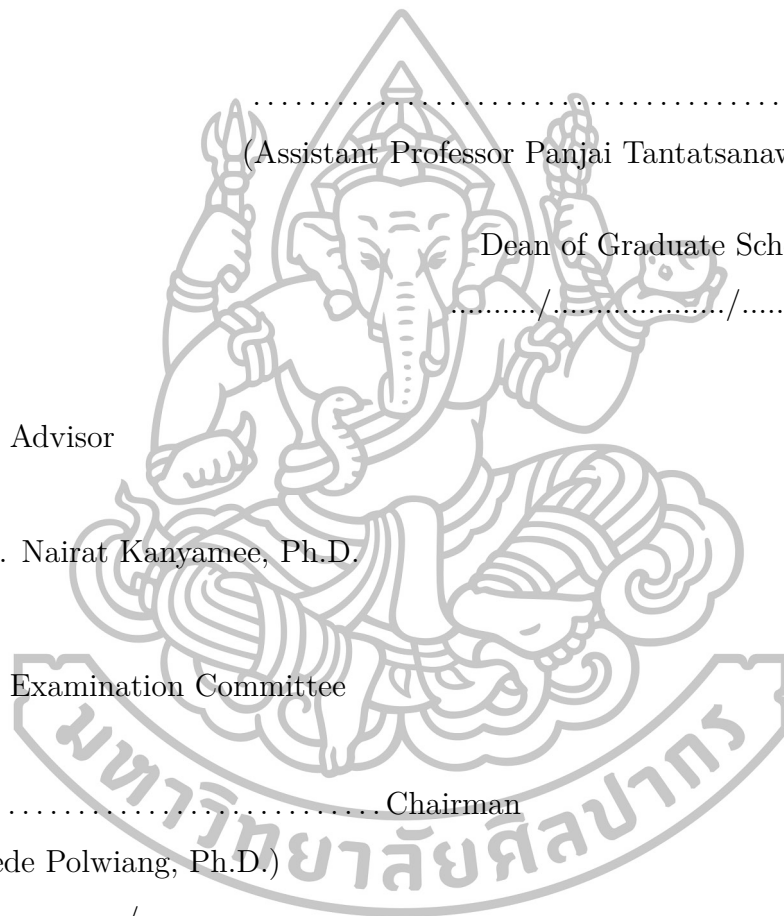
(Dr. Warin Sripunya, Ph.D.)

...../...../.....

..... Member

(Dr. Nairat Kanyamee, Ph.D.)

...../...../.....



56305201 : MAJOR : MATHEMATICS

KEY WORD : THREE-BODY PROBLEM / HAMILTONIAN SYSTEM / SPECTRAL COLLOCATION METHOD / SYMPLECTIC METHOD / RUNGE-KUTTA METHOD

KANYAKORN CHEUPRASERT : SPECTRAL COLLOCATION METHODS FOR THE THREE-BODY PROBLEM. THESIS ADVISOR : DR. NAIRAT KANYAMEE, Ph. D. 71 pp.

In this thesis, we propose a method to find the numerical solutions of the three-body problem with an appropriate set of initial conditions by using the spectral collocation methods. We compare and discuss the errors in energy and the CPU times of the numerical results obtained from the spectral collocation methods, the symplectic methods and the Runge-Kutta methods in order to show the accomplishment of the spectral collocation methods.

The numerical results show that the proposed method gives a spectral accuracy for linear and some nonlinear differential equations and gives an impressive accuracy in energy for the three-body problem.

---

Department of Mathematics

Graduate school, Silpakorn University

Student's signature.....

Academic Year 2015

Thesis Advisor's signature.....

56305201 : สาขาคณิตศาสตร์

คำสำคัญ : ปัญหาสามวัตถุ / ระบบฮามิลโทเนียน / วิธีสเปกตรัล / วิธีซิมเพลติก / วิธีรุงเงอ-คุททา

กัลยกร เชื่อประเสริฐ : วิธีการสเปกตรัลคอลลีเคชันสำหรับปัญหาสามวัตถุ. อาจารย์ที่ปรึกษา

วิทยานิพนธ์ : ดร. นัยน์รัตน์ กันยะมี. 71 หน้า.

วิทยานิพนธ์นี้นำเสนอ การหาผลเฉลยเชิงตัวเลขและเซตของเงื่อนไขค่าเริ่มต้นที่เหมาะสมของปัญหาสามวัตถุ โดยใช้วิธีสเปกตรัลคอลลีเคชัน และทำการเปรียบเทียบค่าคลาดเคลื่อนของพลังงาน และเวลาที่ใช้ในการคำนวณที่ได้จากสเปกตรัลคอลลีเคชันเทียบกับวิธีซิมเพลติกและวิธีรุงเงอ-คุททา เพื่อแสดงผลสำเร็จของวิธีสเปกตรัลคอลลีเคชัน

ผลการทดลองเชิงตัวเลขได้แสดงให้เห็นว่าวิธีที่นำเสนอมีความแม่นยำสูงสำหรับสมการเชิงอนุพันธ์เชิงเส้นและสมการเชิงอนุพันธ์ที่ไม่เชิงเส้นบางสมการ และมีความแม่นยำของพลังงานที่น่าพอใจสำหรับปัญหาสามวัตถุ



---

ภาควิชาคณิตศาสตร์

บัณฑิตวิทยาลัย มหาวิทยาลัยศิลปากร

ลายมือชื่อนักศึกษา.....

ปีการศึกษา 2558

ลายมือชื่ออาจารย์ที่ปรึกษาวิทยานิพนธ์.....

## Acknowledgements

This thesis, I would like to express my sincere thanks to my advisor, Dr. Nairat Kanyamee, for understanding me. I am impress with her expertise. I am very grateful for her guidance and teaching, not only in this thesis methodologies but also many other useful tip for working in the future.

In addition, I would like to thank Dr. Sittisede Polwiang and Dr. Warin Sripunya, the chairman and a member of the thesis committee, for their comments and suggestions to improve the manuscript. We would also like to thank the Centre of Excellence in Mathematics, the Commission on Higher Education, for their support during the first year of my study.

Finally, I would like to express my gratitude to my family and my friends for all their support throughout the period of this thesis.

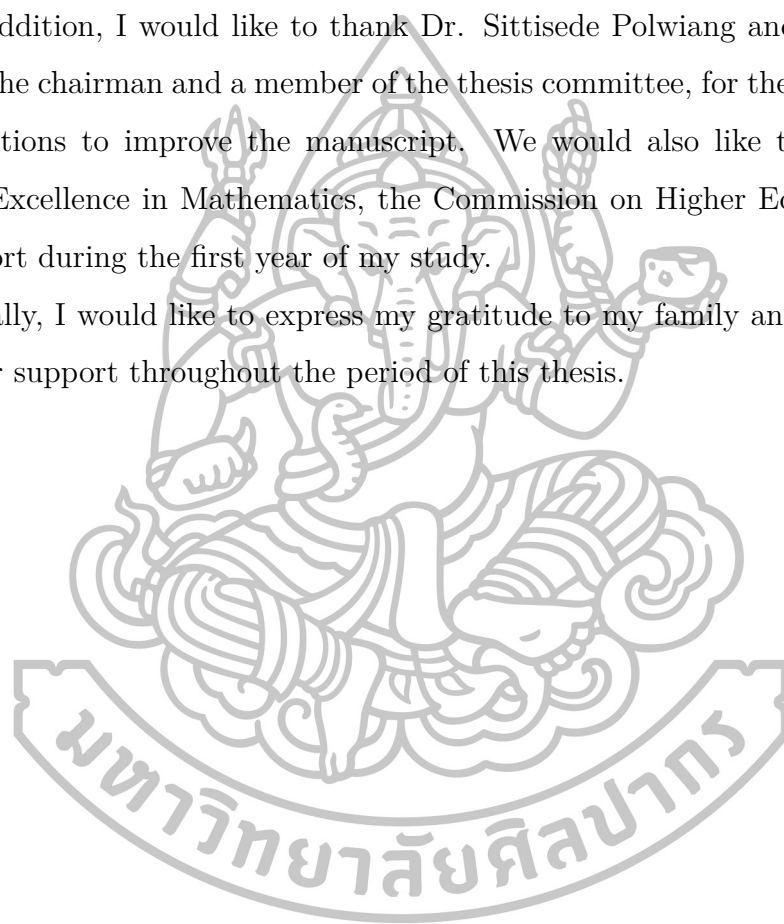
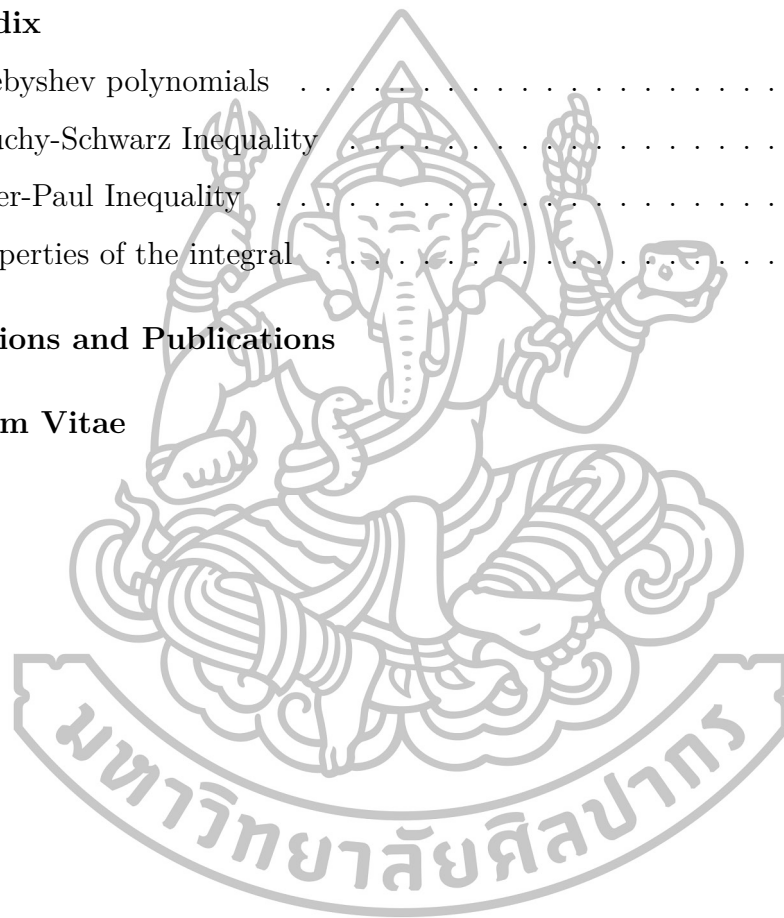


## Table of contents

	Page
<b>Abstract in English</b>	d
<b>Abstract in Thai</b>	e
<b>Acknowledgements</b>	f
<b>List of Figures</b>	k
<b>List of Tables</b>	l
<b>1 Introduction</b>	1
<b>2 Preliminaries</b>	5
2.1 The three-body problem . . . . .	5
2.2 Spectral collocation methods . . . . .	6
<b>3 Chebyshev-Gauss collocation method</b>	9
3.1 Chebyshev polynomials of the first kind . . . . .	9
3.2 Discrete Chebyshev-Gauss expansion [15] . . . . .	11
3.3 Chebyshev-Gauss collocation method . . . . .	14
3.3.1 Single interval Domain . . . . .	22
3.3.2 Multi-interval Domain . . . . .	22
<b>4 Error analysis of the Chebyshev-Gauss collocation method</b>	24
<b>5 Numerical Results</b>	37
5.1 Single interval Domain . . . . .	38
5.2 System of differential equations . . . . .	43



	Page
5.3 The three-body problem . . . . .	47
<b>6 Conclusions</b>	<b>61</b>
<b>References</b>	<b>63</b>
<b>A Appendix</b>	<b>67</b>
A.1 Chebyshev polynomials . . . . .	67
A.2 Cauchy-Schwarz Inequality . . . . .	68
A.3 Peter-Paul Inequality . . . . .	69
A.4 Properties of the integral . . . . .	69
<b>Presentations and Publications</b>	<b>70</b>
<b>Curriculum Vitae</b>	<b>71</b>



## List of Figures

Figures	Page
5.1 Point-wise absolute error of scheme (3.21) when at $T = 0.5, 0.8$ and $1$ . . . . .	39
5.2 Discrete $L^2$ error of scheme (3.21) when at $T = 0.5, 0.8$ and $1$ . . . . .	40
5.3 Point-wise absolute error of scheme (3.21) versus the Chebyshev–Gauss spectral collocation method. . . . .	40
5.4 Discrete $L^2$ error of scheme (3.21) versus the Chebyshev–Gauss spectral collocation method. . . . .	41
5.5 Point-wise absolute error of scheme (3.21) versus the Chebyshev–Gauss spectral collocation method and the convergence rate when $N$ varies. . . . .	41
5.6 Discrete $L^2$ error of scheme (3.21) versus the Chebyshev–Gauss spectral collocation method and the convergence rate when $N$ varies. . . . .	42
5.7 Discrete $L^2$ error of scheme (3.21) versus the Chebyshev–Gauss spectral collocation method and the Legendre–Gauss collocation method. . . . .	42
5.8 Point-wise absolute error of scheme (3.21) when $t = 2000$ , $\tau = 1$ and $N = 17$ . . . . .	43
5.9 Phase plot $p^N(t)$ versus $q^N(t)$ when $M = 10^5$ , $\tau = 0.1$ and $N = 7$ . . . . .	44
5.10 (a) Error in energy of scheme (5.3) versus the Legendre–Gauss collocation method (b) the Chebyshev–Gauss spectral collocation method when $M = 10^5$ , $\tau = 0.1$ and $N = 7$ . . . . .	45
5.11 (a) Phase plot $q_1^N(t)$ versus $p_1^N(t)$ (b) Phase plot $q_1^N(t)$ versus $q_2^N(t)$ when $M = 10^4$ , $\tau = 0.1$ and $N = 7$ . . . . .	46
5.12 Phase plots of $q_N^2$ versus $q_N^1$ by (a) the Chebyshev-Gauss collocation method (b) the first-order symplectic method (c) the fourth-order Runge-Kutta method. . . . .	48
5.13 Phase plots of $q_N^2$ versus $q_N^1$ and $t$ by (a) the Chebyshev-Gauss collocation method (b) the first-order symplectic method (c) the fourth-order Runge-Kutta method. . . . .	48

5.14 (a) Comparison of the relative error in energy between the three collocation methods and the first-order symplectic method (b) Comparison of the relative error in energy between the three collocation methods. . . . .	50
5.15 Phase plots of $q_N^2$ versus $q_N^1$ by (a) the Chebyshev-Gauss collocation method (b) the first-order symplectic method. (c) the fourth-order Runge-Kutta method. .	51
5.16 Phase plots of $q_N^2$ versus $q_N^1$ and $t$ by (a) the Chebyshev-Gauss collocation method (b) The first-order symplectic method (c) The fourth-order Runge-Kutta method. 51	51
5.17 Phase plots of $q_N^2$ versus $q_N^1$ by (a) the Chebyshev-Gauss collocation method (b) the first-order symplectic method (c) the fourth-order Runge-Kutta method. .	52
5.18 Phase plots of $q_N^2$ versus $q_N^1$ and $t$ by (a) the Chebyshev-Gauss collocation method (b) the first-order symplectic method (c) the fourth-order Runge-Kutta method. 52	52
5.19 (a) Comparison of the relative error in energy between the three collocation methods and the first-order symplectic method (b) Comparison of the relative error in energy between the three collocation methods. . . . .	53
5.20 Phase plots of $q_N^2$ versus $q_N^1$ by (a) the Chebyshev-Gauss collocation method (b) the first-order symplectic method (c) the fourth-order Runge-Kutta method. .	54
5.21 Phase plots of $q_N^2$ versus $q_N^1$ and $t$ by (a) the Chebyshev-Gauss collocation method (b) the first-order symplectic method (c) the fourth-order Runge-Kutta method. 54	54
5.22 Phase plots of $q_N^2$ versus $q_N^1$ by (a) the Chebyshev-Gauss collocation method (b) the first-order symplectic method (c) the fourth-order Runge-Kutta method. .	56
5.23 Phase plots of $q_N^2$ versus $q_N^1$ and $t$ by (a) the Chebyshev-Gauss collocation method (b) the first-order symplectic method (c) the fourth-order Runge-Kutta method. 56	56
5.24 Phase plots of $q_N^2$ versus $q_N^1$ by (a) the Chebyshev-Gauss collocation method (b) the first-order symplectic method (c) the fourth-order Runge-Kutta method. .	57
5.25 Phase plots of $q_N^2$ versus $q_N^1$ and $t$ by (a) the Chebyshev-Gauss collocation method (b) the first-order symplectic method (c) the fourth-order Runge-Kutta method. 57	57
5.26 (a) Comparison of the relative error in energy between the three collocation methods and the first-order symplectic method (b) Comparison of the relative error in energy between the three collocation methods. . . . .	58

- 5.27 Phase plots of  $q_N^2$  versus  $q_N^1$  by (a) the Chebyshev-Gauss collocation method (b) the first-order symplectic method (c) the fourth-order Runge-Kutta method. . 59
- 5.28 Phase plots of  $q_N^2$  versus  $q_N^1$  and  $t$  by (a) the Chebyshev-Gauss collocation method (b) the first-order symplectic method (c) the fourth-order Runge-Kutta method. 59



## List of Tables

Tables	Page
5.1 Comparison of the errors and CPU times from the three collocation methods for the system (5.4). . . . .	45
5.2 Comparison of the errors and CPU times from the three collocation methods for Henon Heiles (5.5). . . . .	47
5.3 Comparison of the errors and CPU times between the five methods. . . . .	49
5.4 Comparison of the errors and CPU times between the three collocation methods. . . . .	49
5.5 Comparison of the errors and CPU times between the five methods. . . . .	51
5.6 Comparison of the errors and CPU times between the five methods. . . . .	53
5.7 Comparison of the errors and CPU times between the three collocation methods. . . . .	53
5.8 Comparison of the errors and CPU times between the five methods. . . . .	55
5.9 Comparison of the errors and CPU times between the three collocation methods. . . . .	55
5.10 Comparison of the errors and CPU times between the five methods. . . . .	56
5.11 Comparison of the errors and CPU times between the three collocation methods. . . . .	56
5.12 Comparison of the errors and CPU times between the five methods. . . . .	58
5.13 Comparison of the errors and CPU times between the five methods. . . . .	60

# Chapter 1

## Introduction

The three-body problem arises in the area of classical mechanics. It describes three masses which interact under the gravitational force. The problem was originated from the motion of the Moon under the gravitational force acting between the Sun and the Earth [31]. The three-body problem is considered to be one of the Hamiltonian systems. The Hamiltonian of the system of  $n$  body is denoted by

$$H(\mathbf{p}, \mathbf{q}) = H(p_1, \dots, p_n, q_1, \dots, q_n).$$

The corresponding system of differential equations is given by

$$\begin{aligned} \frac{dp_i}{dt} &= -\frac{\partial H}{\partial q_i} \\ \frac{dq_i}{dt} &= \frac{\partial H}{\partial p_i}, \quad i = 1, 2, \dots, n \end{aligned}$$

where  $p_i$  is the generalized momenta and  $q_i$  is the generalized coordinates.

The three-body problem was first discovered in 1687 by Sir Isaac Newton. He formulated a system of differential equations to describe the motion of the Moon around the Earth. The study revealed that the Moon and Earth influence on each other by a gravitational force and use the initial conditions associated to the equations to predict the motion of two bodies moving in orbit. When another variable is added to generate the three-body system, the relationship of the motion of the Moon under the influence of the Earth and Sun is considered [23, 24, 28]. Later in 1772, Euler established a lunar theory through the study of the restricted three-body problem. About the same time, Lagrange, who followed Euler's lead, introduced a method for describing periodic orbits of general three-body problem.

He discovered the five Lagrange points (equilibrium points) and the Lagrangian equilateral triangle. [24, 26, 31]

In 1836, Jacobi continued to study the restricted system with more variables [26, 31]. Later in 1858, Dirichlet claimed that he had discovered a general method for treating the problem. In addition, he claimed that he had succeeded in proving the stability of the planetary system. However, he died without leaving a proof of his work. Yet, it was presented by his students, Kovalevski and Mittag-leffler [22]. In 1883, Poincaré authored a book about the three-body problem based on the Mean Value Theorem in order to prove that the three-body problem has a relativistic periodic solution. Nevertheless, the analytic solution to the three-body problem still has not been found [3, 4].

Later, Alexey Lapshin revealed a numerical solution to the problem using the fourth order of Runge-Kutta method. He showed the method of solving the restricted problem when one of the masses of the three-body problem is considered to be very small (close to zero) compared to the other two masses. He, moreover, found that the orbit of an object with a small mass moves around the two objects in shape of the eight and ellipses [21]. Feng Kang afterwards offered a new method to determine the numerical solution of such differential equations called the symplectic methods, which preserve the area and, thus, reduce variability in solutions [17, 30].

In 2011, Kanyamee and Zhang considered the Hamiltonian of the Earth-Moon-Satellite system. They described the motion of a satellite around the Earth and Moon by setting the Earth and Moon on the  $x$ -axis, while the coordinates  $(x, y)$  represented the satellite coordinate in the orbit around the Earth and Moon. They compared the spectral collocation methods with the first-order symplectic method. The orbits obtained from the symplectic method seemed to be thicker than the collocation methods, especially the left and right corner. Moreover, when comparing the error in energy and CPU times, the spectral collocation methods provide small error and less time than the symplectic method. However, the convergence rate of the spectral collocation methods is of the first order, which

could be improved. Additionally, they did not provide the set of appropriate initial conditions for this problem [18].

After that, Zhang Hua et al. proved that the Symplectic Algebraic Dynamics Algorithm (SADA) has high accuracy in finding solutions to describe the long term behavior of the circular restricted three-body problem (CR3BP). They considered the Hamiltonian of the Earth-Moon-Satellite system and compared the SADA of the fourth order with the Runge-Kutta method of fourth order. They eventually found that the SADA method gives better accuracy than Runge-Kutta method in a long-term period [32].

As stated in the beginning of the chapter, the Hamiltonian systems are described by a set of ordinary differential equations . The ordinary differential equations occur mostly in problems in Science and Engineering. There are several numerical methods to solve the initial value problems of the ordinary differential equations. The classical methods such as the Euler method and explicit Runge-Kutta methods are known to provide the numerical solutions with a low accuracy [5] whereas the implicit Runge-Kutta methods give a high accuracy for the numerical results [6, 7, 14]. There are some other high accuracy methods for the ordinary differential equations proposed by Hairer et al. [9], Lambert [20] and Stuart et al. [29].

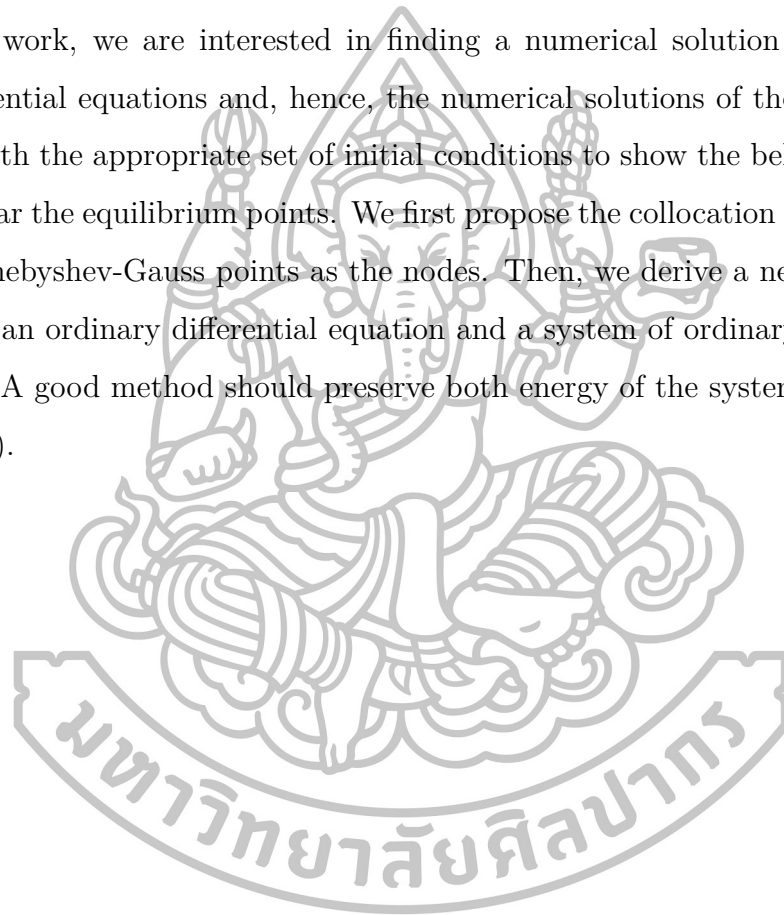
Spectral methods have been successfully used to obtain the numerical solutions of ordinary and partial differential equations. The solutions of the methods are approximated in forms of the expansion of higher-order polynomials [8, 15, 16, 19]. The spectral collocation methods recently capture many researcher's interests as they give a spectral accuracy to the solutions. The smoother the exact solutions, the smaller the numerical errors are [35].

The recent work for solving the ordinary differential equations using the spectral methods are proposed by Guo et al. [2, 11, 12, 14, 33]. They developed the Legendre-Gauss [14] and designed Laguerre-Gauss and Laguerre-Radau type [2, 11] spectral collocation methods for the ordinary differential equations. Furthermore, Kanyamee et al. [18] described the comparison of several spectral



Galerkin and spectral collocation methods and symplectic methods for the Hamiltonian systems. Wang et al. [34, 35] developed the Chebyshev-Gauss spectral collocation methods and developed the Legendre-Gauss collocation methods for nonlinear delay differential equations. El-Baghdady et al. [10] designed a new Chebyshev spectral collocation method for solving a class of one-dimensional linear parabolic partial integro-differential equations.

In this work, we are interested in finding a numerical solution of the ordinary differential equations and, hence, the numerical solutions of the three-body problem with the appropriate set of initial conditions to show the behavior of the solution near the equilibrium points. We first propose the collocation method with  $(N + 1)$  Chebyshev-Gauss points as the nodes. Then, we derive a new algorithm for solving an ordinary differential equation and a system of ordinary differential equations. A good method should preserve both energy of the system  $H$  and the area (orbit).



# Chapter 2

## Preliminaries

In this chapter, we will discuss the three-body problem and the spectral collocation methods.

### 2.1 The three-body problem

We consider the Hamiltonian,  $H$ , of the Earth-Moon-Satellite system given by

$$H(p_x, p_y, x, y) = \frac{p_x^2 + p_y^2}{2} + (yp_x - xp_y) - \left( \frac{1-\mu}{r_1} + \frac{\mu}{r_2} \right)$$

where  $x$  and  $y$  are the displacements along the  $x$ - and  $y$ -axes,  $p_x$  and  $p_y$  are the momenta in the  $x$ - and  $y$ - directions, respectively,  $r_1^2 = (x + \mu)^2 + y^2$ ,  $r_2^2 = (x + \mu - 1)^2 + y^2$  and  $\mu$  is the mass of the Moon. In this paper, we choose  $\mu$  to be 0.01215 times the mass of the Earth [32]. The Hamiltonian  $H$  also represents the energy of the system. The system are known to conserve energy, i.e., the energy is constant along the trajectory [17].

This system describes the motion of the satellite around the Earth and Moon. To formulate the equations, we locate the Earth and the Moon on the  $x$ -axis where the origin is at the center of mass between the two objects. The position of the satellite can be represented by the  $x$ - and  $y$ - coordinates or as the point  $(x, y)$ .

The corresponding system is given by

$$\begin{aligned}
\frac{dp_x}{dt} &= p_y - \frac{(1-\mu)}{r_1^3}(x+\mu) - \frac{\mu}{r_2^3}(x+\mu-1) \\
\frac{dp_y}{dt} &= -p_x - \frac{y}{r_1^3}(1-\mu) - \frac{\mu}{r_2^3}(y) \\
\frac{dx}{dt} &= p_x + y \\
\frac{dy}{dt} &= p_y - x
\end{aligned} \tag{2.1}$$

where  $p(0) = p_0$ ,  $q(0) = q_0$ ,  $x(0) = x_0$  and  $y(0) = y_0$ . For simplicity, we let  $p_x = p_1$ ,  $p_y = p_2$ ,  $x = q_1$  and  $y = q_2$ .

As we discussed in Chapter 1, this system has the five Lagrangian equilibrium points which are  $L_1(0, 0.84, 0.84, 0)$ ,  $L_2(0, 1.16, 1.16, 0)$ ,  $L_3(0, -1.01, -1.01, 0)$ ,  $L_4(-0.87, 0.49, 0.49, 0.87)$  and  $L_5(0.87, 0.49, 0.49, -0.87)$ . The first three points  $L_1, L_2$  and  $L_3$  on the  $x$ -axis are the collinear equilibrium points. These three points are called the unstable saddle points. The other two points  $L_4$  and  $L_5$  are called the nonlinear stable points [32].

## 2.2 Spectral collocation methods

The spectral collocation methods are methods to determine a numerical solution of ordinary differential equations and partial differential equations. The collocation method is defined by considering the residual of the problem. The method requires the residual to vanish at a certain set of grid points. These grid points are called the collocation points. The collocation points denoted by  $x_0, \dots, x_N$  are commonly the set of Gauss-type points [15, 16].

Consider the problem:

$$\begin{cases}
\frac{\partial u(x, t)}{\partial t} = \mathcal{L}u(x, t), & x \in [a, b], \quad t \geq 0 \\
\mathcal{B}_L u = 0, & t \geq 0 \\
\mathcal{B}_R u = 0, & t \geq 0 \\
u(x, 0) = f(x), & x \in [a, b]
\end{cases} \tag{2.2}$$

where  $\mathcal{L}$  is a leading spatial derivative operator,  $\mathcal{B}_L$  and  $\mathcal{B}_R$  are the boundary operators at  $x = a$  and  $x = b$ , respectively.

In the collocation method, we seek a solution  $u_N(x, t) \in \mathcal{P}_N$  of the form

$$u_N(x, t) = \sum_{j=0}^N a_j(t) \phi_j(x) \quad (2.3)$$

where  $\phi_j(x)$  is a polynomial taken from the space

$$\mathcal{P}_N = \text{span} \left\{ \phi_j(x) \in \text{Span} \{x^k\}_{k=0}^j \mid \mathcal{B}_L \phi_j = 0, \quad \mathcal{B}_R \phi_j = 0 \right\}_{j=0}^N.$$

As discussed above, we require the residual to vanish at the collocation points  $x_0, \dots, x_N$ . This yields the  $(N+1)$  equations to determine the unknown expansion coefficients,  $a_j(t), j = 0, \dots, N$ .

$$\mathcal{R}_N(x_j, t) = \frac{\partial u(x_j, t)}{\partial t} - \mathcal{L}u(x_j, t) = 0, \quad 0 \leq j \leq N.$$

Substituting (2.3) into (2.2), we obtain the corresponding  $(N+1)$  equations for (2.2) as

$$\begin{cases} \frac{\partial u_N(x_j, t)}{\partial t} = \mathcal{L}u_N(x_j, t), & 0 \leq j \leq N \\ \mathcal{B}_L u_N = 0, \\ \mathcal{B}_R u_N = 0 \\ u_N(x, 0) = f(x) \end{cases}$$

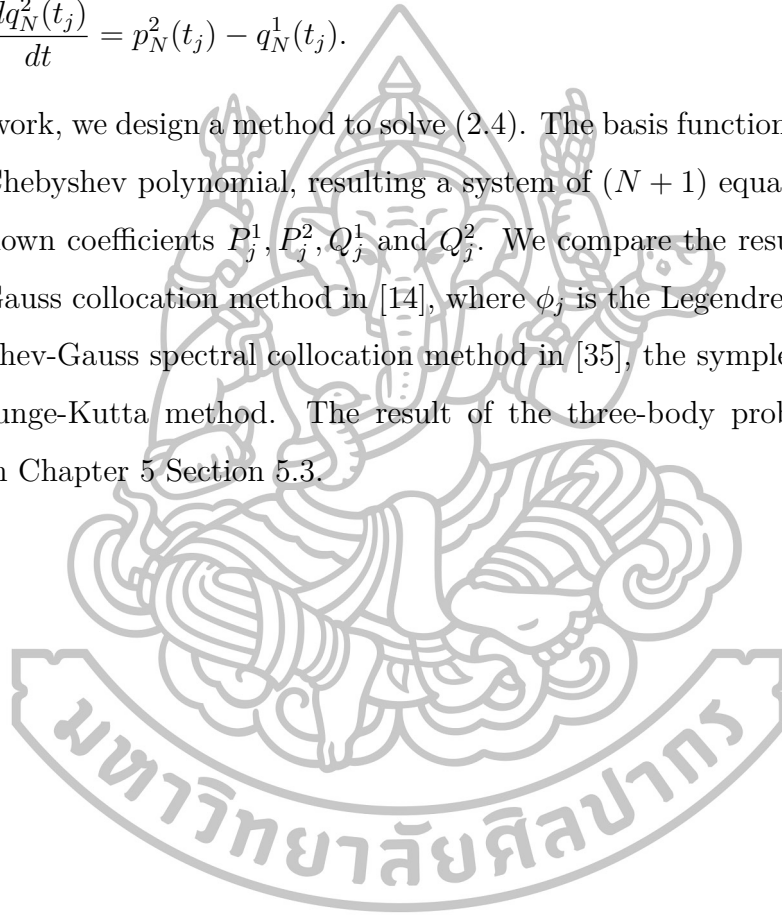
We apply the collocation method to the three-body problem (3.1) using the Gauss points as the collocation points for the problem. The Gauss points  $x_j$  are the zeros of polynomial on the interval  $[-1, 1]$ . These points  $x_j$  are then transformed to the Gauss points  $t_j$  on the interval  $[a, b]$  by  $t_j = \frac{b+a+x_j(b-a)}{2}$ . To find the solution of (3.1), we seek for  $p_N^1(t), p_N^2(t), q_N^1(t), q_N^2(t) \in \mathcal{P}_N$  of the form

$$p_N^1(t) = \sum_{j=0}^N P_j^1 \phi_j(t), \quad p_N^2(t) = \sum_{j=0}^N P_j^2 \phi_j(t), \quad q_N^1(t) = \sum_{j=0}^N Q_j^1 \phi_j(t), \quad q_N^2(t) = \sum_{j=0}^N Q_j^2 \phi_j(t)$$

such that the residual is zero at the points  $t_0, \dots, t_N$ , i.e.,

$$\begin{aligned}
\frac{dp_N^1(t_j)}{dt} &= p_N^2(t_j) - \frac{(1-\mu)}{r_1^3}(q_N^1(t_j) + \mu) - \frac{\mu}{r_2^3}(q_N^1(t_j) + \mu - 1) \\
\frac{dp_N^2(t_j)}{dt} &= -p_N^1(t_j) - \frac{q_N^2(t_j)}{r_1^3}(1-\mu) - \frac{\mu}{r_2^3}(q_N^2(t_j)) \\
\frac{dq_N^1(t_j)}{dt} &= p_N^1(t_j) + q_N^2(t_j) \\
\frac{dq_N^2(t_j)}{dt} &= p_N^2(t_j) - q_N^1(t_j).
\end{aligned} \tag{2.4}$$

In this work, we design a method to solve (2.4). The basis function  $\phi_j$  is chosen to be the Chebyshev polynomial, resulting a system of  $(N + 1)$  equation for each set of unknown coefficients  $P_j^1, P_j^2, Q_j^1$  and  $Q_j^2$ . We compare the results with the Legendre-Gauss collocation method in [14], where  $\phi_j$  is the Legendre polynomial, the Chebyshev-Gauss spectral collocation method in [35], the symplectic method and the Runge-Kutta method. The result of the three-body problem will be discussed in Chapter 5 Section 5.3.



## Chapter 3

# Chebyshev-Gauss collocation method

In this chapter, we describe the Chebyshev polynomials and their properties, in Section 3.1 and 3.2. Then, we introduce the Chebyshev-Gauss collocation method as well as the algorithm for solving an ordinary differential equations in Section 3.3.

### 3.1 Chebyshev polynomials of the first kind

In this section, we consider Chebyshev polynomials of the first kind on the interval  $[-1, 1]$  and the shifted Chebyshev polynomials on the interval  $[0, T]$ .

Chebyshev polynomials of the first kind, denoted  $\mathcal{T}_n(x)$ , are eigenfunctions of the singular Sturm-Liouville equation of the form

$$(1 - x^2) \mathcal{T}_n''(x) - x\mathcal{T}_n'(x) + n^2\mathcal{T}_n(x) = 0, \quad x \in [-1, 1].$$

An alternative representation of the Chebyshev polynomial of degree  $n$  is given by

$$\mathcal{T}_n(x) = \cos(n \arccos(x)).$$

Let  $\mathcal{T}_l(x)$  be the Chebyshev polynomial of degree  $l$  defined on the interval  $[-1, 1]$ .

We define the shifted Chebyshev polynomials  $\mathcal{T}_{T,l}(t)$  on the interval  $[0, T]$ , with the transformation  $x = \frac{2t}{T} - 1$ , by

$$\mathcal{T}_{T,l}(t) = \mathcal{T}_l\left(\frac{2t}{T} - 1\right) = \cos\left(l \cos^{-1}\left(\frac{2t}{T} - 1\right)\right), \quad l = 0, 1, 2, \dots$$

The first few polynomials are illustrated as follows:

$$\begin{aligned}\mathcal{T}_{T,0}(t) &= \cos \left( (0) \cos^{-1} \left( \frac{2t}{T} - 1 \right) \right) = 1, \\ \mathcal{T}_{T,1}(t) &= \cos \left( (1) \cos^{-1} \left( \frac{2t}{T} - 1 \right) \right) = \frac{2t}{T} - 1, \\ \mathcal{T}_{T,2}(t) &= \cos \left( (2) \cos^{-1} \left( \frac{2t}{T} - 1 \right) \right) = \frac{8t^2}{T^2} - \frac{8t}{T} + 1.\end{aligned}$$

By following a property of Chebyshev polynomials, we have the three-term recurrence relation for shifted Chebyshev polynomials

$$\mathcal{T}_{T,l+1}(t) - 2 \left( \frac{2t}{T} - 1 \right) \mathcal{T}_{T,l}(t) + \mathcal{T}_{T,l-1}(t) = 0, \quad l \geq 1. \quad (3.1)$$

The shifted Chebyshev polynomials are also orthogonal on the interval  $[0, T]$  ( see Appendix A.1 ), i.e.

$$\int_0^T \mathcal{T}_{T,l}(t) \mathcal{T}_{T,m}(t) \omega^{-\frac{1}{2}}(t) dt = \frac{1}{2} \pi c_l \delta_{l,m}, \quad l \geq 0 \quad (3.2)$$

where  $\omega(t) = t(T-t)$ ,  $c_0 = 2$ ,  $c_l = 1$  and  $\delta_{l,m}$  is the Kronecker symbol.

Consider any function  $u \in L^2_{\omega^{-\frac{1}{2}}}(0, T)$ . A Chebyshev expansion of a function  $u$  is

$$u(t) = \sum_{l=0}^{\infty} \hat{u}_l \mathcal{T}_{T,l}(t). \quad (3.3a)$$

where the expansion coefficients,  $\hat{u}_l$ , are constants. Multiplying both sides of (3.3a) by  $\mathcal{T}_{T,l}(t)$  and  $\omega^{-\frac{1}{2}}(t)$  and integrating with respect to  $t$  over  $[0, T]$  gives

$$\begin{aligned}\int_0^T \mathcal{T}_{T,l}(t) u(t) \omega^{-\frac{1}{2}}(t) dt &= \int_0^T \mathcal{T}_{T,l}(t) \left( \sum_{l=0}^{\infty} \hat{u}_l \mathcal{T}_{T,l}(t) \right) \omega^{-\frac{1}{2}}(t) dt \\ &= \sum_{l=0}^{\infty} \int_0^T \mathcal{T}_{T,l}(t) \hat{u}_l \mathcal{T}_{T,l}(t) \omega^{-\frac{1}{2}}(t) dt \\ &= \int_0^T \mathcal{T}_{T,0}(t) \mathcal{T}_{T,0}(t) \hat{u}_0 \omega^{-\frac{1}{2}}(t) dt + \int_0^T \mathcal{T}_{T,1}(t) \mathcal{T}_{T,1}(t) \hat{u}_1 \omega^{-\frac{1}{2}}(t) dt + \dots \\ &= \int_0^T \mathcal{T}_{T,l}(t) \mathcal{T}_{T,l}(t) \omega^{-\frac{1}{2}}(t) \hat{u}_l dt \\ &= \frac{1}{2} \pi c_l \hat{u}_l \\ \therefore \hat{u}_l &= \frac{2}{\pi c_l} \int_0^T \frac{u(t) \mathcal{T}_{T,l}(t)}{\sqrt{t(T-t)}} dt. \quad (3.3b)\end{aligned}$$

Next, for any positive integer  $N$ , we consider the Chebyshev-Gauss quadrature. Let  $\{(x_j^N, \omega_j^N)\}_{j=0}^N$  be the Chebyshev nodes (where  $x$  are the zeros of  $\mathcal{T}_{N+1}(x)$ ) and corresponding weights on the interval  $(-1, 1)$ . We define the shifted Chebyshev-Gauss nodes and the corresponding weights on  $(0, T)$  as

$$t_{T,j}^N = \frac{T}{2}(x_j^N + 1), \quad 0 \leq j \leq N \quad \text{and} \quad \omega_{T,j}^N = \frac{T}{2}\omega_j^N, \quad 0 \leq j \leq N.$$

Let  $\mathcal{P}_N(0, T)$  be the set of polynomials of degree at most  $N$  on  $[a, b]$ . According to the Gauss-type quadrature rule. The Gaussian quadrature is exact for all polynomials  $p(x) \in \mathcal{P}_{2N+1}$ . As a results, for any  $\phi \in \mathcal{P}_{2N+1}(-1, 1)$ ,

$$\int_{-1}^1 \frac{\phi(x)}{\sqrt{1-x^2}} dx = \frac{\pi}{N+1} \sum_{j=0}^N \phi(x_j^N).$$

Hence, for any  $\phi \in \mathcal{P}_{2N+1}(0, T)$ , we have:

$$\begin{aligned} \int_0^T \frac{\phi(t)}{\sqrt{t(T-t)}} dt &= \int_{-1}^1 \phi\left(\frac{T}{2}(x+1)\right) \left(\frac{1}{\frac{T}{2}\sqrt{1-x^2}}\right) \frac{T}{2} dx \\ &= \int_{-1}^1 \frac{\phi\left(\frac{T}{2}(x+1)\right)}{\sqrt{1-x^2}} dx \\ &= \frac{\pi}{N+1} \sum_{j=0}^N \phi\left(\frac{T}{2}(x_j^N + 1)\right) \quad (\text{by Gaussian quadrature [16]}) \\ &= \frac{\pi}{N+1} \sum_{j=0}^N \phi(t_{T,j}^N). \end{aligned} \tag{3.4}$$

### 3.2 Discrete Chebyshev-Gauss expansion [15]

In the continuous  $L^2_{\omega^{-\frac{1}{2}}}(0, T)$  space, we define the inner product and  $L^2_{\omega^{-\frac{1}{2}}}$ -norm as

$$(u, v)_T = \int_0^T u(t)v(t)dt \quad \text{and} \quad \|u\|_T = (u, u)_T^{1/2} \quad \text{for } u, v \in L^2_{\omega^{-\frac{1}{2}}}(0, T).$$

For the discrete expansion, using the Chebyshev-Gauss quadrature formula, the discrete inner product and norm on  $(0, T)$  is defined by

$$(u, v)_{T,N} = \frac{\pi}{N+1} \sum_{j=0}^N u(t_{T,j}^N)v(t_{T,j}^N) \quad \text{and} \quad \|u\|_{T,N} = (u, u)_{T,N}^{1/2} \tag{3.5}$$



where  $u, v \in L^2_{\omega^{-\frac{1}{2}}}(0, T)$ .

It follows from (3.4) that for any  $\phi\psi \in \mathcal{P}_{2N+1}(0, T)$  and  $\varphi \in \mathcal{P}_N(0, T)$ ,

$$(\phi, \psi)_T = \int_0^T \phi(t)\psi(t)\omega^{-\frac{1}{2}}(t)dt = \frac{\pi}{N+1} \sum_{j=0}^N \phi(t_{T,j}^N)\psi(t_{T,j}^N) = (\phi, \psi)_{T,N} \quad (3.6a)$$

and the two norms  $\|\varphi\|_T^2$  and  $\|\varphi\|_{T,N}^2$  coincide, i.e.

$$\|\varphi\|_T^2 = \int_0^T \varphi(t)\varphi(t)\omega^{-\frac{1}{2}}(t)dt = \frac{\pi}{N+1} \sum_{j=0}^N \varphi(t_{T,j}^N)\varphi(t_{T,j}^N) = \|\varphi\|_{T,N}^2. \quad (3.6b)$$

Recall the Chebyshev expansion in (3.3a), the truncated continuous expansion of  $u$  is considered as the projection of  $u$  on the finite dimensional space  $\mathcal{B}_{(N+1)}$  of the form

$$u(t) = \sum_{l=0}^{N+1} \hat{u}_l^N \mathcal{T}_{T,l}(t). \quad (3.7)$$

where  $\mathcal{B}_{(N+1)} = \text{span} \{t^k : 0 \leq k \leq N+1\}$  with the coefficients

$$\hat{u}_l^N = \frac{2}{\pi c_l} (u, \mathcal{T}_{T,l})_T = \frac{2}{\pi c_l} (u, \mathcal{T}_{T,l})_{T,N}, \quad 0 \leq l \leq N \quad \text{and} \quad \hat{u}_{N+1}^N = \frac{2}{\pi c_{N+1}} (u, \mathcal{T}_{T,N+1})_T.$$

Let  $\mathcal{I}_{T,N}u$  be the discrete Chebyshev-Gauss expansion of any  $u$  in  $L^2_{\omega^{-\frac{1}{2}}}(0, T)$ .

Using the Chebyshev-Gauss quadrature, we define the discrete approximation of  $u$

$$\mathcal{I}_{T,N}u(t) = \sum_{l=0}^N \tilde{u}_l^N \mathcal{T}_{T,l}(t) \quad (3.8)$$

where the discrete expansion coefficients are

$$\tilde{u}_l^N = \frac{2}{(N+1)c_l} \sum_{j=0}^N u(t_{T,j}^N) \mathcal{T}_{T,l}(t_{T,j}^N), \quad 0 \leq l \leq N.$$

This  $\mathcal{I}_{T,N}u \in \mathcal{P}_N(0, T)$  and it interpolates  $u$  at all the Gaussian quadrature points [15].

$$\mathcal{I}_{T,N}u(t_{T,j}^N) = \sum_{l=0}^N \tilde{u}_l^N \mathcal{T}_{T,l}(t_{T,j}^N) = \sum_{l=0}^N u(t_{T,j}^N) \mathcal{L}_l(t_{T,j}^N) = u(t_{T,j}^N), \quad 0 \leq j \leq N. \quad (3.9)$$

where  $\mathcal{L}_l(t)$  is the Lagrange polynomials based on the Chebyshev-Gauss nodes.

From (3.6a) and (3.9), we have

$$(u, \phi)_{T,N} \stackrel{(3.9)}{=} (\mathcal{I}_{T,N}u, \phi)_T \stackrel{(3.6a)}{=} (\mathcal{I}_{T,N}u, \phi)_{T,N}, \quad \forall \phi \in \mathcal{P}_{N+1}(0, T). \quad (3.10)$$

Using (3.10) and the above statement that  $\mathcal{T}_{T,l}(t) \in \mathcal{P}_N(0, T)$ , the discrete expansion coefficients  $\tilde{u}_l^N$  in (3.8) can be written as

$$\begin{aligned}
\mathcal{T}_{T,l}(t)\mathcal{I}_{T,N}u(t)\omega^{-\frac{1}{2}}(t) &= \mathcal{T}_{T,l}(t) \left( \sum_{l=0}^N \tilde{u}_l^N \mathcal{T}_{T,l}(t) \right) \omega^{-\frac{1}{2}}(t) \\
\int_0^T \mathcal{T}_{T,l}(t)\mathcal{I}_{T,N}u(t)\omega^{-\frac{1}{2}}(t)dt &= \int_0^T \mathcal{T}_{T,l}(t) \left( \sum_{l=0}^N \tilde{u}_l^N \mathcal{T}_{T,l}(t) \right) \omega^{-\frac{1}{2}}(t)dt \\
\int_0^T \mathcal{T}_{T,l}(t)\mathcal{I}_{T,N}u(t)\omega^{-\frac{1}{2}}(t)dt &= \int_0^T \mathcal{T}_{T,l}(t)\mathcal{T}_{T,0}(t)\tilde{u}_0^N\omega^{-\frac{1}{2}}(t)dt + \dots \\
&\quad + \int_0^T \mathcal{T}_{T,l}(t)\mathcal{T}_{T,n}(t)\tilde{u}_n^N\omega^{-\frac{1}{2}}(t)dt \\
(\mathcal{I}_{T,N}u, \mathcal{T}_{T,l})_T &= \frac{1}{2}\pi c_l \tilde{u}_l^N \\
\tilde{u}_l^N &= \frac{2}{\pi c_l} (\mathcal{I}_{T,N}u, \mathcal{T}_{T,l})_T \\
\therefore \tilde{u}_l^N &= \frac{2}{\pi c_l} (\mathcal{I}_{T,N}u, \mathcal{T}_{T,l})_T = \frac{2}{\pi c_l} (\mathcal{I}_{T,N}u, \mathcal{T}_{T,l})_{T,N}, \quad 0 \leq l \leq N. \quad (3.11)
\end{aligned}$$

Next, we consider the relationship between the coefficients of the truncated continuous Chebyshev expansion in (3.7) and the discrete expansion in (3.8). For any  $u \in \mathcal{P}_{N+1}(0, T)$ , the coefficients  $\hat{u}_l^N$  and  $\tilde{u}_l^N$  determined in (3.7) and (3.11) gives

$$\tilde{u}_l^N = \frac{2}{\pi c_l} (\mathcal{I}_{T,N}u, \mathcal{T}_{T,l})_{T,N} \stackrel{(3.9)}{=} \frac{2}{\pi c_l} (u, \mathcal{T}_{T,l})_{T,N} \stackrel{(3.6a)}{=} \frac{2}{\pi c_l} (u, \mathcal{T}_{T,l})_T, \quad 0 \leq l \leq N.$$

Therefore, for any  $u \in \mathcal{P}_{N+1}(0, T)$ ,

$$\hat{u}_l^N = \tilde{u}_l^N, \quad 0 \leq l \leq N. \quad (3.12)$$

The result from (3.12) gives the comparison of the discrete norm and the  $L^2_{\omega^{-\frac{1}{2}}}$ -norm of  $u \in \mathcal{P}_{N+1}(0, T)$  as follows:

$$\begin{aligned}
\|u\|_{T,N}^2 &\stackrel{(3.5)}{=} (u, u)_{T,N} \\
&= \frac{\pi}{N+1} \sum_{j=0}^N u(t_{T,j}^N)u(t_{T,j}^N) \\
&\stackrel{(3.9)}{=} \frac{\pi}{N+1} \sum_{j=0}^N \mathcal{I}_{T,N}u(t_{T,j}^N)\mathcal{I}_{T,N}u(t_{T,j}^N) \\
&\stackrel{(3.5)}{=} (\mathcal{I}_{T,N}u, \mathcal{I}_{T,N}u)_{T,N} \\
&= \|\mathcal{I}_{T,N}u\|_{T,N}^2
\end{aligned}$$

$$\begin{aligned}
&\stackrel{(3.6b)}{=} \|\mathcal{I}_{T,N}u\|_T^2 \\
&\stackrel{(3.8)}{=} \left( \sum_{l=0}^N \tilde{u}_l^N \mathcal{T}_{T,l}, \sum_{l=0}^N \tilde{u}_l^N \mathcal{T}_{T,l} \right)_T \\
&= \int_0^T \left( \sum_{l=0}^N \tilde{u}_l^N \mathcal{T}_{T,l}(t) \right) \left( \sum_{l=0}^N \tilde{u}_l^N \mathcal{T}_{T,l}(t) \right) \omega^{-\frac{1}{2}}(t) dt \\
&= \int_0^T \left( \sum_{l=0}^N (\tilde{u}_l^N)^2 \mathcal{T}_{T,l}(t) \mathcal{T}_{T,l}(t) \right) \omega^{-\frac{1}{2}}(t) dt \\
&= \sum_{l=0}^N \left( (\tilde{u}_l^N)^2 \int_0^T \mathcal{T}_{T,l}(t) \mathcal{T}_{T,l}(t) \omega^{-\frac{1}{2}}(t) dt \right) \\
&= \sum_{l=0}^N (\tilde{u}_l^N)^2 \int_0^T \mathcal{T}_{T,l}^2(t) \omega^{-\frac{1}{2}}(t) dt \\
&\stackrel{(3.12)}{=} \sum_{l=0}^N (\hat{u}_l^N)^2 \int_0^T \mathcal{T}_{T,l}^2(t) \omega^{-\frac{1}{2}}(t) dt \\
&\leq \sum_{l=0}^{N+1} (\hat{u}_l^N)^2 \int_0^T \mathcal{T}_{T,l}^2(t) \omega^{-\frac{1}{2}}(t) dt \\
&= \int_0^T \sum_{l=0}^{N+1} (\hat{u}_l^N \mathcal{T}_{T,l}(t))^2 \omega^{-\frac{1}{2}}(t) dt \\
&\stackrel{(3.7)}{=} \int_0^T (u(t))^2 \omega^{-\frac{1}{2}}(t) dt \\
\therefore \|u\|_{T,N}^2 &\leq \|u\|_T^2. \tag{3.13}
\end{aligned}$$

### 3.3 Chebyshev-Gauss collocation method

In this section, we introduce a Chebyshev-Gauss collocation method to obtain a numerical solution of ordinary differential equations. Consider the first-order ordinary differential equation on the interval  $[0, T]$  of the form

$$\begin{cases} \frac{d}{dt}X(t) = f(X(t), t), & 0 < t \leq T \\ X(0) = X_0. \end{cases} \tag{3.14}$$

For the spectral collocation method, we find  $X^N(t) \in \mathcal{P}_{N+1}(0, T)$  such that

$$\begin{cases} \frac{d}{dt}X^N(t_{T,j}^N) = f(X^N(t_{T,j}^N), t_{T,j}^N), & 0 \leq j \leq N \\ X^N(0) = X_0. \end{cases} \tag{3.15}$$

which implies the residual error vanishes at the collocation points  $t_{T,j}^N, j = 0, \dots, N$  or

$$R_N(X^N(t_{T,j}^N), t_{T,j}^N) = \frac{d}{dt}X^N(t_{T,j}^N) - f(X^N(t_{T,j}^N), t_{T,j}^N) = 0.$$

In the Chebyshev collocation, we seek a solution  $X^N(t) \in \mathcal{P}_{N+1}(0, T)$  of the form

$$X^N(t) = \sum_{l=0}^{N+1} \hat{X}_l^N \mathcal{T}_{T,l}(t), \quad 0 < t \leq T. \quad (3.16)$$

As a result, we have that  $X^N(t)\mathcal{T}_{T,l}(t) \in \mathcal{P}_{2N+1}(0, T)$  for  $0 \leq l \leq N$ . Multiplying (3.16) by  $\mathcal{T}_{T,l}(t)\omega^{-\frac{1}{2}}(t)$  and integrating the result over the interval  $[0, T]$  together with (3.7), we obtain

$$\begin{aligned} \int_0^T \mathcal{T}_{T,l}(t)X^N(t)\omega^{-\frac{1}{2}}(t)dt &= \int_0^T \mathcal{T}_{T,l}(t) \left( \sum_{l=0}^{N+1} \hat{X}_l^N \mathcal{T}_{T,l}(t) \right) \omega^{-\frac{1}{2}}(t)dt \\ (X^N, \mathcal{T}_{T,l})_T &\stackrel{(3.2)}{=} \frac{1}{2} \pi c_l \hat{X}_l^N \\ \hat{X}_l^N &= \frac{2}{\pi c_l} (X^N, \mathcal{T}_{T,l})_T \\ &\stackrel{(3.6a)}{=} \frac{2}{\pi c_l} (X^N, \mathcal{T}_{T,l})_{T,N} \\ &\stackrel{(3.5)}{=} \left( \frac{2}{\pi c_l} \right) \left( \frac{\pi}{N+1} \right) \sum_{j=0}^N X^N(t_{T,j}^N) \mathcal{T}_{T,l}(t_{T,j}^N) \\ \therefore \hat{X}_l^N &= \frac{2}{c_l(N+1)} \sum_{j=0}^N X^N(t_{T,j}^N) \mathcal{T}_{T,l}(t_{T,j}^N), \quad 0 \leq l \leq N. \quad (3.17) \end{aligned}$$

So far, we only obtain the coefficients  $\hat{X}_l^N$  for  $0 \leq l \leq N$ . We still need to find the last coefficient  $\hat{X}_{N+1}^N$ . Considering  $t = 0$  in (3.16),  $X_0 = \sum_{l=0}^{N+1} \hat{X}_l^N \mathcal{T}_{T,l}(0)$ . By using the property  $\mathcal{T}_{T,l}(0) = (-1)^l$  and (3.17), we obtain

$$\begin{aligned} X^N(t) &= \hat{X}_{N+1}^N \mathcal{T}_{T,N+1}(t) + \sum_{l=0}^N \hat{X}_l^N \mathcal{T}_{T,l}(t) \\ X^N(0) &= \hat{X}_{N+1}^N \mathcal{T}_{T,N+1}(0) + \sum_{l=0}^N \hat{X}_l^N \mathcal{T}_{T,l}(0) \\ \mathcal{T}_{T,N+1}(0)X^N(0) &= \mathcal{T}_{T,N+1}(0)\hat{X}_{N+1}^N \mathcal{T}_{T,N+1}(0) + \mathcal{T}_{T,N+1}(0) \sum_{l=0}^N \hat{X}_l^N \mathcal{T}_{T,l}(0) \end{aligned}$$

$$\begin{aligned}
(-1)^{N+1}X_0 &= (-1)^{2N+2}\hat{X}_{N+1}^N + (-1)^{N+1}\sum_{l=0}^N\hat{X}_l^N(-1)^l \\
\hat{X}_{N+1}^N &= (-1)^{N+1}X_0 + \sum_{l=0}^N(-1)^{N+l}\hat{X}_l^N \\
&= (-1)^{N+1}X_0 + \sum_{l=0}^N(-1)^{N+l}\left(\sum_{j=0}^N\frac{2}{c_l(N+1)}X^N(t_{T,j}^N)\mathcal{T}_{T,l}(t_{T,j}^N)\right) \\
\therefore \hat{X}_{T,N+1}^N &= (-1)^{N+1}X_0 + \frac{2}{N+1}\sum_{l=0}^N\sum_{j=0}^N\frac{(-1)^{N+l}}{c_l}X^N(t_{T,j}^N)\mathcal{T}_{T,l}(t_{T,j}^N). \quad (3.18)
\end{aligned}$$

To derive the derivative term,  $\frac{d}{dt}X^N$ , for the equation, we consider the recurrence relation

$$\frac{d}{dt}\mathcal{T}_{T,l}(t) = \binom{l}{l-2}\frac{d}{dt}\mathcal{T}_{T,l-2}(t) + \frac{4(l)}{T}\mathcal{T}_{T,l-1}(t).$$

Due to the nature the Chebyshev polynomial, we divide  $l$  into two different cases.

**Case I**  $l$  is even,

$$\frac{d}{dt}\mathcal{T}_{T,2}(t) = 2\left(\frac{4}{T}\right)\mathcal{T}_{T,1}(t)$$

$$\frac{d}{dt}\mathcal{T}_{T,4}(t) = (2)\mathcal{T}_{T,2}(t) + 4\left(\frac{4}{T}\right)\mathcal{T}_{T,3}(t)$$

$$= \left[4\left(\frac{4}{T}\right)\mathcal{T}_{T,1}(t)\right] + \left[4\left(\frac{4}{T}\right)\mathcal{T}_{T,3}(t)\right]$$

$$\frac{d}{dt}\mathcal{T}_{T,6}(t) = \left(\frac{6}{4}\right)\mathcal{T}_{T,4}(t) + 6\left(\frac{4}{T}\right)\mathcal{T}_{T,5}(t)$$

$$= \frac{6}{4}\left[4\left(\frac{4}{T}\right)\mathcal{T}_{T,1}(t) + 4\left(\frac{4}{T}\right)\mathcal{T}_{T,3}(t)\right] + \left[6\left(\frac{4}{T}\right)\mathcal{T}_{T,5}(t)\right]$$

$$= \left[6\left(\frac{4}{T}\right)\mathcal{T}_{T,1}(t)\right] + \left[6\left(\frac{4}{T}\right)\mathcal{T}_{T,3}(t)\right] + \left[6\left(\frac{4}{T}\right)\mathcal{T}_{T,5}(t)\right]$$

$$\frac{d}{dt}\mathcal{T}_{T,8}(t) = \left(\frac{8}{6}\right)\mathcal{T}_{T,6}(t) + 8\left(\frac{4}{T}\right)\mathcal{T}_{T,7}(t)$$

$$= \frac{8}{6}\left[6\left(\frac{4}{T}\right)\mathcal{T}_{T,1}(t) + 6\left(\frac{4}{T}\right)\mathcal{T}_{T,3}(t) + 6\left(\frac{4}{T}\right)\mathcal{T}_{T,5}(t)\right] + \left[8\left(\frac{4}{T}\right)\mathcal{T}_{T,7}(t)\right]$$

$$= \left[8\left(\frac{4}{T}\right)\mathcal{T}_{T,1}(t)\right] + \left[8\left(\frac{4}{T}\right)\mathcal{T}_{T,3}(t)\right] + \left[8\left(\frac{4}{T}\right)\mathcal{T}_{T,5}(t)\right] + \left[8\left(\frac{4}{T}\right)\mathcal{T}_{T,7}(t)\right]$$

$$\frac{d}{dt}\mathcal{T}_{T,10}(t) = \left(\frac{10}{8}\right)\mathcal{T}_{T,8}(t) + 10\left(\frac{4}{T}\right)\mathcal{T}_{T,9}(t)$$

$$\begin{aligned}
&= \frac{10}{8} \left[ 8 \left( \frac{4}{T} \right) \mathcal{T}_{T,1}(t) + 8 \left( \frac{4}{T} \right) \mathcal{T}_{T,3}(t) + 8 \left( \frac{4}{T} \right) \mathcal{T}_{T,5}(t) + 8 \left( \frac{4}{T} \right) \mathcal{T}_{T,7}(t) \right] \\
&+ \left[ 10 \left( \frac{4}{T} \right) \mathcal{T}_{T,9}(t) \right] \\
&= \left[ 10 \left( \frac{4}{T} \right) \mathcal{T}_{T,1}(t) \right] + \left[ 10 \left( \frac{4}{T} \right) \mathcal{T}_{T,3}(t) \right] + \left[ 10 \left( \frac{4}{T} \right) \mathcal{T}_{T,5}(t) \right] \\
&+ \left[ 10 \left( \frac{4}{T} \right) \mathcal{T}_{T,7}(t) \right] + \left[ 10 \left( \frac{4}{T} \right) \mathcal{T}_{T,9}(t) \right] \\
&\therefore \frac{d}{dt} \mathcal{T}_{T,l}(t) = \sum_{m=1}^{\frac{l}{2}} (l) \left( \frac{4}{T} \right) \mathcal{T}_{T,l-(2m-1)}(t), \quad l = 2, 4, 6, \dots
\end{aligned}$$

**Case II** We consider  $l$  is odd,

$$\begin{aligned}
\frac{d}{dt} \mathcal{T}_{T,1}(t) &= \left( \frac{2}{T} \right) \mathcal{T}_{T,0}(t) \\
\frac{d}{dt} \mathcal{T}_{T,3}(t) &= (3) \mathcal{T}_{T,1}(t) + \left[ 3 \left( \frac{4}{T} \right) \mathcal{T}_{T,2}(t) \right] \\
&= \left[ 3 \left( \frac{2}{T} \right) \mathcal{T}_{T,0}(t) \right] + \left[ 3 \left( \frac{4}{T} \right) \mathcal{T}_{T,2}(t) \right] \\
\frac{d}{dt} \mathcal{T}_{T,5}(t) &= \left( \frac{5}{3} \right) \mathcal{T}_{T,3}(t) + \left[ 5 \left( \frac{4}{T} \right) \mathcal{T}_{T,4}(t) \right] \\
&= \frac{5}{3} \left[ 3 \left( \frac{2}{T} \right) \mathcal{T}_{T,0}(t) + 3 \left( \frac{4}{T} \right) \mathcal{T}_{T,2}(t) \right] + \left[ 5 \left( \frac{4}{T} \right) \mathcal{T}_{T,4}(t) \right] \\
&= \left[ 5 \left( \frac{2}{T} \right) \mathcal{T}_{T,0}(t) \right] + \left[ 5 \left( \frac{4}{T} \right) \mathcal{T}_{T,2}(t) \right] + \left[ 5 \left( \frac{4}{T} \right) \mathcal{T}_{T,4}(t) \right] \\
\frac{d}{dt} \mathcal{T}_{T,7}(t) &= \left( \frac{7}{5} \right) \mathcal{T}_{T,5}(t) + \left[ 7 \left( \frac{4}{T} \right) \mathcal{T}_{T,6}(t) \right] \\
&= \frac{7}{5} \left[ 5 \left( \frac{2}{T} \right) \mathcal{T}_{T,0}(t) + 5 \left( \frac{4}{T} \right) \mathcal{T}_{T,2}(t) + 5 \left( \frac{4}{T} \right) \mathcal{T}_{T,4}(t) \right] + \left[ 7 \left( \frac{4}{T} \right) \mathcal{T}_{T,6}(t) \right] \\
&= \left[ 7 \left( \frac{2}{T} \right) \mathcal{T}_{T,0}(t) \right] + \left[ 7 \left( \frac{4}{T} \right) \mathcal{T}_{T,2}(t) \right] + \left[ 7 \left( \frac{4}{T} \right) \mathcal{T}_{T,4}(t) \right] + \left[ 7 \left( \frac{4}{T} \right) \mathcal{T}_{T,6}(t) \right] \\
\frac{d}{dt} \mathcal{T}_{T,9}(t) &= \left( \frac{9}{7} \right) \mathcal{T}_{T,7}(t) + \left[ 9 \left( \frac{4}{T} \right) \mathcal{T}_{T,8}(t) \right] \\
&= \frac{9}{7} \left[ 7 \left( \frac{2}{T} \right) \mathcal{T}_{T,0}(t) + 7 \left( \frac{4}{T} \right) \mathcal{T}_{T,2}(t) + 7 \left( \frac{4}{T} \right) \mathcal{T}_{T,4}(t) + 7 \left( \frac{4}{T} \right) \mathcal{T}_{T,6}(t) \right] \\
&+ \left[ 9 \left( \frac{4}{T} \right) \mathcal{T}_{T,8}(t) \right]
\end{aligned}$$

$$\begin{aligned}
&= \left[ 9 \left( \frac{2}{T} \right) \mathcal{T}_{T,0}(t) \right] + \left[ 9 \left( \frac{4}{T} \right) \mathcal{T}_{T,2}(t) \right] + \left[ 9 \left( \frac{4}{T} \right) \mathcal{T}_{T,4}(t) \right] \\
&+ \left[ 9 \left( \frac{4}{T} \right) \mathcal{T}_{T,6}(t) \right] + \left[ 9 \left( \frac{4}{T} \right) \mathcal{T}_{T,8}(t) \right] \\
\therefore \frac{d}{dt} \mathcal{T}_{T,l}(t) &= \left( \sum_{m=1}^{\frac{l-1}{2}} (l) \left( \frac{4}{T} \right) \mathcal{T}_{T,l-(2m-1)}(t) \right) + \frac{2(l)}{T}, \quad l = 1, 3, 5, \dots
\end{aligned}$$

Hence, we use (3.17) and (3.18) to obtain

$$\begin{aligned}
\frac{d}{dt} X^N(t) &= \sum_{l=1}^{N+1} \hat{X}_l^N \frac{d}{dt} \mathcal{T}_{T,l}(t) \\
&= \hat{X}_{N+1}^N \frac{d}{dt} \mathcal{T}_{T,N+1}(t) + \sum_{l=1}^N \hat{X}_l^N \frac{d}{dt} \mathcal{T}_{T,l}(t) \\
&= \left( (-1)^{N+1} X_0 + \frac{2}{N+1} \sum_{l=0}^N \sum_{j=0}^N \frac{(-1)^{N+l}}{c_l} X^N(t_{T,j}^N) \mathcal{T}_{T,l}(t_{T,j}^N) \right) \frac{d}{dt} \mathcal{T}_{T,N+1}(t) \\
&+ \left( \sum_{l=1}^N \sum_{j=0}^N \frac{2}{(N+1)c_l} X^N(t_{T,j}^N) \mathcal{T}_{T,l}(t_{T,j}^N) \right) \frac{d}{dt} \mathcal{T}_{T,l}(t) \\
&= (-1)^{N+1} X_0 \frac{d}{dt} \mathcal{T}_{T,N+1}(t) + \left( \sum_{l=1}^N \sum_{j=0}^N \frac{2}{(N+1)c_l} X^N(t_{T,j}^N) \mathcal{T}_{T,l}(t_{T,j}^N) \right) \frac{d}{dt} \mathcal{T}_{T,l}(t) \\
&+ \frac{2}{N+1} \left( \sum_{l=0}^N \sum_{j=0}^N \frac{(-1)^{N+l}}{c_l} X^N(t_{T,j}^N) \mathcal{T}_{T,l}(t_{T,j}^N) \right) \frac{d}{dt} \mathcal{T}_{T,N+1}(t).
\end{aligned}$$

We consider  $N$  into two different cases,

**Case**  $N$  is odd and  $l$  is even

$$\begin{aligned}
\frac{d}{dt} X^N(t) &= \sum_{l=1}^{N+1} \hat{X}_l^N \frac{d}{dt} \mathcal{T}_{T,l}(t) = \hat{X}_{N+1}^N \frac{d}{dt} \mathcal{T}_{T,N+1}(t) + \sum_{l=1}^N \hat{X}_l^N \frac{d}{dt} \mathcal{T}_{T,l}(t) \\
&= \left( (-1)^{N+1} X_0 + \frac{2}{N+1} \sum_{l=0}^N \sum_{j=0}^N \frac{(-1)^{N+l}}{c_l} X^N(t_{T,j}^N) \mathcal{T}_{T,l}(t_{T,j}^N) \right) \\
&\times \left( \frac{4}{T} \sum_{m=1}^{\frac{N+1}{2}} (N+1) \mathcal{T}_{T,N-(2m-2)}(t_{T,k}^N) \right) + \left( \sum_{l=1}^N \sum_{j=0}^N \frac{2}{c_l(N+1)} X^N(t_{T,j}^N) \mathcal{T}_{T,l}(t_{T,j}^N) \right) \\
&\times \left( \frac{4}{T} \sum_{m=1}^{\frac{l}{2}} (l) \mathcal{T}_{T,l-(2m-1)}(t_{T,k}^N) \right)
\end{aligned}$$

$$\begin{aligned}
&= \left[ \frac{4(-1)^{N+1}X_0(N+1)}{T} \sum_{m=1}^{\frac{N+1}{2}} \mathcal{T}_{T,N-(2m-2)}(t_{T,k}^N) \right] \\
&+ \frac{8}{T} \left[ \sum_{l=0}^N \sum_{j=0}^N \frac{(-1)^{N+l}}{c_l} X^N(t_{T,j}^N) \mathcal{T}_{T,l}(t_{T,j}^N) \left( \sum_{m=1}^{\frac{N+1}{2}} \mathcal{T}_{T,N-(2m-2)}(t_{T,k}^N) \right) \right] \\
&+ \frac{8}{T(N+1)} \left[ \sum_{l=1}^N \sum_{j=0}^N \frac{1}{c_l} X^N(t_{T,j}^N) \mathcal{T}_{T,l}(t_{T,j}^N) \left( \sum_{m=1}^{\frac{l}{2}} (l) \mathcal{T}_{T,l-(2m-1)}(t_{T,k}^N) \right) \right]
\end{aligned}$$

**Case**  $N$  is odd and  $l$  is odd

$$\begin{aligned}
\frac{d}{dt}X^N(t) &= \sum_{l=1}^{N+1} \hat{X}_l^N \frac{d}{dt} \mathcal{T}_{T,l}(t) = \hat{X}_{N+1}^N \frac{d}{dt} \mathcal{T}_{T,N+1}(t) + \sum_{l=1}^N \hat{X}_l^N \frac{d}{dt} \mathcal{T}_{T,l}(t) \\
&= \left( (-1)^{N+1}X_0 + \frac{2}{N+1} \sum_{l=0}^N \sum_{j=0}^N \frac{(-1)^{N+l}}{c_l} X^N(t_{T,j}^N) \mathcal{T}_{T,l}(t_{T,j}^N) \right) \\
&\times \left( \frac{4}{T} \sum_{m=1}^{\frac{N+1}{2}} (N+1) \mathcal{T}_{T,N-(2m-2)}(t_{T,k}^N) \right) + \left( \sum_{l=1}^N \sum_{j=0}^N \frac{2}{c_l(N+1)} X^N(t_{T,j}^N) \mathcal{T}_{T,l}(t_{T,j}^N) \right) \\
&\times \left( \left( \frac{4}{T} \sum_{m=1}^{\frac{l-1}{2}} (l) \mathcal{T}_{T,N-(2m-2)}(t_{T,k}^N) \right) + \frac{2(l)}{T} \right) \\
&= \left[ \frac{4(-1)^{N+1}X_0(N+1)}{T} \sum_{m=1}^{\frac{N+1}{2}} \mathcal{T}_{T,N-(2m-2)}(t_{T,k}^N) \right] \\
&+ \frac{8}{T} \sum_{l=0}^N \sum_{j=0}^N \frac{(-1)^{N+l}}{c_l} X^N(t_{T,j}^N) \mathcal{T}_{T,l}(t_{T,j}^N) \left( \sum_{m=1}^{\frac{N+1}{2}} \mathcal{T}_{T,N-(2m-2)}(t_{T,k}^N) \right) \\
&+ \frac{8}{T(N+1)} \sum_{l=1}^N \sum_{j=0}^N \frac{1}{c_l} X^N(t_{T,j}^N) \mathcal{T}_{T,l}(t_{T,j}^N) \left( \left( \sum_{m=1}^{\frac{l-1}{2}} (l) \mathcal{T}_{T,l-(2m-1)}(t_{T,k}^N) \right) + \frac{l}{2} \right).
\end{aligned}$$

**Case**  $N$  is even and  $l$  is even

$$\begin{aligned}
\frac{d}{dt}X^N(t) &= \sum_{l=1}^{N+1} \hat{X}_l^N \frac{d}{dt} \mathcal{T}_{T,l}(t) = \hat{X}_{N+1}^N \frac{d}{dt} \mathcal{T}_{T,N+1}(t) + \sum_{l=1}^N \hat{X}_l^N \frac{d}{dt} \mathcal{T}_{T,l}(t) \\
&= \left( (-1)^{N+1}X_0 + \frac{2}{N+1} \sum_{l=0}^N \sum_{j=0}^N \frac{(-1)^{N+l}}{c_l} X^N(t_{T,j}^N) \mathcal{T}_{T,l}(t_{T,j}^N) \right) \\
&\times \left( \left( \frac{4}{T} \sum_{m=1}^{\frac{N}{2}} (N+1) \mathcal{T}_{T,N-(2m-2)}(t_{T,k}^N) \right) + \frac{2(N+1)}{T} \right)
\end{aligned}$$



$$\begin{aligned}
& + \left( \sum_{l=1}^N \sum_{j=0}^N \frac{2}{c_l(N+1)} X^N(t_{T,j}^N) \mathcal{T}_{T,l}(t_{T,j}^N) \right) \times \left( \frac{4}{T} \sum_{m=1}^{\frac{l}{2}} (l) \mathcal{T}_{T,l-(2m-1)}(t_{T,k}^N) \right) \\
& = \left[ \frac{4(-1)^{N+1} X_0(N+1)}{T} \left( \left( \sum_{m=1}^{\frac{N}{2}} \mathcal{T}_{T,N-(2m-2)}(t_{T,k}^N) \right) + \frac{1}{2} \right) \right] \\
& + \frac{8}{T} \sum_{l=0}^N \sum_{j=0}^N \frac{(-1)^{N+l}}{c_l} X^N(t_{T,j}^N) \mathcal{T}_{T,l}(t_{T,j}^N) \left( \left( \sum_{m=1}^{\frac{N}{2}} \mathcal{T}_{T,N-(2m-2)}(t_{T,k}^N) \right) + \frac{1}{2} \right) \\
& + \frac{8}{T(N+1)} \sum_{l=1}^N \sum_{j=0}^N \frac{1}{c_l} X^N(t_{T,j}^N) \mathcal{T}_{T,l}(t_{T,j}^N) \left( \sum_{m=1}^{\frac{l}{2}} (l) \mathcal{T}_{T,l-(2m-1)}(t_{T,k}^N) \right).
\end{aligned}$$

Case  $N$  is even and  $l$  is odd

$$\begin{aligned}
\frac{d}{dt} X^N(t) & = \sum_{l=1}^{N+1} \hat{X}_l^N \frac{d}{dt} \mathcal{T}_{T,l}(t) = \hat{X}_{N+1}^N \frac{d}{dt} \mathcal{T}_{T,N+1}(t) + \sum_{l=1}^N \hat{X}_l^N \frac{d}{dt} \mathcal{T}_{T,l}(t) \\
& = \left( (-1)^{N+1} X_0 + \frac{2}{N+1} \sum_{l=0}^N \sum_{j=0}^N \frac{(-1)^{N+l}}{c_l} X^N(t_{T,j}^N) \mathcal{T}_{T,l}(t_{T,j}^N) \right) \\
& \times \left( \left( \frac{4}{T} \sum_{m=1}^{\frac{N}{2}} (N+1) \mathcal{T}_{T,N-(2m-2)}(t_{T,k}^N) \right) + \frac{2(N+1)}{T} \right) \\
& + \left( \sum_{l=1}^N \sum_{j=0}^N \frac{2}{c_l(N+1)} X^N(t_{T,j}^N) \mathcal{T}_{T,l}(t_{T,j}^N) \right) \\
& \times \left( \left( \frac{4}{T} \sum_{m=1}^{\frac{l-1}{2}} (l) \mathcal{T}_{T,l-(2m-1)}(t_{T,k}^N) \right) + \frac{2(l)}{T} \right) \\
& = \left[ \frac{4(-1)^{N+1} X_0(N+1)}{T} \left( \left( \sum_{m=1}^{\frac{N}{2}} \mathcal{T}_{T,N-(2m-2)}(t_{T,k}^N) \right) + \frac{1}{2} \right) \right] \\
& + \frac{8}{T} \sum_{l=0}^N \sum_{j=0}^N \frac{(-1)^{N+l}}{c_l} X^N(t_{T,j}^N) \mathcal{T}_{T,l}(t_{T,j}^N) \left( \left( \sum_{m=1}^{\frac{N}{2}} \mathcal{T}_{T,N-(2m-2)}(t_{T,k}^N) \right) + \frac{1}{2} \right) \\
& + \frac{8}{T(N+1)} \sum_{l=1}^N \sum_{j=0}^N \frac{1}{c_l} X^N(t_{T,j}^N) \mathcal{T}_{T,l}(t_{T,j}^N) \left( \left( \sum_{m=1}^{\frac{l-1}{2}} (l) \mathcal{T}_{T,l-(2m-1)}(t_{T,k}^N) \right) + \frac{l}{2} \right).
\end{aligned}$$

For simplicity, we let

$$\begin{aligned}
 a_{k,j}^N = \frac{8}{N+1} \left( \sum_{l=1}^N \frac{1}{c_l} \mathcal{T}_{T,l}(t_{T,j}^N) \right) \times & \begin{cases} \sum_{m=1}^{\frac{l}{2}} (l) \mathcal{T}_{T,l-(2m-1)}(t_{T,k}^N), & l \text{ is even} \\ \left( \sum_{m=1}^{\frac{l-1}{2}} (l) \mathcal{T}_{T,l-(2m-1)}(t_{T,k}^N) \right) + \frac{l}{2}, & l \text{ is odd} \end{cases} \\
 + 8 \left( \sum_{l=0}^N \frac{(-1)^{N+l}}{c_l} \mathcal{T}_{T,l}(t_{T,j}^N) \right) \times & \begin{cases} \sum_{m=1}^{\frac{N+1}{2}} \mathcal{T}_{T,N-(2m-2)}(t_{T,k}^N), & N \text{ is odd} \\ \left( \sum_{m=1}^{\frac{N}{2}} \mathcal{T}_{T,N-(2m-2)}(t_{T,k}^N) \right) + \frac{1}{2}, & N \text{ is even} \end{cases}
 \end{aligned} \tag{3.19a}$$

and

$$b_k^N = (4(N+1)(-1)^{N+1}) \times \begin{cases} \sum_{m=1}^{\frac{N+1}{2}} \mathcal{T}_{T,N-(2m-2)}(t_{T,k}^N), & N \text{ is odd} \\ \left( \sum_{m=1}^{\frac{N}{2}} \mathcal{T}_{T,N-(2m-2)}(t_{T,k}^N) \right) + \frac{1}{2}, & N \text{ is even.} \end{cases} \tag{3.19b}$$

Therefore,

$$\frac{d}{dt} X^N(t_{T,k}) = \frac{1}{T} \sum_{j=0}^N a_{k,j}^N X^N(t_{T,j}^N) + \frac{X_0}{T} b_k^N, \quad 0 \leq k \leq N. \tag{3.20}$$

Substituting (3.20) into the left hand side of (3.15) yields the following matrix equation of (3.20)

$$A^N \mathbf{X}^N = (T) F^N(\mathbf{X}^N) - X_0 b^N. \tag{3.21}$$

where  $A^N$  is the matrix with the entries  $a_{k,j}^N$ ,  $0 \leq j, k \leq N$ , given in (3.19a),

$$\begin{aligned}
 \mathbf{X}^N &= (X^N(t_{T,0}^N), X^N(t_{T,1}^N), \dots, X^N(t_{T,N}^N))^T, \\
 F^N(\mathbf{X}^N) &= (f(X^N(t_{T,0}^N), t_{T,0}^N), f(X^N(t_{T,1}^N), t_{T,1}^N), \dots, f(X^N(t_{T,N}^N), t_{T,N}^N))^T, \\
 b^N &= (b_0^N, b_1^N, \dots, b_N^N)^T.
 \end{aligned}$$

We solve this system for the solution  $\mathbf{X}^N = (X^N(t_{T,0}^N), X^N(t_{T,1}^N), \dots, X^N(t_{T,N}^N))^T$ .

The last step of our algorithm is to determine  $X^N(t)$  at the right end (or  $X^N(T)$ ). This value will be used as the initial value of the consecutive interval when considering a domain decomposition. To compute  $X^N(t)$ , we use the values of  $\{X^N(t_{T,k}^N)\}_{k=0}^N$  which are obtained from (3.21) together with (3.18). Since  $\mathcal{T}_{T,l}(T) = 1$ , we get

$$\begin{aligned}
X^N(T) &= \sum_{l=0}^{N+1} \hat{X}_l \\
&= \hat{X}_{N+1} + \sum_{l=0}^N \hat{X}_l \\
&= \left[ (-1)^{N+1} X_0 + \frac{2}{N+1} \sum_{l=0}^N \sum_{j=0}^N \frac{(-1)^{N+1}}{c_l} X^N(t_{T,j}^N) \mathcal{T}_{T,l}(t_{T,j}^N) \right] \\
&\quad + \left[ \sum_{l=0}^N \sum_{j=0}^N \frac{2}{c_l(N+1)} X^N(t_{T,j}^N) \mathcal{T}_{T,l}(t_{T,j}^N) \right] \\
&= (-1)^{N+1} X_0 + \left[ \frac{2}{N+1} \sum_{l=0}^N \sum_{j=0}^N \frac{((-1)^{N+l} + 1)}{c_l} X^N(t_{T,j}^N) \mathcal{T}_{T,l}(t_{T,j}^N) \right].
\end{aligned} \tag{3.22}$$

### 3.3.1 Single interval Domain

For the domain containing only one interval, we apply the algorithm in (3.21) directly. The scheme (3.21) is an implicit scheme. We apply an iterative method to solve the system.

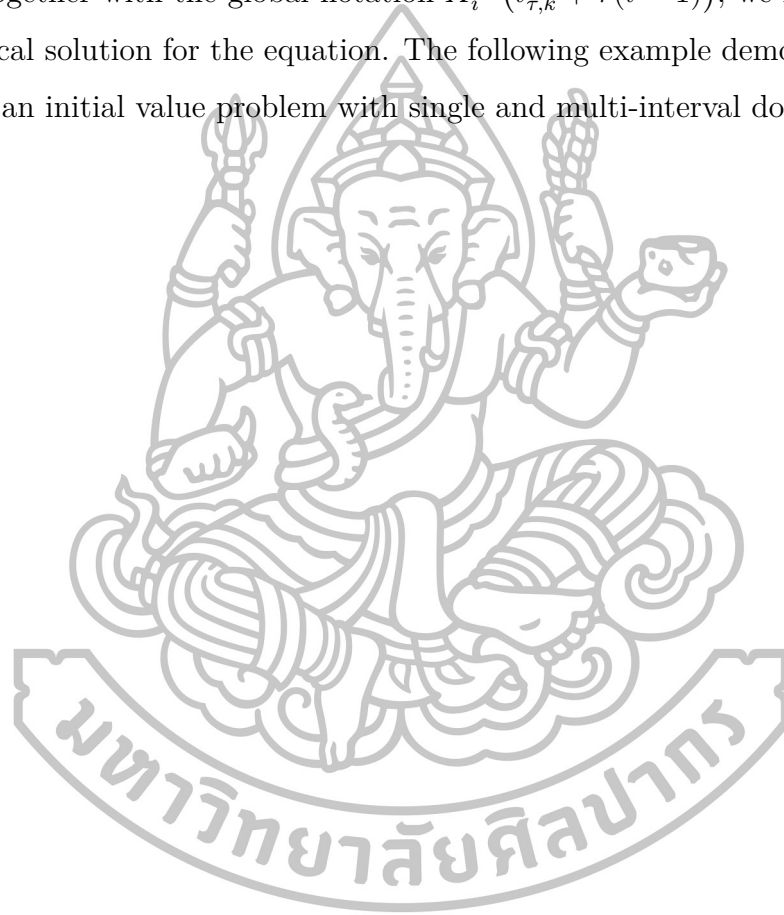
### 3.3.2 Multi-interval Domain

For the domain decomposition, we break the domain  $[0, T]$  into  $M$  subintervals where each of which is of length  $\tau = \frac{T}{M}$ . We first evaluate the solution  $X_1^N(t)$  on the first subinterval  $[0, \tau]$  with the given initial condition  $X(0) = X_0$ . Then, we compute the end point value of  $X_1^N(\tau)$  and set it as the initial condition for the next subinterval. By continuing the process, the solution on the  $i$ -th interval can

be evaluated by finding  $X_i^N(t) \in \mathcal{P}_{2N+1}(0, \tau)$ ,  $2 \leq i \leq M$  such that

$$\begin{cases} \frac{d}{dt} X_i^N(t_{\tau,k}^N) = f(X_i^N(t_{\tau,k}^N), \tau(i-1) + t_{\tau,k}^N), & 0 \leq k \leq N, 2 \leq i \leq M \\ X_i^N(0) = X_{i-1}^N(\tau). \end{cases} \quad (3.23)$$

The value of  $X_i^N(t_{\tau,k}^N)$  is the local value for each subinterval. Patching all the solutions together with the global notation  $X_i^N(t_{\tau,k}^N + \tau(i-1))$ , we finally arrive the numerical solution for the equation. The following example demonstrates the solution of an initial value problem with single and multi-interval domains.



## Chapter 4

# Error analysis of the Chebyshev-Gauss collocation method

In this chapter, we analyze the error of the solution obtained from scheme (3.15). The error analysis has been completed by Yang et al. in [35]. We will follow their proof in detail in this chapter. We first compare the numerical solution  $X^N(t)$  with the Chebyshev-Gauss interpolation  $\mathcal{I}_{T,N}X(t)$ . Let

$$G_1^N(t) = \mathcal{I}_{T,N} \frac{d}{dt} X(t) - \frac{d}{dt} \mathcal{I}_{T,N} X(t).$$

Then,

$$\frac{d}{dt} \mathcal{I}_{T,N} X(t) = \mathcal{I}_{T,N} \frac{d}{dt} X(t) - G_1^N(t).$$

At  $t = t_{T,j}^N$ ,

$$\begin{aligned} \frac{d}{dt} \mathcal{I}_{T,N} X(t_{T,j}^N) &= \mathcal{I}_{T,N} \frac{d}{dt} X(t_{T,j}^N) - G_1^N(t_{T,j}^N) \\ &\stackrel{(3.15)}{=} \mathcal{I}_{T,N} f(X(t_{T,j}^N), t_{T,j}^N) - G_1^N(t_{T,j}^N) \\ &\stackrel{(3.9)}{=} f(\mathcal{I}_{T,N} X(t_{T,j}^N), t_{T,j}^N) - G_1^N(t_{T,j}^N), \quad 0 \leq j \leq N. \end{aligned} \quad (4.1)$$

Let  $E^N(t) = X^N(t) - \mathcal{I}_{T,N}X(t)$ . Then  $\frac{d}{dt} E^N(t) = \frac{d}{dt} X^N(t) - \frac{d}{dt} \mathcal{I}_{T,N}X(t)$ .

$$\therefore \frac{d}{dt} E^N(t_{T,j}^N) = \frac{d}{dt} X^N(t_{T,j}^N) - \frac{d}{dt} \mathcal{I}_{T,N}X(t_{T,j}^N).$$

Using (3.15) and (4.1),

$$\begin{aligned} \frac{d}{dt} E^N(t_{T,j}^N) &= f(X(t_{T,j}^N), t_{T,j}^N) - (f(\mathcal{I}_{T,N}X(t_{T,j}^N), t_{T,j}^N) - G_1^N(t_{T,j}^N)) \\ &= f(X(t_{T,j}^N), t_{T,j}^N) - f(\mathcal{I}_{T,N}X(t_{T,j}^N), t_{T,j}^N) + G_1^N(t_{T,j}^N). \end{aligned}$$

Moreover, we let  $G_2^N(t_{T,j}^N) = f(X^N(t_{T,j}^N), t_{T,j}^N) - f(\mathcal{I}_{T,N}X(t_{T,j}^N), t_{T,j}^N)$ . The equation (3.15) becomes

$$\begin{cases} \frac{d}{dt}E^N(t_{T,j}^N) = G_1^N(t_{T,j}^N) + G_2^N(t_{T,j}^N), & 0 \leq j \leq N \\ E^N(0) = X_0 - \mathcal{I}_{T,N}X(0). \end{cases} \quad (4.2)$$

We define  $R_N(t) = t^{-1}(E^N(t) - E^N(0))$ . Obviously,  $tR_N(t) \in \mathcal{P}_N(0, T)$ ,

$$\begin{aligned} tR_N(t) &= E^N(t) - E^N(0) \\ E^N(t) &= tR_N(t) + E^N(0) \\ \frac{d}{dt}E^N(t) &= \frac{d}{dt}(tR_N(t)) + \frac{d}{dt}E^N(0) \\ \therefore \frac{d}{dt}E^N(t) &= \frac{d}{dt}(tR_N(t)). \end{aligned}$$

Multiplying (4.2) by  $2(T-t)\left(\frac{\pi}{N+1}\right)R_N(t_{T,j}^N)$  and sum from  $j = 0$  to  $N$ , we have

$$\begin{aligned} \sum_{j=0}^N 2(T-t)\left(\frac{\pi}{N+1}\right)R_N(t_{T,j}^N)\frac{d}{dt}E^N(t_{T,j}^N) &= \sum_{j=0}^N 2(T-t)\left(\frac{\pi}{N+1}\right)R_N(t_{T,j}^N)G_1^N(t_{T,j}^N) \\ &\quad + \sum_{j=0}^N 2(T-t)\left(\frac{\pi}{N+1}\right)R_N(t_{T,j}^N)G_2^N(t_{T,j}^N) \\ 2\left(\frac{\pi}{N+1}\right)\sum_{j=0}^N (T-t)R_N(t_{T,j}^N)\frac{d}{dt}E^N(t_{T,j}^N) &= 2\left(\frac{\pi}{N+1}\right)\sum_{j=0}^N (T-t)R_N(t_{T,j}^N)G_1^N(t_{T,j}^N) \\ &\quad + 2\left(\frac{\pi}{N+1}\right)\sum_{j=0}^N (T-t)R_N(t_{T,j}^N)G_2^N(t_{T,j}^N) \\ \therefore 2\left((T-t)R_N, \frac{d}{dt}E^N\right)_{T,N} &= A_1^N + A_2^N \end{aligned} \quad (4.3)$$

where  $A_1^N = 2(G_1^N, (T-t)R_N)_{T,N}$  and  $A_2^N = 2(G_2^N, (T-t)R_N)_{T,N}$ .

From (3.6a),

$$\begin{aligned} 2\left((T-t)R_N, \frac{d}{dt}E^N\right)_{T,N} &= 2\left((T-t)R_N, \frac{d}{dt}(tR_N(t))\right)_{T,N} \\ 2\left((T-t)R_N, \frac{d}{dt}(tR_N(t))\right)_{T,N} &\stackrel{(3.6a)}{=} 2\left((T-t)R_N, \frac{d}{dt}(tR_N(t))\right)_T \\ &= 2\int_0^T (T-t)R_N(t)\left(\frac{d}{dt}(tR_N(t))\right)\left(\frac{1}{\sqrt{t(T-t)}}\right)dt \end{aligned}$$

$$\begin{aligned}
&= 2 \int_0^T (T-t)R_N(t) \left( t \frac{d}{dt} R_N(t) + R_N(t) \right) \left( \frac{1}{\sqrt{t(T-t)}} \right) dt \\
&= 2 \int_0^T R_N(t) \left( \frac{t(T-t)}{\sqrt{t(T-t)}} \right) \frac{d}{dt} R_N(t) dt + 2 \int_0^T R_N^2(t) \left( \frac{T-t}{\sqrt{t(T-t)}} \right) dt \\
&= 2 \int_0^T R_N(t) \left( \sqrt{t(T-t)} \right) \frac{d}{dt} R_N(t) dt + 2 \int_0^T R_N^2(t) \left( \frac{T-t}{\sqrt{t(T-t)}} \right) dt.
\end{aligned}$$

By integrating by parts, we have

$$\begin{aligned}
2 \left( (T-t)R_N, \frac{d}{dt} E^N \right)_{T,N} &= 2 \left( \left[ \frac{R_N^2(t)}{2} \left( \sqrt{t(T-t)} \right) \right]_0^T - \int_0^T \frac{R_N^2(t)}{2} \left( \frac{T-2t}{2\sqrt{t(T-t)}} \right) dt \right) \\
&\quad + 2 \int_0^T R_N^2(t) \left( \frac{T-t}{\sqrt{t(T-t)}} \right) dt \\
&= 2 \int_0^T R_N^2(t) \left( \frac{T-t}{\sqrt{t(T-t)}} \right) dt - \int_0^T R_N^2(t) \left( \frac{T-2t}{2\sqrt{t(T-t)}} \right) dt \\
&= \int_0^T R_N^2(t) \left( \frac{1}{\sqrt{t(T-t)}} \right) \left( 2T-2t - \frac{T}{2} + t \right) dt \\
&= \int_0^T R_N^2(t) \left( \frac{1}{\sqrt{t(T-t)}} \right) \left( \frac{3}{2}T - t \right) dt \\
&= \frac{3}{2} \int_0^T R_N^2(t) \left( \frac{T}{\sqrt{t(T-t)}} \right) dt - \int_0^T R_N^2(t) \left( \frac{t}{\sqrt{t(T-t)}} \right) dt \\
&\geq \frac{3}{2} \int_0^T R_N^2(t) \left( \frac{T}{\sqrt{t(T-t)}} \right) dt - \int_0^T R_N^2(t) \left( \frac{T}{\sqrt{t(T-t)}} \right) dt \\
&= \left( \frac{3T}{2} - T \right) \int_0^T R_N^2(t) \left( \frac{1}{\sqrt{t(T-t)}} \right) dt \\
&= \frac{T}{2} \int_0^T R_N^2(t) \left( \frac{1}{\sqrt{t(T-t)}} \right) dt \\
&= \frac{T}{2} \|R_N\|_T^2.
\end{aligned}$$

Therefore,

$$2 \left( (T-t)R_N, \frac{d}{dt} E^N \right)_{T,N} \geq \frac{T}{2} \|R_N\|_T^2. \quad (4.4)$$

Because of  $G_1^N(t) \in \mathcal{P}_N(0, T)$  and (3.6a), it follows that, for any  $\epsilon > 0$ ,

$$|A_1^N| = |2(G_1^N, (T-t)R_N)_{T,N}|$$

$$\begin{aligned}
& \stackrel{(3.6a)}{=} |2(G_1^N, (T-t)R_N)_T| \\
& \leq 2 \int_0^T |G_1^N(T-t)R_N| dt \\
& \leq 2 \|G_1^N\|_T \|(T-t)R_N\|_T \quad (\text{by Cauchy-Schwarz Inequality [8, 25]}) \\
& \leq 2 \left( \frac{\epsilon}{2T} \|(T-t)R_N\|_T^2 + \frac{T}{2\epsilon} \|G_1^N\|_T^2 \right) \quad (\text{by Peter-Paul Inequality [25]}) \\
& = \frac{\epsilon}{T} \|(T-t)R_N\|_T^2 + \frac{T}{\epsilon} \|G_1^N\|_T^2 \\
& \leq \frac{\epsilon}{T} \|TR_N\|_T^2 + \frac{T}{\epsilon} \|G_1^N\|_T^2 \\
& = \epsilon T \|R_N\|_T^2 + \frac{T}{\epsilon} \|G_1^N\|_T^2 \\
\therefore |A_1^N| & \leq \epsilon T \|t^{-1} (E^N(t) - E^N(0))\|_T^2 + \frac{T}{\epsilon} \|G_1^N\|_T^2. \tag{4.5}
\end{aligned}$$

The above together with (4.3) and (4.4) leads to

$$\begin{aligned}
\frac{T}{2} \|R_N\|_T^2 & \stackrel{(4.4)}{\leq} 2 \left\| (T-t)R_N, \frac{d}{dt} E^N \right\|_{T,N} \\
\frac{T}{2} \|t^{-1} (E^N(t) - E^N(0))\|_T^2 & \leq 2 \left\| (T-t)R_N, \frac{d}{dt} E^N \right\|_{T,N} \\
\frac{T}{2} \|t^{-1} (E^N(t) - E^N(0))\|_T^2 & \stackrel{(4.3)}{\leq} A_1^N + A_2^N \\
\frac{T}{2} \|t^{-1} (E^N(t) - E^N(0))\|_T^2 & \stackrel{(4.5)}{\leq} \epsilon T \|t^{-1} (E^N(t) - E^N(0))\|_T^2 + \frac{T}{\epsilon} \|G_1^N\|_T^2 + A_2^N \\
\left( \frac{T}{2} - \epsilon T \right) \|t^{-1} (E^N(t) - E^N(0))\|_T^2 & \leq \frac{T}{\epsilon} \|G_1^N\|_T^2 + A_2^N \\
\therefore \left( \frac{1}{2} - \epsilon \right) T \|t^{-1} (E^N(t) - E^N(0))\|_T^2 & \leq \frac{T}{\epsilon} \|G_1^N\|_T^2 + A_2^N. \tag{4.6}
\end{aligned}$$

We would like to estimate the error of  $X$  at the end point  $t = T$ . We start with the estimation of  $\|G_1^N\|_T$ . Let  $\mathcal{I}_N$  be the Chebyshev-Gauss interpolation on the interval  $(-1, 1)$  and  $\chi(t) = 1 - t^2$ . According to a standard interpolation error [13] with  $\alpha = \beta = \gamma = \delta = -\frac{1}{2}$ , for any  $v \in H_{\chi^{r-\frac{1}{2}}}^r(-1, 1)$  and integer  $1 \leq r \leq N + 1$ ,

$$\|\mathcal{I}_N v - v\|_{L^2_{\chi^{-\frac{1}{2}}}(-1,1)}^2 \leq cN^{-2r} \int_{-1}^1 \chi^{r-\frac{1}{2}} \left( \frac{d^r}{dt^r} v(t) \right)^2 dt.$$

Furthermore, by a standard interpolation error [13] with  $\alpha = \beta = -\frac{1}{2}$ , for any  $v \in H_{\chi^{r-\frac{3}{2}}}^r(-1, 1)$  and integer  $2 \leq r \leq N + 1$ ,



$$\left\| \frac{d}{dt} (\mathcal{I}_N v - v) \right\|_{L^2_{x^{-\frac{1}{2}}(-1,1)}}^2 \leq cN^{4-2r} \int_{-1}^1 \chi^{r-\frac{3}{2}} \left( \frac{d^r}{dt^r} v(t) \right)^2 dt.$$

where  $c$  is a generic positive constant independent of  $T, N$  and any function.

For the shift Chebyshev polynomial on  $[0, T]$ , we have

$$\|\mathcal{I}_{T,N} v - v\|_T^2 \leq cN^{-2r} \int_0^T \omega^{r-\frac{1}{2}}(t) \left( \frac{d^r}{dt^r} v(t) \right)^2 dt. \quad (4.7)$$

$$\left\| \frac{d}{dt} (\mathcal{I}_{T,N} v - v) \right\|_T^2 \leq cN^{4-2r} \int_0^T \omega^{r-\frac{3}{2}}(t) \left( \frac{d^r}{dt^r} v(t) \right)^2 dt. \quad (4.8)$$

Furthermore, by (4.7) with  $v = \frac{d}{dt} X(t)$  and  $r = r - 1$ , for  $2 \leq r \leq N + 2$ , we obtain

$$\begin{aligned} \left\| \mathcal{I}_{T,N} \frac{d}{dt} X - \frac{d}{dt} X \right\|_T^2 &\leq cN^{-2(r-1)} \int_0^T \omega^{(r-\frac{1}{2})-1}(t) \left( \frac{d^{r-1}}{dt^{r-1}} \left( \frac{d}{dt} X(t) \right) \right)^2 dt \\ &\leq cN^{-2r-2} \int_0^T \omega^{r-\frac{3}{2}}(t) \left( \frac{d^r}{dt^r} X(t) \right)^2 dt. \end{aligned} \quad (4.9)$$

Therefore,

$$\begin{aligned} \|G_1^N\|_T^2 &= \int_0^T \left| \mathcal{I}_{T,N} \frac{d}{dt} X - \frac{d}{dt} \mathcal{I}_{T,N} X \right|^2 dt \\ &= \int_0^T \left| \mathcal{I}_{T,N} \frac{d}{dt} X - \frac{d}{dt} \mathcal{I}_{T,N} X + \frac{d}{dt} X - \frac{d}{dt} X \right|^2 dt \\ &= \int_0^T \left| \left( \mathcal{I}_{T,N} \frac{d}{dt} X - \frac{d}{dt} X \right) + \left( -\frac{d}{dt} \mathcal{I}_{T,N} X + \frac{d}{dt} X \right) \right|^2 dt \\ &= \left\| \left( \mathcal{I}_{T,N} \frac{d}{dt} X - \frac{d}{dt} X \right) + \left( -\frac{d}{dt} \mathcal{I}_{T,N} X + \frac{d}{dt} X \right) \right\|_T^2 \\ &\leq \left\| \mathcal{I}_{T,N} \frac{d}{dt} X - \frac{d}{dt} X \right\|_T^2 + \left\| \frac{d}{dt} \mathcal{I}_{T,N} X - \frac{d}{dt} X \right\|_T^2 \\ &\stackrel{(4.8), (4.9)}{\leq} cN^{-2r-2} \int_0^T \omega^{r-\frac{3}{2}}(t) \left( \frac{d^r}{dt^r} X(t) \right)^2 dt + cN^{4-2r} \int_0^T \omega^{r-\frac{3}{2}} \left( \frac{d^r}{dt^r} X(t) \right)^2 dt \\ \therefore \|G_1^N\|_T^2 &\leq cN^{4-2r} \int_0^T \omega^{r-\frac{3}{2}} \left( \frac{d^r}{dt^r} X(t) \right)^2 dt. \end{aligned} \quad (4.10)$$

Substituting (4.10) into (4.6),

$$\left( \frac{1}{2} - \epsilon \right) T \|t^{-1} (E^N(t) - E^N(0))\|_T^2 \leq c\epsilon^{-1} T N^{4-2r} \int_0^T \omega^{r-\frac{3}{2}} \left( \frac{d^r}{dt^r} X(t) \right)^2 dt + A_2^N. \quad (4.11)$$

**Proposition 4.1.** [35] If  $f(z, t)$  satisfies the following Lipschitz condition:

$$|f(z_1, t) - f(z_2, t)| \leq \gamma |z_1 - z_2|, \quad \gamma > 0 \quad (4.12)$$

and  $0 < \gamma T \leq \beta < \frac{1}{4}$ , where  $\beta$  is a certain constant. Then the system (3.15) has a unique solution.

**Theorem 4.1.** [35] Assume that  $f(z, t)$  fulfills the Lipschitz condition (4.12). Then for any  $X \in H_{\omega^{r-\frac{3}{2}}}^r(0, T)$  with integers  $2 \leq r \leq N + 1$ , we have

$$\|X - X^N\|_{L^2(0, T)}^2 \leq \frac{T}{2} \|X - X^N\|_T^2 \leq c_\beta T^2 N^{4-2r} \int_0^T \omega^{r-\frac{3}{2}}(t) \left( \frac{d^r}{dt^r} X(t) \right)^2 dt, \quad (4.13)$$

$$|X(T) - X^N(T)|^2 \leq c_\beta T^2 N^{4-2r} \int_0^T \omega^{r-\frac{3}{2}}(t) \left( \frac{d^r}{dt^r} X(t) \right)^2 dt \quad (4.14)$$

where  $c_\beta$  is a positive constant depending only on  $\beta$ .

**Proof** [35] We can prove Theorem 4.1 by (4.12), (3.13) and

$A_2^N = 2(G_2^N, (T-t)R^N)_{T, N}$  where  $G_2^N(t_{T, j}^N) = f(X^N(t_{T, j}^N), t_{T, j}^N) - f(\mathcal{I}_{T, N}X(t_{T, j}^N), t_{T, j}^N)$ ,

$$\begin{aligned} \|G_2^N\|_{T, N}^2 &= \frac{\pi}{N+1} \sum_{j=0}^N |f(X^N(t_{T, j}^N), t_{T, j}^N) - f(\mathcal{I}_{T, N}X(t_{T, j}^N), t_{T, j}^N)|^2 \\ &\stackrel{(4.12)}{\leq} \frac{\pi}{N+1} \sum_{j=0}^N \gamma^2 |X(t_{T, j}^N) - \mathcal{I}_{T, N}X(t_{T, j}^N)|^2 \\ &= \gamma^2 \|X - \mathcal{I}_{T, N}X\|_{T, N}^2 \\ &\stackrel{(3.13)}{\leq} \gamma^2 \|X - \mathcal{I}_{T, N}X\|_T^2 \\ &= \gamma^2 \|E^N\|_T^2 \end{aligned}$$

$$\therefore \|G_2^N\|_{T, N}^2 \leq \gamma^2 \|E^N\|_T^2. \quad (4.15)$$

Since  $G_2^N \in \mathcal{P}_N(0, T)$  and (3.6a) and (4.15), for any  $\gamma > 0$ ,

$$\begin{aligned} A_2^N &= 2(G_2^N, (T-t)R_N)_{T, N} \\ &\stackrel{(3.6a)}{=} 2(G_2^N, (T-t)R_N)_T \\ &\leq 2 \int_0^T |G_2^N(T-t)R_N| dt \\ &\leq 2 \|G_2^N\|_T \|(T-t)R_N\|_T \quad (\text{by Cauchy-Schwarz Inequality [8, 25]}) \\ &\leq 2 \left( \frac{\gamma}{2} \|(T-t)R_N\|_T^2 + \frac{1}{2\gamma} \|G_2^N\|_T^2 \right) \quad (\text{by Peter-Paul Inequality [25]}) \\ &= \gamma \|(T-t)R_N\|_T^2 + \frac{1}{\gamma} \|G_2^N\|_T^2 \end{aligned}$$

$$\begin{aligned}
&\leq \gamma \|TR_N\|_T^2 + \frac{1}{\gamma} \|G_2^N\|_T^2, \quad t \in [0, T] \\
&= \gamma T^2 \|R_N\|_N^2 + \frac{1}{\gamma} \|G_2^N\|_T^2 \\
\therefore A_2^N &\stackrel{(4.15)}{\leq} \gamma T^2 \|t^{-1} (E^N(t) - E^N(0))\|_T^2 + \gamma \|E^N\|_T^2. \quad (4.16)
\end{aligned}$$

Substituting (4.16) into (4.11),

$$\begin{aligned}
\left(\frac{1}{2} - \epsilon\right) T \|t^{-1} (E^N(t) - E^N(0))\|_T^2 &\leq \gamma T^2 \|t^{-1} (E^N(t) - E^N(0))\|_T^2 + \gamma \|E^N\|_T^2 \\
&\quad + c\epsilon^{-1} T N^{4-2r} \int_0^T \omega^{r-\frac{3}{2}} \left(\frac{d^r}{dt^r} X(t)\right)^2 dt \\
\left(\frac{1}{2} - \epsilon - \gamma T\right) T \|t^{-1} (E^N(t) - E^N(0))\|_T^2 &\leq \frac{cT}{\epsilon} N^{4-2r} \int_0^T \omega^{r-\frac{3}{2}} \left(\frac{d^r}{dt^r} X(t)\right)^2 dt + \gamma \|E^N\|_T^2. \quad (4.17)
\end{aligned}$$

Consider,

$$\begin{aligned}
\|E^N\|_T^2 &= \|E^N(t) - E^N(0) + E^N(0)\|_T^2 \\
&= \int_0^T [(E^N(t) - E^N(0)) + E^N(0)] dt \\
&\leq \|E^N(t) - E^N(0)\|_T \|E^N(0)\|_T \quad (\text{by Cauchy-Schwarz Inequality [8, 25]}) \\
&\leq \frac{\epsilon}{2} \|E^N(t) - E^N(0)\|_T^2 + \frac{1}{2\epsilon} \|E^N(0)\|_T^2 \quad (\text{by Peter-Paul Inequality [25]}) \\
&\leq \epsilon \|E^N(t) - E^N(0)\|_T^2 + \epsilon^{-1} \|E^N(0)\|_T^2 \\
&\leq (1 + \epsilon) \|E^N(t) - E^N(0)\|_T^2 + (1 + \epsilon^{-1}) \|E^N(0)\|_T^2 \\
&\leq (1 + \epsilon) \|(Tt^{-1})(E^N(t) - E^N(0))\|_T^2 \\
&\quad + (1 + \epsilon^{-1}) |E^N(0)|^2, \quad \left(\because \frac{T}{t} \geq 1, \forall t \in [0, T]\right) \\
&\leq (1 + \epsilon) \|(Tt^{-1})(E^N(t) - E^N(0))\|_T^2 + \pi (1 + \epsilon^{-1}) |E^N(0)|^2 \\
\therefore \|E^N\|_2^T &\leq (1 + \epsilon) T^2 \|t^{-1} (E^N(t) - E^N(0))\|_T^2 + \pi (1 + \epsilon^{-1}) |E^N(0)|^2. \quad (4.18)
\end{aligned}$$

For small  $\epsilon > 0$  such that  $\epsilon + \gamma T \leq \frac{1}{2}$  or  $\left(\frac{1}{2} - \epsilon - \gamma T\right) \geq 0$ , we multiply both sides of (4.18) by  $\left(\frac{1}{2} - \epsilon - \gamma T\right)$ , inequality become

$$\begin{aligned}
\left(\frac{1}{2} - \epsilon - \gamma T\right) \|E^N\|_2^T &\leq (1 + \epsilon) T^2 \left(\frac{1}{2} - \epsilon - \gamma T\right) \|t^{-1} (E^N(t) - E^N(0))\|_T^2 \\
&\quad + \pi (1 + \epsilon^{-1}) \left(\frac{1}{2} - \epsilon - \gamma T\right) |E^N(0)|^2
\end{aligned}$$

$$\begin{aligned}
\left(\frac{1}{2} - \epsilon - \gamma T\right) \|E^N\|_2^T &\stackrel{(4.17)}{\leq} (1 + \epsilon) T \left( \gamma \|E^N\|_T^2 + \frac{CTN^{4-2r}}{\epsilon} \int_0^T \omega^{r-\frac{3}{2}} \left(\frac{d^r}{dt^r} X(t)\right)^2 dt \right) \\
&\quad + \pi (1 + \epsilon^{-1}) \left(\frac{1}{2} - \epsilon - \gamma T\right) |E^N(0)|^2 \\
\left(\frac{1}{2} - \epsilon - 2\gamma T - \epsilon\gamma T\right) \|E^N\|_2^T &\leq (1 + \epsilon) c\epsilon^{-1} T^2 N^{4-2r} \int_0^T \omega^{r-\frac{3}{2}} \left(\frac{d^r}{dt^r} X(t)\right)^2 dt \\
&\quad + \pi (1 + \epsilon^{-1}) \left(\frac{1}{2} - \epsilon - \gamma T\right) |E^N(0)|^2
\end{aligned}$$

Since  $c$  is a generic positive constant independent of  $T, N$  and any function, we define a new constant to be  $(1 + \epsilon)c$ . Then

$$\begin{aligned}
\left(\frac{1}{2} - \epsilon - 2\gamma T - \epsilon\gamma T\right) \|E^N\|_2^T &\leq c\epsilon^{-1} T^2 N^{4-2r} \int_0^T \omega^{r-\frac{3}{2}} \left(\frac{d^r}{dt^r} X(t)\right)^2 dt \\
&\quad + \pi (1 + \epsilon^{-1}) \left(\frac{1}{2} - \epsilon - \gamma T\right) |E^N(0)|^2. \quad (4.19)
\end{aligned}$$

On the other hand, for any  $v \in H_{\omega^{-\frac{1}{2}}}^1(0, T)$  ( see Appendix of [35] ),

$$\max_{t \in [0, T]} |v(t)|^2 \leq \frac{\pi}{4} \left( \|v\|_T^2 + T^2 \left\| \frac{dv}{dt} \right\|_T^2 \right). \quad (4.20)$$

From (4.2), (4.7), (4.8) and (4.20), we obtain

$$\begin{aligned}
|E^N(0)|^2 &\stackrel{(4.2)}{=} |\mathcal{I}_{T,N} X(0) - X(0)|^2 \\
&\stackrel{(4.20)}{\leq} \frac{\pi}{4} \left( \|\mathcal{I}_{T,N} X(0) - X(0)\|_T^2 + \left\| \frac{d}{dt} (\mathcal{I}_{T,N} X(0) - X(0)) \right\|_T^2 \right) \\
&\leq \|\mathcal{I}_{T,N} X(0) - X(0)\|_T^2 + \left\| \frac{d}{dt} (\mathcal{I}_{T,N} X(0) - X(0)) \right\|_T^2 \\
&\stackrel{(4.7),(4.8)}{\leq} cN^{-2r} \int_0^T \omega^{r-\frac{1}{2}} \left(\frac{d^r}{dt^r} X(t)\right)^2 dt + cT^2 N^{4-2r} \int_0^T \omega^{r-\frac{3}{2}} \left(\frac{d^r}{dt^r} X(t)\right)^2 dt.
\end{aligned}$$

Consider

$$\begin{aligned}
0 \leq t(T-t) &\leq \frac{T^2}{4} \quad (\text{maximum value of function } f(t) = t(T-t), \forall t \in [0, T] ) \\
\therefore t(T-t) &< T^2.
\end{aligned}$$

For  $\omega = t(T-t)$ ,

$$\begin{aligned}
\omega^{r-\frac{3}{2}}(t(T-t)) &\leq \omega^{r-\frac{3}{2}} T^2, \quad \forall t \in [0, T] \\
\omega^{r-\frac{3}{2}+1} &\leq \omega^{r-\frac{3}{2}} T^2 \\
\omega^{r-\frac{1}{2}} &\leq \omega^{r-\frac{3}{2}} T^2
\end{aligned}$$

$$\omega^{r-\frac{1}{2}} \left( \frac{d^r}{dt^r} X(t) \right)^2 \leq \omega^{r-\frac{3}{2}} T^2 \left( \frac{d^r}{dt^r} X(t) \right)^2.$$

Since  $\omega^{r-\frac{1}{2}} \left( \frac{d^r}{dt^r} X(t) \right)^2 \leq \omega^{r-\frac{3}{2}} T^2 \left( \frac{d^r}{dt^r} X(t) \right)^2$  and  $\omega^{r-\frac{1}{2}} \left( \frac{d^r}{dt^r} X(t) \right)^2$  and  $\omega^{r-\frac{3}{2}} T^2 \left( \frac{d^r}{dt^r} X(t) \right)^2$  are integrable on  $[0, T]$ . By properties of the integral [27], we have

$$\int_0^T \omega^{r-\frac{1}{2}} \left( \frac{d^r}{dt^r} X(t) \right)^2 \leq \int_0^T \omega^{r-\frac{3}{2}} T^2 \left( \frac{d^r}{dt^r} X(t) \right)^2. \quad (4.21)$$

Thus,

$$\begin{aligned} |E^N(0)|^2 &\leq cN^{-2r} \int_0^T \omega^{r-\frac{3}{2}} T^2 \left( \frac{d^r}{dt^r} X(t) \right)^2 dt + cT^2 N^{4-2r} \int_0^T \omega^{r-\frac{3}{2}} \left( \frac{d^r}{dt^r} X(t) \right)^2 dt \\ &= cT^2 N^{-2r} \int_0^T \omega^{r-\frac{3}{2}} \left( \frac{d^r}{dt^r} X(t) \right)^2 dt + cT^2 N^{4-2r} \int_0^T \omega^{r-\frac{3}{2}} \left( \frac{d^r}{dt^r} X(t) \right)^2 dt \\ \therefore |E^N(0)|^2 &\leq cT^2 N^{4-2r} \int_0^T \omega^{r-\frac{3}{2}} \left( \frac{d^r}{dt^r} X(t) \right)^2 dt. \end{aligned} \quad (4.22)$$

Substituting (4.22) into (4.19), we give that

$$\begin{aligned} \left( \frac{1}{2} - \epsilon - 2\gamma T - \epsilon\gamma T \right) \|E^N\|_T^2 &\leq c\epsilon^{-1} T^2 N^{4-2r} \int_0^T \omega^{r-\frac{3}{2}} \left( \frac{d^r}{dt^r} X(t) \right)^2 dt + \pi (1 + \epsilon^{-1}) \\ &\quad \times \left( \frac{1}{2} - \epsilon - \gamma T \right) cT^2 N^{4-2r} \int_0^T \omega^{r-\frac{3}{2}} \left( \frac{d^r}{dt^r} X(t) \right)^2 dt \\ &\leq \left( 1 + \left( \epsilon\pi (1 + \epsilon^{-1}) \left( \frac{1}{2} - \epsilon - \gamma T \right) \right) \right) \\ &\quad \times \left( c\epsilon^{-1} T^2 N^{4-2r} \int_0^T \omega^{r-\frac{3}{2}} \left( \frac{d^r}{dt^r} X(t) \right)^2 dt \right). \end{aligned}$$

From, page 30, we choose  $\epsilon + \gamma T \leq \frac{1}{2}$ , it follows that

$$\begin{aligned} \left( \frac{1}{2} - \epsilon - 2\gamma T - \epsilon\gamma T \right) \|E^N\|_T^2 &\leq \left( 1 + \left( \epsilon\pi (1 + \epsilon^{-1}) \left( \frac{1}{2} - \frac{1}{2} \right) \right) \right) \\ &\quad \times \left( c\epsilon^{-1} T^2 N^{4-2r} \int_0^T \omega^{r-\frac{3}{2}} \left( \frac{d^r}{dt^r} X(t) \right)^2 dt \right) \\ \therefore \left( \frac{1}{2} - \epsilon - 2\gamma T - \epsilon\gamma T \right) \|E^N\|_T^2 &\leq c\epsilon^{-1} T^2 N^{4-2r} \int_0^T \omega^{r-\frac{3}{2}} \left( \frac{d^r}{dt^r} X(t) \right)^2 dt. \end{aligned} \quad (4.23)$$

**Claim :**  $\frac{1}{2} - \epsilon - 2\gamma T - \epsilon\gamma T \geq \frac{1}{4} - \beta$  and, hence,  $\frac{1}{\frac{1}{2} - \epsilon - 2\gamma T - \epsilon\gamma T} \leq \frac{1}{\frac{1}{4} - \beta}$ .

Since  $0 < \gamma T \leq \beta < \frac{1}{4}$ , then  $\frac{1}{4} - \gamma T \geq \frac{1}{4} - \beta > 0$ .

We consider

$$\begin{aligned} \frac{1}{2} - \epsilon - 2\gamma T - \epsilon\gamma T &= \left(\frac{1}{4} - \gamma T\right) + \left(\frac{1}{4} - \gamma T\right) - \epsilon(1 + \gamma T) \\ &= \frac{1}{4} - \gamma T, \quad \left(\because \text{let } \left(\frac{1}{4} - \gamma T\right) - \epsilon(1 + \gamma T) = 0\right) \\ &\geq \frac{1}{4} - \beta \\ \therefore \frac{1}{\frac{1}{2} - \epsilon - 2\gamma T - \epsilon\gamma T} &\leq \frac{1}{\frac{1}{4} - \beta}. \end{aligned} \quad (4.24)$$

Let  $\epsilon = \frac{\frac{1}{4} - \gamma T}{1 + \gamma T}$ . Then by (4.24), we have that

$$\begin{aligned} \|E^N\|_T^2 &\leq \left(\frac{1}{\frac{1}{2} - \epsilon - 2\gamma T - \epsilon\gamma T}\right) c\epsilon^{-1} T^2 N^{4-2r} \int_0^T \omega^{r-\frac{3}{2}} \left(\frac{d^r}{dt^r} X(t)\right)^2 dt \\ &\stackrel{(4.24)}{\leq} \left(\frac{1}{\frac{1}{4} - \beta}\right) cT^2 N^{4-2r} \int_0^T \omega^{r-\frac{3}{2}} \left(\frac{d^r}{dt^r} X(t)\right)^2 dt \\ \therefore \|E^N\|_T^2 &\leq c_\beta T^2 N^{4-2r} \int_0^T \omega^{r-\frac{3}{2}} \left(\frac{d^r}{dt^r} X(t)\right)^2 dt \end{aligned} \quad (4.25)$$

where  $c_\beta$  is a positive constant depending only on  $\beta$ .

Consider

$$\begin{aligned} \|X - X^N\|_T^2 &= \|X - \mathcal{I}_{T,N}X + \mathcal{I}_{T,N}X - X^N\|_T^2 \\ &\leq \|X - \mathcal{I}_{T,N}X\|_T^2 + \|X^N - \mathcal{I}_{T,N}X\|_T^2. \end{aligned}$$

Using (4.7), (4.25) and (4.21), we have

$$\begin{aligned} \|X - X^N\|_T^2 &\stackrel{(4.7), (4.25)}{\leq} cN^{-2r} \int_0^T \omega^{r-\frac{1}{2}} \left(\frac{d^r}{dt^r} X(t)\right)^2 dt + c_\beta T^2 N^{4-2r} \int_0^T \omega^{r-\frac{3}{2}} \left(\frac{d^r}{dt^r} X(t)\right)^2 dt \\ &\stackrel{(4.21)}{\leq} cT^2 N^{-2r} \int_0^T \omega^{r-\frac{3}{2}} \left(\frac{d^r}{dt^r} X(t)\right)^2 dt + c_\beta T^2 N^{4-2r} \int_0^T \omega^{r-\frac{3}{2}} \left(\frac{d^r}{dt^r} X(t)\right)^2 dt \\ \therefore \|X - X^N\|_T^2 &\leq c_\beta T^2 N^{4-2r} \int_0^T \omega^{r-\frac{3}{2}} \left(\frac{d^r}{dt^r} X(t)\right)^2 dt \end{aligned} \quad (4.26)$$

where  $c_\beta$  is a positive constant depending only on  $\beta$ .

Next, we consider

$$\int_0^T (X(t) - X^N(t))^2 dt = \int_0^T (X(t) - X^N(t))^2 \omega^{\frac{1}{2}}(t) \omega^{-\frac{1}{2}}(t) dt.$$

Since  $t(T-t) \leq \frac{T^2}{4}$  or  $\sqrt{t(T-t)} \leq \frac{T}{2}$  and  $\omega = t(T-t)$ , then  $0 \leq \omega^{\frac{1}{2}}(t) \leq \frac{T}{2}$  and  $\omega^{-\frac{1}{2}}(t) \geq 0$  for  $t \in [0, T]$ . Thus,

$$\begin{aligned} \int_0^T (X(t) - X^N(t))^2 dt &\leq \frac{T}{2} \int_0^T (X(t) - X^N(t))^2 \omega^{-\frac{1}{2}}(t) dt \\ &= \frac{T}{2} \|X - X^N\|_T^2 \\ \therefore \int_0^T (X(t) - X^N(t))^2 dt &\leq \frac{T}{2} \|X - X^N\|_T^2. \end{aligned} \quad (4.27)$$

By applying the inequality (4.27), we then arrive the inequality (4.13) in Theorem 4.1.

We next prove the inequality (4.14). We first estimate  $|X(T) - X^N(T)|^2$ .

Consider

$$\begin{aligned} |X(T) - X^N(T)|^2 &= |X(T) - \mathcal{I}_{T,N}X(T) + \mathcal{I}_{T,N}X(T) - X^N(T)|^2 \\ &\leq |X(T) - \mathcal{I}_{T,N}X(T)|^2 + |X^N(T) - \mathcal{I}_{T,N}X(T)|^2. \end{aligned} \quad (4.28)$$

Using (4.20), (4.7), (4.8) and (4.21), we have

$$\begin{aligned} |X(T) - \mathcal{I}_{T,N}X(T)|^2 &\stackrel{(4.20)}{\leq} \frac{\pi}{4} \left( \|X - \mathcal{I}_{T,N}X\|_T^2 + T^2 \left\| \frac{d}{dt} (X - \mathcal{I}_{T,N}X) \right\|_T^2 \right) \\ &\leq \|X - \mathcal{I}_{T,N}X\|_T^2 + T^2 \left\| \frac{d}{dt} (X - \mathcal{I}_{T,N}X) \right\|_T^2 \\ &\stackrel{(4.7),(4.8)}{\leq} cN^{-2r} \int_0^T \omega^{r-\frac{1}{2}} \left( \frac{d^r}{dt^r} X(t) \right)^2 dt \\ &\quad + cT^2 N^{4-2r} \int_0^T \omega^{r-\frac{3}{2}} \left( \frac{d^r}{dt^r} X(t) \right)^2 dt \\ &\stackrel{(4.21)}{\leq} cT^2 N^{-2r} \int_0^T \omega^{r-\frac{3}{2}} \left( \frac{d^r}{dt^r} X(t) \right)^2 dt \\ &\quad + cT^2 N^{4-2r} \int_0^T \omega^{r-\frac{3}{2}} \left( \frac{d^r}{dt^r} X(t) \right)^2 dt \\ \therefore |X(T) - \mathcal{I}_{T,N}X(T)|^2 &\leq cT^2 N^{4-2r} \int_0^T \omega^{r-\frac{3}{2}} \left( \frac{d^r}{dt^r} X(t) \right)^2 dt. \end{aligned} \quad (4.29)$$

Next, we estimate  $|\mathcal{I}_{T,N}X(T) - X^N(T)|^2$ . By (4.20) give that

$$\begin{aligned} |\mathcal{I}_{T,N}X(T) - X^N(T)|^2 &\stackrel{(4.20)}{\leq} \frac{\pi}{4} \left( \|\mathcal{I}_{T,N}X - X^N\|_T^2 + T^2 \left\| \frac{d}{dt} (\mathcal{I}_{T,N}X - X^N) \right\|_T^2 \right) \\ &= \frac{\pi}{4} \left( \|E^N\|_T^2 + T^2 \left\| \frac{d}{dt} E^N \right\|_T^2 \right) \end{aligned}$$

$$\therefore |\mathcal{I}_{T,N}X(T) - X^N(T)|^2 \leq \frac{\pi}{4} \left( \|E^N\|_T^2 + T^2 \left\| \frac{d}{dt} E^N \right\|_T^2 \right). \quad (4.30)$$

Since  $\frac{d}{dt}E^N \in \mathcal{P}_N(0, T)$  and (3.5), (3.6b) and (4.2), we get that

$$\begin{aligned} \left\| \frac{d}{dt} E^N \right\|_T^2 &\stackrel{(3.6b)}{=} \left\| \frac{d}{dt} E^N \right\|_{T,N}^2 \\ &\stackrel{(3.5)}{=} \left( \frac{d}{dt} E^N, \frac{d}{dt} E^N \right)_{T,N} \\ &\stackrel{(4.2)}{=} \left( G_1^N + G_2^N, \frac{d}{dt} E^N \right)_{T,N} \\ &\leq \left\| (G_1^N + G_2^N) \frac{d}{dt} E^N \right\|_{T,N} \\ &\leq \|G_1^N + G_2^N\|_{T,N} \left\| \frac{d}{dt} E^N \right\|_{T,N} \\ &\leq \left( \|G_1^N\|_{T,N} + \|G_2^N\|_{T,N} \right) \left\| \frac{d}{dt} E^N \right\|_{T,N} \\ &\stackrel{(3.6b)}{=} \left( \|G_1^N\|_T + \|G_2^N\|_{T,N} \right) \left\| \frac{d}{dt} E^N \right\|_T \\ \therefore \left\| \frac{d}{dt} E^N \right\|_T &\leq \|G_1^N\|_T + \|G_2^N\|_{T,N}. \end{aligned} \quad (4.31)$$

Substituting (4.10), (4.15) and (4.25) into (4.31), we have

$$\left\| \frac{d}{dt} E^N \right\|_T^2 \leq cN^{4-2r} \int_0^T \omega^{r-\frac{3}{2}} \left( \frac{d^r}{dt^r} X(t) \right)^2 dt + c_\beta \gamma^2 T^2 N^{4-2r} \int_0^T \omega^{r-\frac{3}{2}} \left( \frac{d^r}{dt^r} X(t) \right)^2 dt. \quad (4.32)$$

Since  $0 < \gamma T \leq \beta < \frac{1}{4}$  and substituting (4.32) and (4.25) into (4.30),

$$\begin{aligned} |\mathcal{I}_{T,N}X(T) - X^N(T)|^2 &\leq \frac{\pi}{4} \left( c_\beta T^2 N^{4-2r} \int_0^T \omega^{r-\frac{3}{2}} \left( \frac{d^r}{dt^r} X(t) \right)^2 dt \right) \\ &\quad + \frac{\pi}{4} \left( cT^2 N^{4-2r} \int_0^T \omega^{r-\frac{3}{2}} \left( \frac{d^r}{dt^r} X(t) \right)^2 dt \right) \\ &\quad + c_\beta T^4 N^{4-2r} \int_0^T \omega^{r-\frac{3}{2}} \left( \frac{d^r}{dt^r} X(t) \right)^2 dt \\ \therefore |\mathcal{I}_{T,N}X(T) - X^N(T)|^2 &\leq c_\beta T^2 N^{4-2r} \int_0^T \omega^{r-\frac{3}{2}} \left( \frac{d^r}{dt^r} X(t) \right)^2 dt. \end{aligned} \quad (4.33)$$



Moreover, by (4.28), (4.29) and (4.33), we obtain

$$\begin{aligned} |X(T) - X^N(T)|^2 &\leq (c + c_\beta) T^2 N^{4-2r} \int_0^T \omega^{r-\frac{3}{2}} \left( \frac{d^r}{dt^r} X(t) \right)^2 dt \\ &= c_\beta T^2 N^{4-2r} \int_0^T \omega^{r-\frac{3}{2}} \left( \frac{d^r}{dt^r} X(t) \right)^2 dt. \end{aligned}$$

Hence,

$$|X(T) - X^N(T)|^2 \leq c_\beta T^2 N^{4-2r} \int_0^T \omega^{r-\frac{3}{2}} \left( \frac{d^r}{dt^r} X(t) \right)^2 dt. \quad (4.34)$$

■



# Chapter 5

## Numerical Results

In this chapter, we present some numerical results to support the method in (3.21). We consider two errors, the discrete  $L^2$  error and the point-wise absolute error, in order to compare the results obtained from the Chebyshev–Gauss collocation method, the Legendre–Gauss collocation method in [14] and the Chebyshev–Gauss collocation method in [35]. For the systems of differential equations, we compare the error in the total energy of the systems and CPU times of those three collocation methods.

For the three-body problem, we present the numerical solutions, the maximum error in energy and CPU times and consider some sets of initial conditions of this problem to examine the behavior of the solution near the equilibrium points. We compare the result from the three collocation methods with the symplectic method and the Runge-Kutta method. The symplectic method is known to preserve the area (or orbit). However, it may not preserve the energy of the system. The Runge-Kutta method is a traditional method. It preserves the area when the time is not large, but there may be a phase shift when  $t$  increases.

The numerical results are obtained by using an Intel(R) Core(TM) i5-2410 CPU @ 2.30GHz RAM 4.00 GB computer.

For simplicity, we use the following notations,

- CGC : Chebyshev-Gauss collocation method (3.21).
- LGC : Legendre-Gauss collocation method in [14].
- CGC-Yang : Chebyshev-Gauss spectral collocation method in [35].

- Symp1 : The first-order symplectic method.
- RK4 : The fourth-order Runge-Kutta method.
- The point-wise absolute error

$$E_{T,p} = |X(T) - X^N(T)|.$$

- The discrete  $L^2$  error

$$E_{T,d} = \|X - X^N\|_{T,N}.$$

- The point-wise absolute error for systems of differential equations

$$E^N(t) = \sqrt{(p^N(t) - P(t))^2 + (q^N(t) - Q(t))^2}.$$

- The maximum error in energy for systems of differential equations

$$E_H(\tau) = |H(P(0), Q(0)) - H(P(\tau), Q(\tau))|.$$

## 5.1 Single interval Domain

**Example 5.1.1.** We use scheme (3.21) to solve the problem

$$\begin{cases} \frac{d}{dt}X(t) = f(X(t), t), & 0 < t \leq T \\ X(0) = 1. \end{cases} \quad (5.1)$$

with

$$f(X(t), t) = \exp\left(\frac{1}{5}\sin(X(t))\right) + \frac{3}{2}(t+1)^{\frac{1}{2}} + 10\cos(2t) - \exp\left(\frac{1}{5}\sin((t+1)^{\frac{3}{2}} + 5\sin(2t))\right).$$

The exact solution of this problem is

$$X(t) = (t+1)^{\frac{3}{2}} + 5\sin(2t)$$

which oscillates and grows to infinity as  $t$  increases. The corresponding function on right side,  $f(X(t), t)$ , satisfies the Lipschitz condition as follows. Consider

$$f(X_1(t), t) - f(X_2(t), t) = \exp\left(\frac{1}{5}\sin(X_1(t))\right) - \exp\left(\frac{1}{5}\sin(X_2(t))\right).$$

By Mean Value Theorem [1], we have

$$\frac{\exp\left(\frac{1}{5}\sin(X_1(t))\right) - \exp\left(\frac{1}{5}\sin(X_2(t))\right)}{X_1(t) - X_2(t)} = \frac{1}{5}\exp\left(\frac{1}{5}\sin(X_c(t))\right)\cos(X_c(t))$$

for some  $X_c(t)$  between  $X_1(t)$  and  $X_2(t)$ .

Since  $|\sin(X_c(t))| \leq 1$  and  $|\cos(X_c(t))| \leq 1$ , we get

$$\left| \frac{\exp\left(\frac{1}{5}\sin(X_1(t))\right) - \exp\left(\frac{1}{5}\sin(X_2(t))\right)}{X_1(t) - X_2(t)} \right| \leq \frac{1}{5}e^{\frac{1}{5}}$$

$$\left| \exp\left(\frac{1}{5}\sin(X_1(t))\right) - \exp\left(\frac{1}{5}\sin(X_2(t))\right) \right| \leq \frac{1}{5}e^{\frac{1}{5}}|X_1(t) - X_2(t)|.$$

Thus,  $|f(X(t), t)|$  fulfills the Lipschitz condition with  $\gamma = \frac{1}{5}e^{\frac{1}{5}}$ . It follows from Proposition 4.1 and Theorem 4.1 that the equation (5.1) has a unique solution and has the error estimates in (4.13) and (4.14).

We implement the algorithm by using this function  $f(X(t), t)$ . The figures below illustrate the errors by the spectral collocation methods defined at the beginning of the section. In Figure 5.1, we plot the point-wise absolute error at  $T = 0.5, 0.8$  and  $1$  with different value of  $N$ . We observe that the point-wise absolute error decreases as  $N$  increases and  $T$  decreases. Furthermore, The errors oscillates between odd and even  $N$ . The rate of convergence when  $N$  is even is faster than the rate when  $N$  is odd.

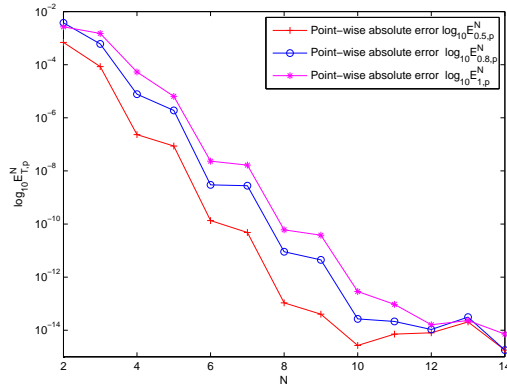


Figure 5.1: Point-wise absolute error of scheme (3.21) when at  $T = 0.5, 0.8$  and  $1$ .

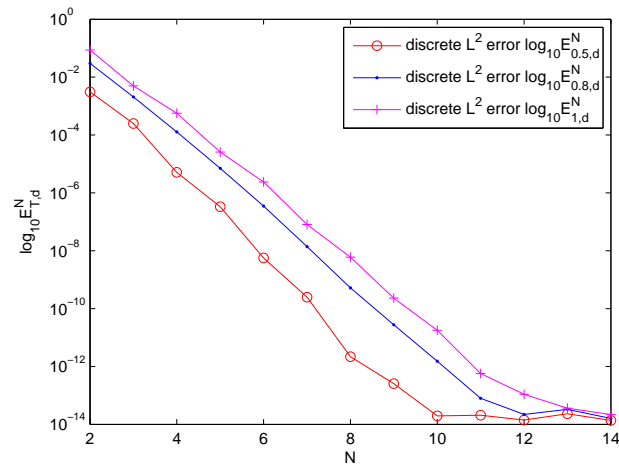


Figure 5.2: Discrete  $L^2$  error of scheme (3.21) when at  $T = 0.5, 0.8$  and  $1$ .

Figure 5.2, we present the discrete  $L^2$  error at  $T = 0.5, 0.8$  and  $1$  with various of  $N$ . There is only slight oscillation for the discrete  $L^2$  errors. The error decreases as  $N$  increases and  $T$  decreases. In Figures 5.3 and 5.4, we compare the Chebyshev–Gauss collocation method in (3.21) and the Chebyshev–Gauss spectral collocation method in [35]. The point-wise absolute error and the discrete  $L^2$  error of two methods are nearly coincide. The rate from both methods are of the same order.

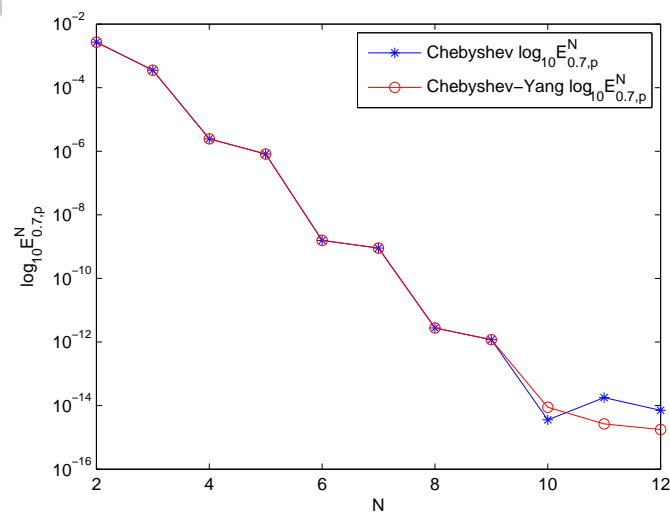


Figure 5.3: Point-wise absolute error of scheme (3.21) versus the Chebyshev–Gauss spectral collocation method.

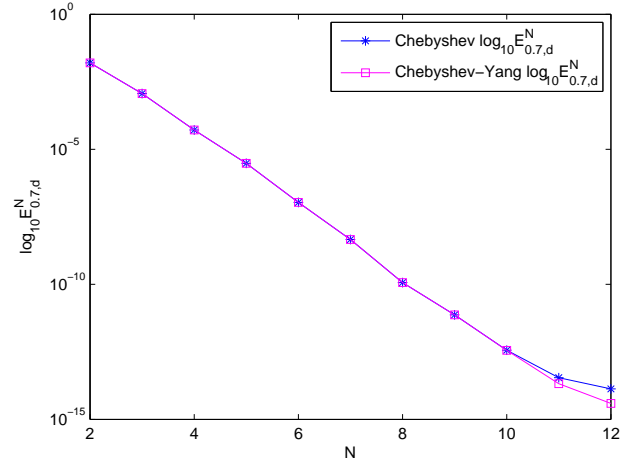


Figure 5.4: Discrete  $L^2$  error of scheme (3.21) versus the Chebyshev–Gauss spectral collocation method.

The rate of convergence of the point-wise absolute errors and the discrete  $L^2$  errors from the Chebyshev–Gauss collocation in (3.21) and the Chebyshev–Gauss spectral collocation method in [35] shown in Figures 5.5 and 5.6 demonstrate the spectral accuracy. We plot the point-wise absolute errors of the two methods and estimate them by comparing with the function in Figure 5.5. It follows that convergence rate is of order  $\mathcal{O}(e^{-3.1N})$ . Similarly, as shown in Figure 5.6, the convergence rate of the discrete  $L^2$  error is of order  $\mathcal{O}(N^{-4.33\sqrt{N}})$ .

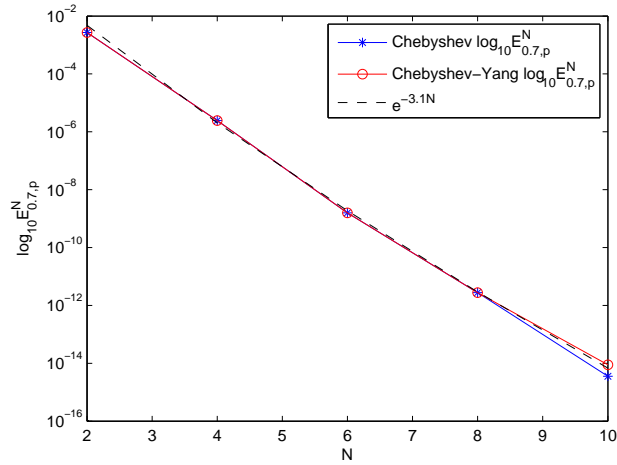


Figure 5.5: Point-wise absolute error of scheme (3.21) versus the Chebyshev–Gauss spectral collocation method and the convergence rate when  $N$  varies.

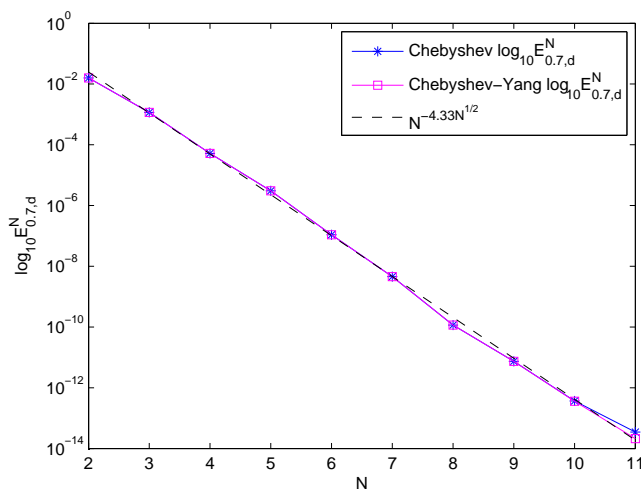


Figure 5.6: Discrete  $L^2$  error of scheme (3.21) versus the Chebyshev–Gauss spectral collocation method and the convergence rate when  $N$  varies.

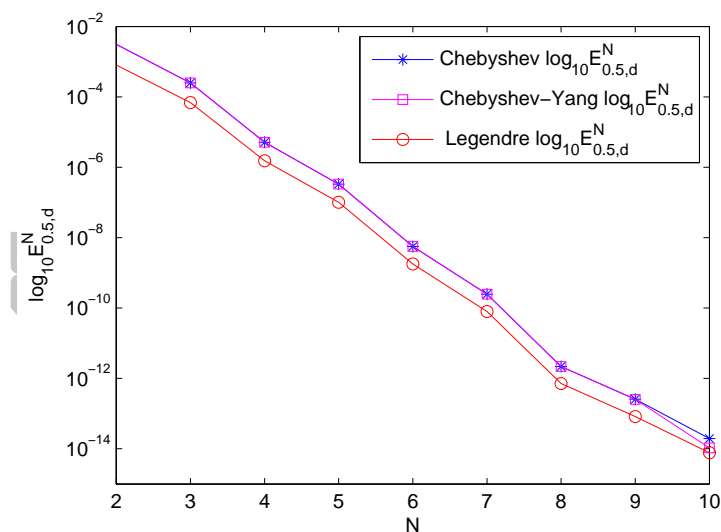


Figure 5.7: Discrete  $L^2$  error of scheme (3.21) versus the Chebyshev–Gauss spectral collocation method and the Legendre–Gauss collocation method.

In Figure 5.7, we compare the Chebyshev–Gauss collocation method in (3.21) with the Legendre–Gauss collocation method and the Chebyshev–Gauss spectral collocation method in [35]. We observe that the discrete  $L^2$  error of the Legendre–Gauss collocation method decay slightly faster as  $N$  increases and the two Chebyshev–Gauss collocation methods are of the same rate.

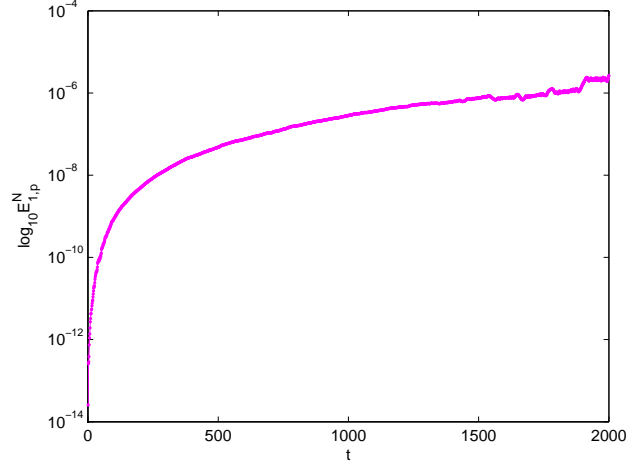


Figure 5.8: Point-wise absolute error of scheme (3.21) when  $t = 2000$ ,  $\tau = 1$  and  $N = 17$ .

Figure 5.8 shows the point-wise absolute error of the Chebyshev–Gauss collocation method in (3.21). We observe that the point-wise absolute error grows rapidly when the time is less than 200 seconds then it increases at a slower rate and slightly oscillates as  $t$  increases.

## 5.2 System of differential equations

For the system of differential equations, we denote the vectors

$$\begin{aligned}\vec{\mathbf{X}}(t) &= (X_1(t), X_2(t), \dots, X_n(t))^T \\ \vec{F}(\vec{\mathbf{X}}(t)) &= \left( f_1(\vec{\mathbf{X}}(t), t), f_2(\vec{\mathbf{X}}(t), t), \dots, f_n(\vec{\mathbf{X}}(t), t) \right)^T.\end{aligned}$$

We can apply the algorithm in (3.21) to the system of equations. The solution can be determined in a similar way. Consider the system

$$\begin{cases} \frac{d}{dt} \vec{\mathbf{X}}(t) = \vec{F}(\vec{\mathbf{X}}(t), t), & 0 < t \leq T \\ \vec{\mathbf{X}}(0) = \vec{\mathbf{X}}_0. \end{cases} \quad (5.2)$$

In spectral collocation method, we approximate the solution of (5.2) as follows.

Find  $\vec{X}^N(t) \in (\mathcal{P}_{N+1}(0, T))^n$  such that

$$\begin{cases} \frac{d}{dt} \vec{X}^N(t_{T,j}^N) = \vec{F}(\vec{X}^N(t_{T,j}^N), t_{T,j}^N), & 0 \leq j \leq N, 0 < t \leq T \\ \vec{X}^N(0) = \vec{X}_0. \end{cases} \quad (5.3)$$



We evaluate each  $X_i(t)$  by applying (3.21) together with an iterative method.

In the examples below, we presents the numerical solution of linear and non-linear Hamiltonian systems. We are interested in the long-term behavior of the system. A good algorithm should preserve both the area (orbit) and the energy of the system [18].

**Example 5.2.1.** Consider the Hamiltonian system

$$\begin{aligned} p'(t) &= -q(t) + 1, & 0 < t \leq \tau \\ q'(t) &= p(t), & 0 < t \leq \tau \\ p(0) &= 1, & q(0) = 1. \end{aligned} \tag{5.4}$$

with the exact solution

$$p(t) = \cos(t) + \sin(t) \quad \text{and} \quad q(t) = \sin^2(t) + \sin(t) + \cos^2(t) - \cos(t).$$

The corresponding Hamiltonian function of this system is  $H(p, q) = \frac{1}{2}p^2 + \frac{1}{2}q^2 - q$ .

The total energy of the system is  $E = \frac{1}{2}p^2(0) + \frac{1}{2}q^2(0) - q(0) = \frac{1}{2}$ .

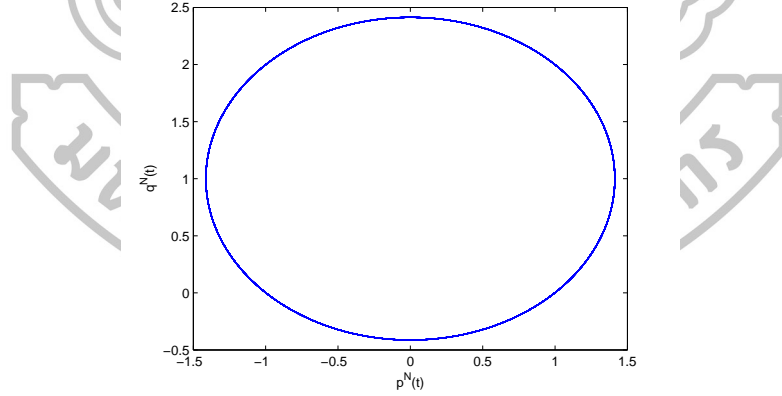


Figure 5.9: Phase plot  $p^N(t)$  versus  $q^N(t)$  when  $M = 10^5$ ,  $\tau = 0.1$  and  $N = 7$ .

Figure 5.9 represents the phase plots of  $p^N(t)$  and  $q^N(t)$  by using the Chebyshev–Gauss collocation method when  $M = 10^5$ ,  $\tau = 0.1$  and  $N = 7$ . The other two collocation methods also present the same orbit. We see that the orbit preserves the area as it does not shift from the exact solution when  $t$  is large.

In Figures 5.10(a) and 5.10(b), we compare the error in energy of the Chebyshev–Gauss collocation method in (5.3) with the Legendre–Gauss collocation method

and the Chebyshev–Gauss spectral collocation method in [35]. The error in energy from the Chebyshev–Gauss collocation method in (5.3) is smaller than the error from the Legendre–Gauss collocation method. However, the errors are still larger than that from the Chebyshev–Gauss spectral collocation method in [35]. The three methods show a constant growth (with respect to the log scale) of the error, but the point-wise absolute error from [35] slightly oscillates as  $t$  increases.

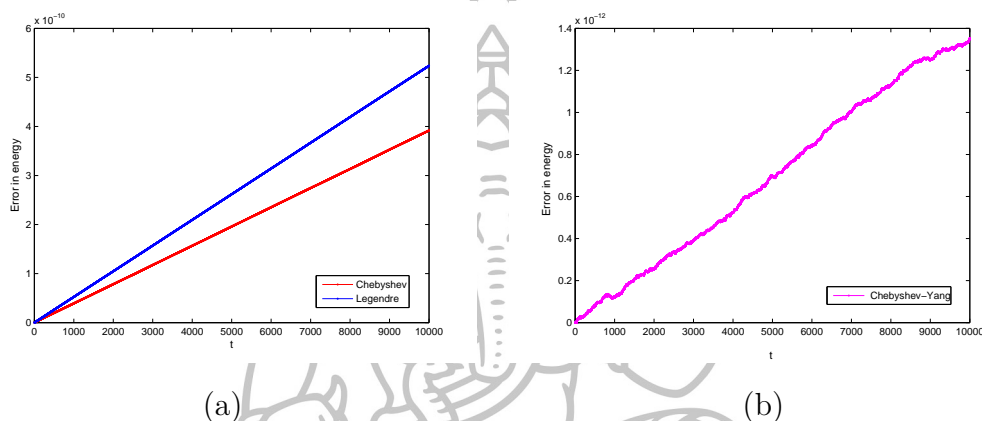


Figure 5.10: (a) Error in energy of scheme (5.3) versus the Legendre–Gauss collocation method (b) the Chebyshev–Gauss spectral collocation method when  $M = 10^5$ ,  $\tau = 0.1$  and  $N = 7$ .

$N$		7	9	11	13	17	21
$\tau$		0.1	0.25	0.5	1	2	4
$E^N(t)$	CGC	2.77e-11	1.77e-11	3.28e-11	2.48e-11	8.14e-11	2.62e-11
	LGC	3.70e-11	1.50e-11	3.44e-11	3.51e-11	5.05e-11	3.40e-11
	CGC–Yang	1.15e-13	1.36e-13	2.33e-13	3.27e-12	3.27e-12	4.82e-12
$E_H(t)$	CGC	3.92e-11	3.92e-11	5.06e-11	3.48e-11	9.22e-11	3.21e-11
	LGC	5.24e-11	2.12e-11	4.70e-11	4.32e-11	3.26e-11	4.81e-11
	CGC–Yang	1.36e-13	8.30e-14	4.54e-14	3.71e-13	6.26e-14	4.00e-13
CPU Times	CGC	15.60	25.20	42.07	87.14	221.91	659.08
	LGC	19.04	31.14	56.20	124.27	379.50	743.33
	CGC–Yang	33.32	70.70	197.68	539.41	1.35e3	2.15e3

Table 5.1: Comparison of the errors and CPU times from the three collocation methods for the system (5.4).

Table 5.1 represents the point-wise absolute error  $E^N(t)$ , the maximum error

of energy  $E_H(\tau)$  and the CPU times when  $M = 10^4$  with different values of  $\tau$  and  $N$  of the system (5.4). We have the Chebyshev–Gauss spectral collocation method in [35] preserves energy better and the point-wise absolute error less than the other two methods. However, when we compared the CPU times, it takes much longer than the time taken from the other two methods. The Chebyshev–Gauss collocation method (5.3) gives the best CPU times.

**Example 5.2.2.** Consider the Henon–Heiles system

$$\begin{aligned} p_1'(t) &= -q_1(t) - 2q_1(t)q_2(t), & 0 < t \leq \tau \\ p_2'(t) &= -q_2(t) - 2q_1^2(t) + q_2^2(t), & 0 < t \leq \tau \\ q_1'(t) &= p_1(t), & 0 < t \leq \tau \\ q_2'(t) &= p_2(t), & 0 < t \leq \tau \end{aligned} \quad (5.5)$$

with initial conditions  $p_1(0) = 0.011$ ,  $p_2(0) = 0$ ,  $q_1(0) = 0.013$  and  $q_2(0) = -0.4$ .

The corresponding Hamiltonian function of this system is

$$H(p_1, p_2, q_1, q_2) = \frac{1}{2} (p_1^2 + p_2^2 + q_1^2 + q_2^2) + q_1^2 q_2 - \frac{1}{3} q_2^3.$$

The total energy of the system with respect to the initial conditions is

$$E = \frac{1}{2} (p_1^2(0) + p_2^2(0) + q_1^2(0) + q_2^2(0)) + q_1(0)^2 q_2(0) - \frac{1}{3} q_2^3(0) = 0.1014.$$

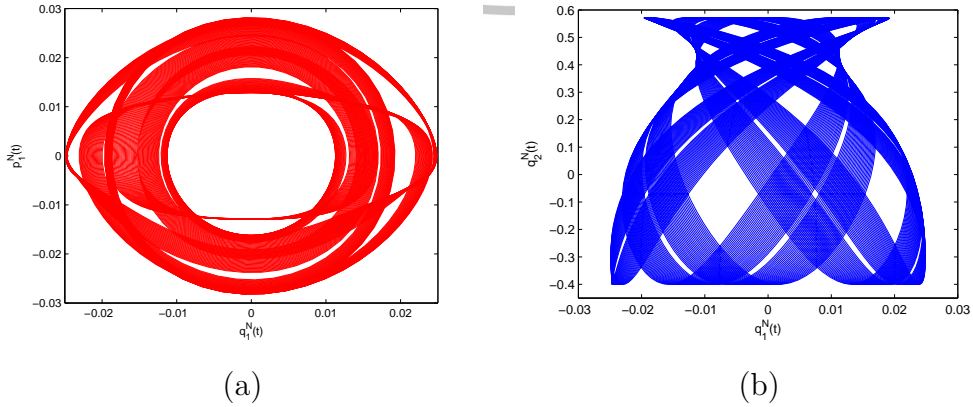


Figure 5.11: (a) Phase plot  $q_1^N(t)$  versus  $p_1^N(t)$  (b) Phase plot  $q_1^N(t)$  versus  $q_2^N(t)$  when  $M = 10^4$ ,  $\tau = 0.1$  and  $N = 7$ .

Figures 5.11(a) and 5.11(b) illustrate the phase plots of  $p_1^N(t)$  and  $q_1^N(t)$  and the phase plots of  $q_1^N(t)$  and  $q_2^N(t)$ , respectively, by using the Chebyshev–Gauss collocation method (5.3) when  $M = 10^4$ ,  $\tau = 0.1$  and  $N = 7$ . The other two collocation methods also present the same orbit.

$N$		7	9	11	13	17	21
$\tau$		0.1	0.25	0.5	1	2	4
$E_H(t)$	CGC	5.91e-12	1.10e-12	8.41e-12	9.30e-12	2.29e-11	1.85e-11
	LGC	3.45e-12	2.28e-11	9.48e-12	9.79e-12	4.19e-11	2.09e-11
	CGC-Yang	1.21e-14	6.34e-15	2.39e-15	1.42e-14	2.73e-14	2.47e-12
CPU Times	CGC	10.69	158.19	290.49	54.59	221.91	659.08
	LGC	13.12	18.24	24.58	34.66	77.84	141.30
	CGC-Yang	6.54	9.20	16.05	43.08	163.52	407.01

Table 5.2: Comparison of the errors and CPU times from the three collocation methods for Henon Heiles (5.5).

Table 5.2 illustrates the maximum error of energy  $E_H(\tau)$  and CPU times when  $M = 10^4$  with different values of  $\tau$  and  $N$  of the system (5.5). From the table, the method (5.3) and the Legendre–Gauss collocation method provide the error in energy of the same order. In this example, the Chebyshev–Gauss spectral collocation method in [35] preserves energy better. However, when we compared the CPU times, the time from the Chebyshev–Gauss spectral collocation method in [35] grows as  $\tau$  and  $N$  increases. The CPU times of the method (5.3) and the Legendre–Gauss collocation method are close to each other when  $\tau$  and  $N$  are small.

### 5.3 The three-body problem

For the three-body problem, as shown in (2.4), apply the algorithm (3.21) to the system

$$\begin{aligned}\frac{dp_N^1(t_j)}{dt} &= p_N^2(t_j) - \frac{(1-\mu)}{r_1^3}(q_N^1(t_j) + \mu) - \frac{\mu}{r_2^3}(q_N^1(t_j) + \mu - 1) \\ \frac{dp_N^2(t_j)}{dt} &= -p_N^1(t_j) - \frac{q_N^2(t_j)}{r_1^3}(1-\mu) - \frac{\mu}{r_2^3}(q_N^2(t_j))\end{aligned}$$

$$\begin{aligned}\frac{dq_N^1(t_j)}{dt} &= p_N^1(t_j) + q_N^2(t_j) \\ \frac{dq_N^2(t_j)}{dt} &= p_N^2(t_j) - q_N^1(t_j).\end{aligned}$$

In all the figures below, we used  $N = 18, \tau = 0.02$  on the interval  $[0, 360]$  and  $M = \frac{360}{\tau}$  for the collocation methods and  $h = 0.001$  for the symplectic and the Runge-Kutta methods.

According to the theoretical result of the three-body problem, the system has three unstable saddle points. We first examine the orbital behavior of the satellite. We choose the initial conditions to present the orbit around the center of mass.

**Example 5.3.1.** Orbital behavior

We consider the first set of initial conditions,  $p_1(0) = 1.259185, p_2(0) = -1.259185, q_1(0) = -0.25$  and  $q_2(0) = -0.25$ . With this set of initial conditions, the phase plot of  $q_1$  and  $q_2$  illustrates an orbit.

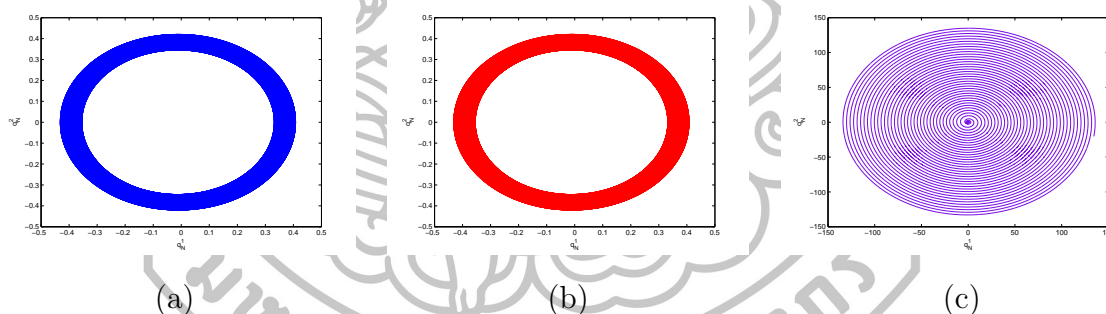


Figure 5.12: Phase plots of  $q_N^2$  versus  $q_N^1$  by (a) the Chebyshev-Gauss collocation method (b) the first-order symplectic method (c) the fourth-order Runge-Kutta method.

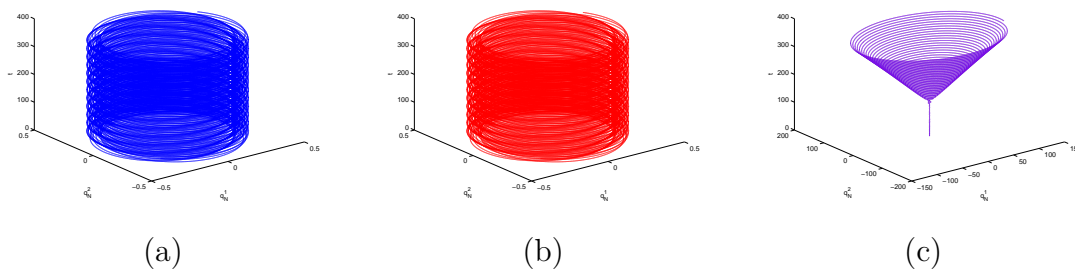


Figure 5.13: Phase plots of  $q_N^2$  versus  $q_N^1$  and  $t$  by (a) the Chebyshev-Gauss collocation method (b) the first-order symplectic method (c) the fourth-order Runge-Kutta method.

In Figures 5.12 and 5.13, we compare the phase plots of  $q_N^1$  and  $q_N^2$  of the Chebyshev-Gauss collocation method with the first-order symplectic method and the fourth-order Runge-Kutta method. We observe that the orbit from the symplectic method is almost the same as the orbit from the Chebyshev-Gauss collocation method, whereas the loop from the Runge-Kutta method spins out and diverges as  $t$  increases. The other two collocation methods also present the similar orbit to Figures 5.12(a) and 5.13(a).

Method	Time (secs.)	Error in energy
CGC	209.912	6.92004e-10
LGC	180.254	1.34285e-9
CGC-Yang	168.261	3.68594e-14
Symp1	1115.715	9.48892e-5
RK4	345.514	1.56437

Table 5.3: Comparison of the errors and CPU times between the five methods.

Method	Time (secs.)	Error in energy
CGC	351.484	1.03391e-10
LGC	256.714	1.36782e-9
CGC-Yang	190.982	8.52651e-14

Table 5.4: Comparison of the errors and CPU times between the three collocation methods.

Table 5.3 illustrates the maximum error in energy and CPU times when  $N = 18$ ,  $\tau = 0.02$  on the interval  $[0, 360]$  and  $M = \frac{360}{\tau}$  for the collocation methods and when  $h = 0.001$  for the symplectic and the Runge-Kutta methods. From the table, the collocation methods preserve energy better and give the better CPU times than the symplectic method and the Runge-Kutta method. In Table 5.4, we present the maximum error in energy and CPU times when  $M = 10^4$ ,  $N = 20$  and  $\tau = 0.1$  for the collocation methods. From the table, the Chebyshev-Gauss spectral collocation method preserves energy better and gives the best CPU times.

In Figure 5.14, we compare the errors in energy of the Chebyshev-Gauss collocation method with the Legendre-Gauss collocation method and the Chebyshev-Gauss spectral collocation method and the first-order symplectic method. The errors from the three collocations are much smaller (lie at the bottom of Figure 5.14(a)) compared to the symplectic. If we compare among the collocation

methods, we see that the Chebyshev-Gauss collocation method is better than the Legendre-Gauss collocation method, but still has higher error than the Chebyshev-Gauss spectral collocation method.

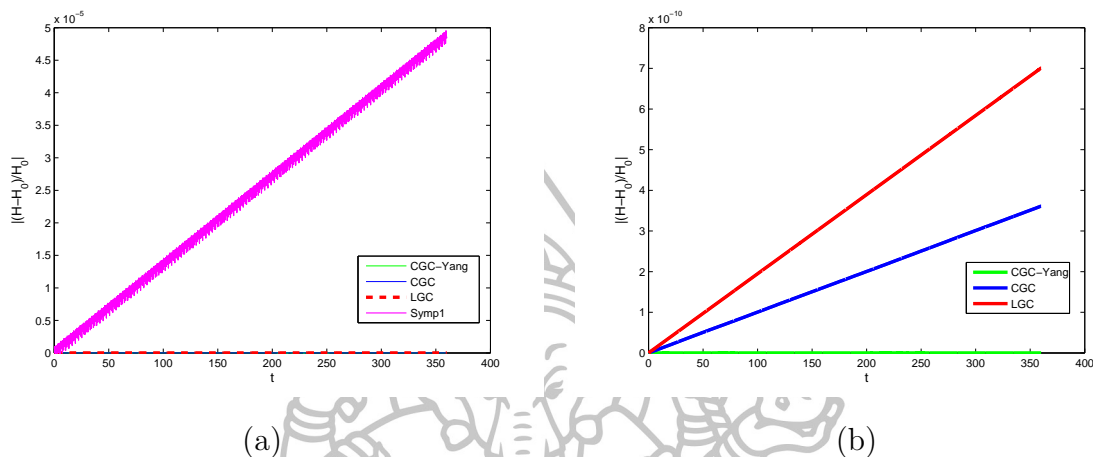


Figure 5.14: (a) Comparison of the relative error in energy between the three collocation methods and the first-order symplectic method. (b) Comparison of the relative error in energy between the three collocation methods.

### Example 5.3.2. Chaotic behavior

In this example, we examine the chaotic behavior of the solution. We consider the set of initial conditions close to  $L_2$ . The set of initial conditions is  $p_1(0) = 0$ ,  $p_2(0) = 1.22165$ ,  $q_1(0) = 1.1$  and  $q_2(0) = 0$  [32].

In Figures 5.15 and 5.16, we compare the phase plots of  $q_N^1$  and  $q_N^2$  of the Chebyshev-Gauss collocation method with the first-order symplectic method and the fourth-order Runge-Kutta method. We observe that the phase plot from the Chebyshev-Gauss collocation method is nested in an oval shape around the saddle point  $L_2$ . The orbit from the symplectic method starts from a point outside then presents a nested in an oval shape. The orbit from the fourth-order Runge-Kutta method is thick and grows as  $t$  increases. The other two collocation methods also present the similar orbit to Figures 5.15(a) and 5.16(a).

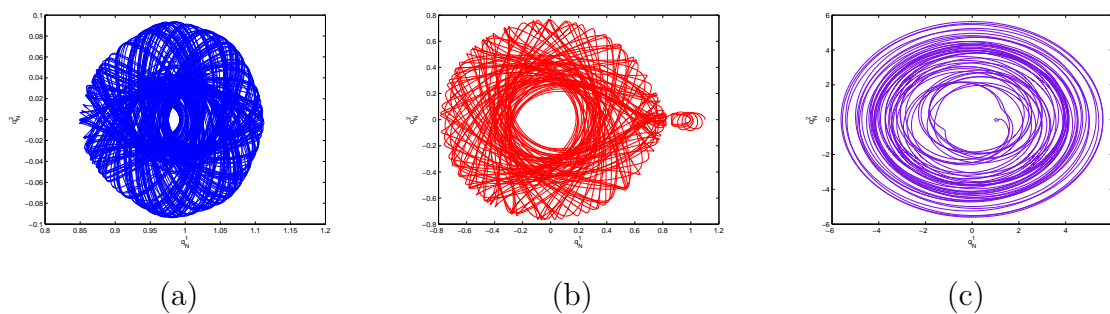


Figure 5.15: Phase plots of  $q_N^2$  versus  $q_N^1$  by (a) the Chebyshev-Gauss collocation method (b) the first-order symplectic method. (c) the fourth-order Runge-Kutta method.

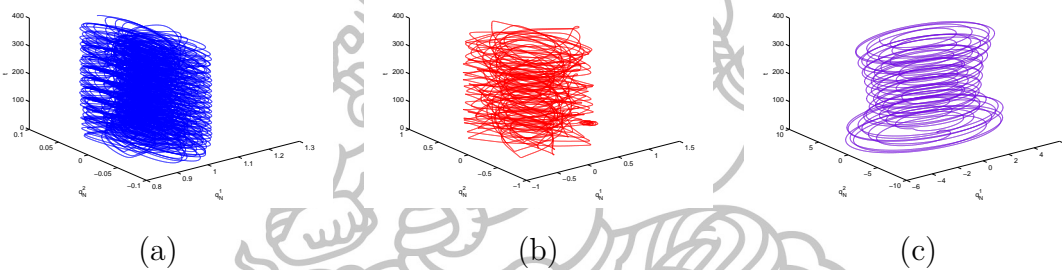


Figure 5.16: Phase plots of  $q_N^2$  versus  $q_N^1$  and  $t$  by (a) the Chebyshev-Gauss collocation method (b) The first-order symplectic method (c) The fourth-order Runge-Kutta method.

Method	Time (secs.)	Error in energy
CGC	236.126	1.30388e-3
LGC	199.451	2.46555e-4
CGC-Yang	148.078	1.38244e-4
Symp1	1053.726	3.73057e-3
RK4	339.844	0.26926

Table 5.5: Comparison of the errors and CPU times between the five methods.

Table 5.5 illustrates the maximum error in energy and CPU times when  $N = 18$ ,  $\tau = 0.02$  on the interval  $[0, 360]$  and  $M = \frac{360}{\tau}$  for the collocation methods and when  $h = 0.001$  for the symplectic and the Runge-Kutta methods. For the chaotic case, the errors in energy from the collocation methods and the symplectic method are almost of the same order. The methods do not preserve energy well



in this case.

**Example 5.3.3.** The solution near the stable points

In this example, we examine the behavior of the solution near the stable points. We consider the set of initial conditions close to  $L_4$ . The set of initial conditions is  $p_1(0) = -0.9$ ,  $p_2(0) = 0.4$ ,  $q_1(0) = 0.4$  and  $q_2(0) = 0.9$ .

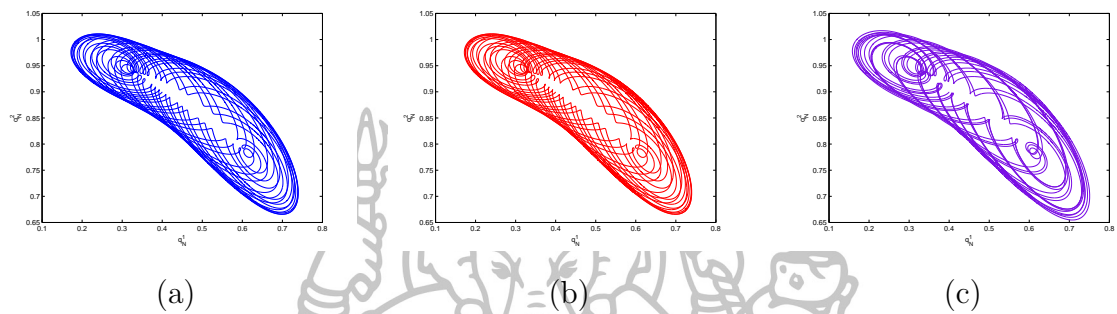


Figure 5.17: Phase plots of  $q_N^2$  versus  $q_N^1$  by (a) the Chebyshev-Gauss collocation method (b) the first-order symplectic method (c) the fourth-order Runge-Kutta method.

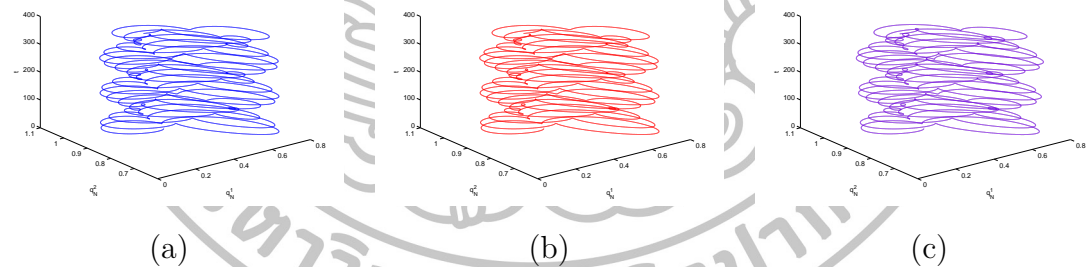


Figure 5.18: Phase plots of  $q_N^2$  versus  $q_N^1$  and  $t$  by (a) the Chebyshev-Gauss collocation method (b) the first-order symplectic method (c) the fourth-order Runge-Kutta method.

In Figures 5.17 and 5.18, we compare the phase plots of  $q_N^1$  and  $q_N^2$  of the Chebyshev-Gauss collocation method with the first-order symplectic method and the fourth-order Runge-Kutta method. We observe that the orbits from the Chebyshev-Gauss collocation method, the first-order symplectic method and the fourth-order Runge-Kutta method present an oval loop which eventually converges to the equilibrium point  $(q_1, q_2) = (0.49, 0.87)$ . The other two collocation methods also present the similar orbit to Figures 5.17(a), 5.18(a).

Table 5.6 represents the maximum error in energy and CPU times when  $N =$

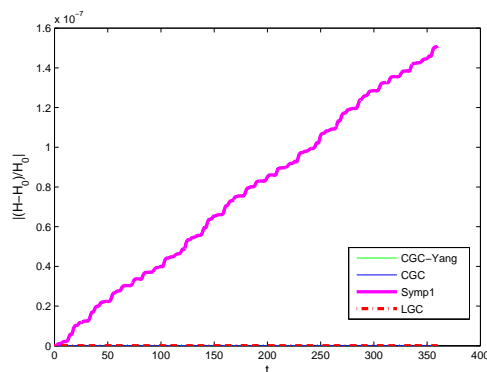
18,  $\tau = 0.02$  on the interval  $[0, 360]$  and  $M = \frac{360}{\tau}$  for the collocation methods and when  $h = 0.001$  for the symplectic and the Runge-Kutta methods. From the table, the collocation methods preserve energy better and give the better CPU times than the symplectic method and the Runge-Kutta method. In Table 5.7, we present the maximum error in energy and CPU times when  $M = 10^4$ ,  $N = 20$  and  $\tau = 0.1$  for the collocation methods. From the table, the Chebyshev-Gauss spectral collocation method preserves energy better and gives the best CPU times.

Method	Time (secs.)	Error in energy
CGC	287.781	4.59632e-13
LGC	260.260	8.19789e-13
CGC-Yang	149.774	1.33226e-15
Symp1	1237.280	2.25572e-7
RK4	353.667	1.79116e-4

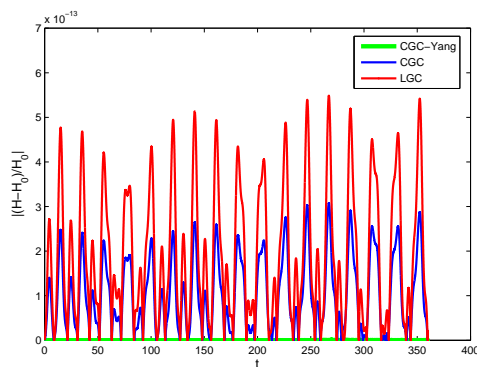
Table 5.6: Comparison of the errors and CPU times between the five methods.

Method	Time (secs.)	Error in energy
CGC	210.539	8.06022e-14
LGC	168.366	4.48752e-13
CGC-Yang	73.670	8.88178e-16

Table 5.7: Comparison of the errors and CPU times between the three collocation methods.



(a)



(b)

Figure 5.19: (a) Comparison of the relative error in energy between the three collocation methods and the first-order symplectic method (b) Comparison of the relative error in energy between the three collocation methods.

In Figure 5.19, we compare the errors in energy of the Chebyshev-Gauss collocation method with the Legendre-Gauss collocation method, the Chebyshev-Gauss

spectral collocation method and the first-order symplectic method. The error from the symplectic method grows larger as  $t$  increases.

**Example 5.3.4.** Orbital behavior

In this example, we examine the case where the phase plots present an orbit with an inner loop. We consider the set of initial conditions  $p_1(0) = -0.16$ ,  $p_2(0) = -0.7$ ,  $q_1(0) = 1.3$  and  $q_2(0) = -0.31$ .

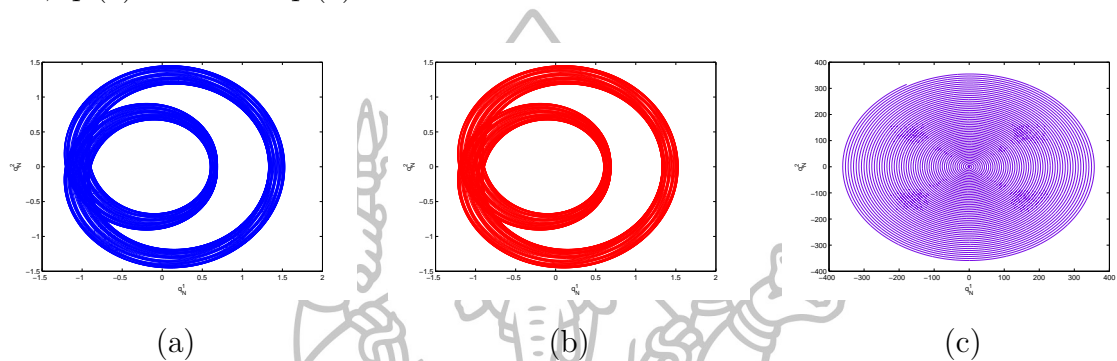


Figure 5.20: Phase plots of  $q_N^2$  versus  $q_N^1$  by (a) the Chebyshev-Gauss collocation method (b) the first-order symplectic method (c) the fourth-order Runge-Kutta method.

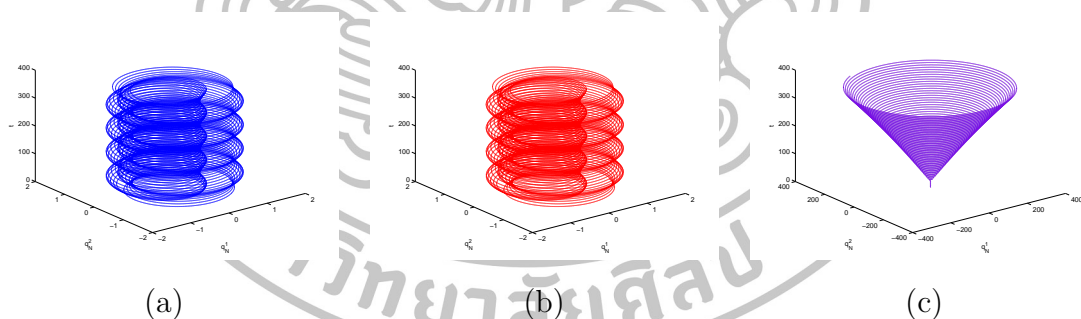


Figure 5.21: Phase plots of  $q_N^2$  versus  $q_N^1$  and  $t$  by (a) the Chebyshev-Gauss collocation method (b) the first-order symplectic method (c) the fourth-order Runge-Kutta method.

In Figures 5.20 and 5.21, we compare the phase plots of  $q_N^1$  and  $q_N^2$  of the Chebyshev-Gauss collocation method with the first-order symplectic method and the fourth-order Runge-Kutta method. We observe that the orbits from the symplectic method are similar to the orbit of the Chebyshev-Gauss collocation method. The phase plot shows a circular orbit with an inner loop on left side where the third mass moves around an object. The orbit of the fourth-order Runge-Kutta method spins out as  $t$  increases. The other two collocation methods also present

a similar orbit to Figures 5.20(a), 5.21(a).

Method	Time (secs.)	Error energy
CGC	203.075	6.67316e-10
LGC	186.929	1.29832e-9
CGC-Yang	126.929	6.40987e-14
Symp1	1239.537	5.09196e-6
RK4	342.127	1.82939

Table 5.8: Comparison of the errors and CPU times between the five methods.

Method	Time (secs.)	Error energy
CGC	213.755	1.06250e-10
LGC	172.932	1.35033e-9
CGC-Yang	113.769	7.09432e-14

Table 5.9: Comparison of the errors and CPU times between the three collocation methods.

Table 5.8 represents the maximum error in energy and CPU times when  $N = 18, \tau = 0.02$  on the interval  $[0, 360]$  and  $M = \frac{360}{\tau}$  for the collocation methods and when  $h = 0.001$  for the symplectic and the Runge-Kutta methods. From the table, the collocation methods preserve energy better and give the better CPU times than the symplectic method and the Runge-Kutta method. In Table 5.9, we present the maximum error in energy and CPU times when  $M = 10^4, N = 20$  and  $\tau = 0.1$  for the collocation methods. From the table, the Chebyshev-Gauss spectral collocation method preserves energy better and gives the best CPU times.

**Example 5.3.5.** The solution near the stable points

In this example, we examine the behavior of the solution near the stable points. We consider the set of initial conditions close to  $L_5$ . The set of initial conditions is  $p_1(0) = 0.83, p_2(0) = 0.55, q_1(0) = 0.55$  and  $q_2(0) = -0.83$ .

In Figures 5.22 and 5.23, we compare the phase plots of  $q_N^1$  and  $q_N^2$  of the Chebyshev-Gauss collocation method with the first-order symplectic method and the fourth-order Runge-Kutta method. We observe that the orbits from the Chebyshev-Gauss collocation method, the first-order symplectic method and the fourth-order Runge-Kutta method present an oval loop which eventually converges to the equilibrium point  $(q_1, q_2) = (0.49, -0.87)$ . The other two collocation methods also present the similar orbit to Figures 5.22(a), 5.23(a).

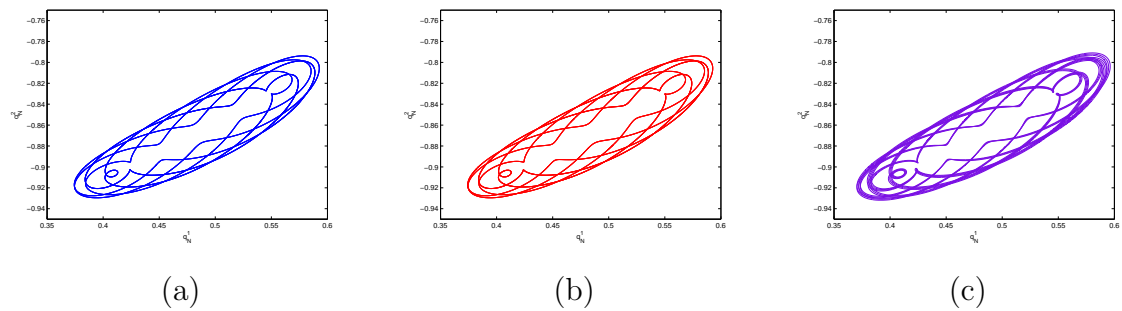


Figure 5.22: Phase plots of  $q_N^2$  versus  $q_N^1$  by (a) the Chebyshev-Gauss collocation method (b) the first-order symplectic method (c) the fourth-order Runge-Kutta method.

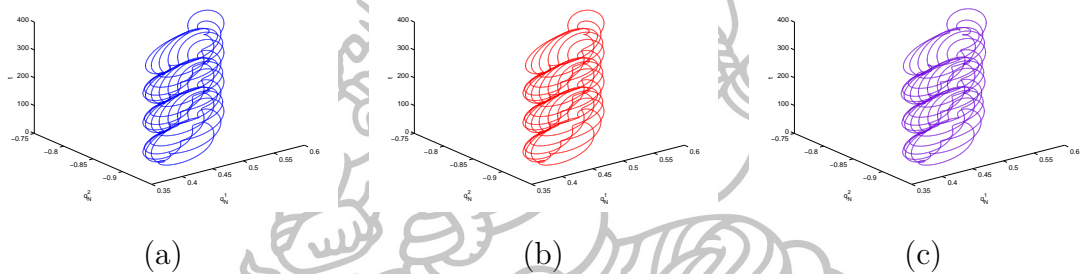


Figure 5.23: Phase plots of  $q_N^2$  versus  $q_N^1$  and  $t$  by (a) the Chebyshev-Gauss collocation method (b) the first-order symplectic method (c) the fourth-order Runge-Kutta method.

Method	Time (secs.)	Error in energy
CGC	323.575	2.10498e-13
LGC	293.721	4.00568e-13
CGC-Yang	148.077	6.66134e-16
Symp1	1214.538	3.98323e-8
RK4	1013.856	2.83977e-5

Table 5.10: Comparison of the errors and CPU times between the five methods.

Method	Time (secs.)	Error in energy
CGC	808.611	5.75096e-14
LGC	256.714	1.36782e-9
CGC-Yang	190.982	8.52651e-14

Table 5.11: Comparison of the errors and CPU times between the three collocation methods.

Table 5.10 illustrates the maximum error in energy and CPU times when  $N = 18$ ,  $\tau = 0.02$  on the interval  $[0, 360]$  and  $M = \frac{360}{\tau}$  for the collocation methods and when  $h = 0.001$  for the symplectic and the Runge-Kutta methods. From the

table, the collocation methods preserve energy better and give the better CPU times than the symplectic method and the Runge-Kutta method. In Table 5.11, we present the maximum error in energy and CPU times when  $M = 10^4$ ,  $N = 20$  and  $\tau = 0.1$  for the collocation methods. From the table, the Chebyshev-Gauss spectral collocation method preserves energy better and gives the best CPU times.

**Example 5.3.6.** The solution near the unstable points

In this example, we examine the behavior of the solution near the unstable points. We consider the set of initial conditions close to  $L_1$ . The set of initial conditions is  $p_1(0) = 0$ ,  $p_2(0) = 0.9025$ ,  $q_1(0) = 0.78$  and  $q_2(0) = 0$ .

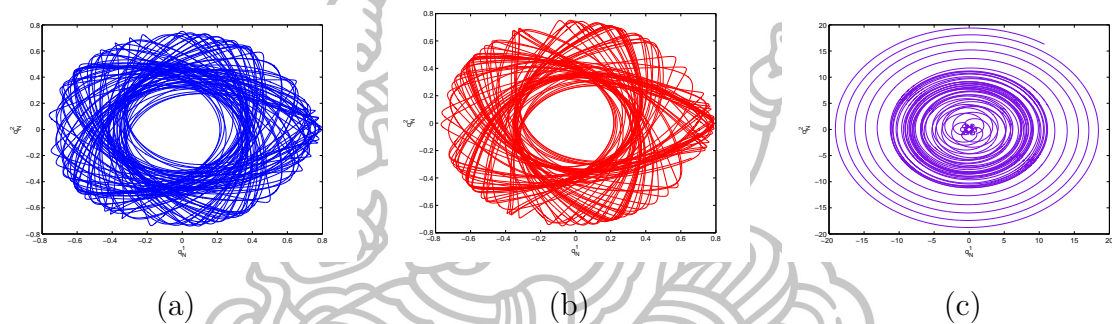


Figure 5.24: Phase plots of  $q_N^2$  versus  $q_N^1$  by (a) the Chebyshev-Gauss collocation method (b) the first-order symplectic method (c) the fourth-order Runge-Kutta method.

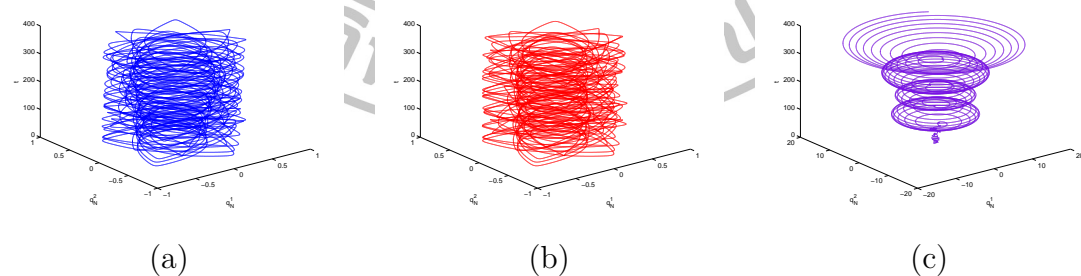


Figure 5.25: Phase plots of  $q_N^2$  versus  $q_N^1$  and  $t$  by (a) the Chebyshev-Gauss collocation method (b) the first-order symplectic method (c) the fourth-order Runge-Kutta method.

In Figures 5.24 and 5.25, we compare the phase plot of  $q_N^1$  and  $q_N^2$  of the Chebyshev-Gauss collocation method with the first-order symplectic method and the fourth-order Runge-Kutta method. We observe that the orbit from the symplectic method is almost the same as the orbit from the Chebyshev-Gauss col-

location method, whereas the loop from the Runge-Kutta method spins out and diverges as  $t$  increases. The other two collocation methods also present the similar orbit to Figures 5.24(a), 5.25(a).

Method	Time (secs.)	Error in energy
CGC	338.415	3.77642e-10
LGC	300.389	7.30468e-10
CGC-Yang	168.403	2.77556e-14
Symp1	1439.647	4.98448e-5
RK4	1116.041	0.21472

Table 5.12: Comparison of the errors and CPU times between the five methods.

Table 5.12 represents the maximum error in energy and CPU times when  $N = 18$ ,  $\tau = 0.02$  on the interval  $[0, 360]$  and  $M = \frac{360}{\tau}$  for the collocation methods and when  $h = 0.001$  for the symplectic and the Runge-Kutta methods. From the table, the collocation methods preserve energy better and give the better CPU times than the symplectic method and the Runge-Kutta method.

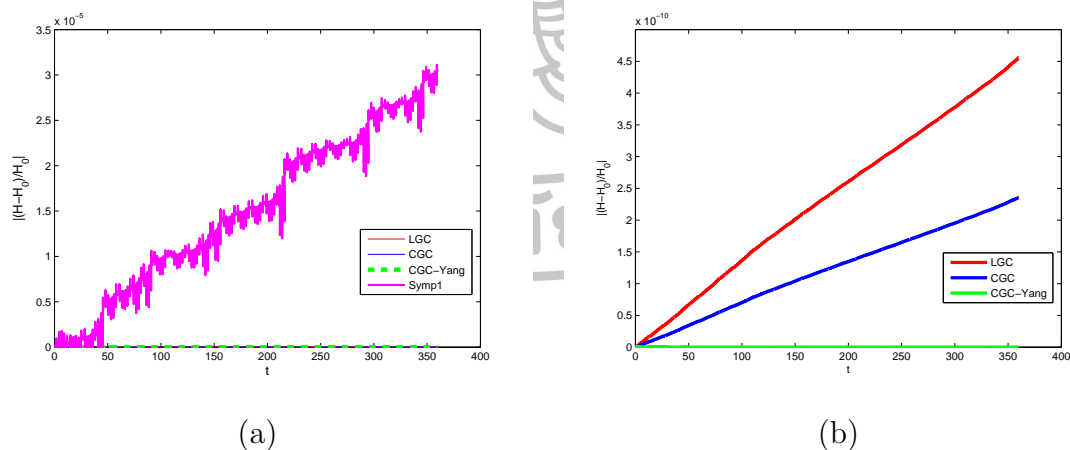


Figure 5.26: (a) Comparison of the relative error in energy between the three collocation methods and the first-order symplectic method (b) Comparison of the relative error in energy between the three collocation methods.

In Figure 5.26, we compare the error in energy of the Chebyshev-Gauss collocation method with the Legendre-Gauss collocation method, the Chebyshev-Gauss spectral collocation method and the first-order symplectic method. The error from

the symplectic method grows larger as  $t$  increases.

**Example 5.3.7.** The solution near the unstable points

In this example, we examine the behavior of the solution near the unstable points. We consider the set of initial conditions close to  $L_3$ . The set of initial condition is  $p_1(0) = 0$ ,  $p_2(0) = -0.9617$ ,  $q_1(0) = -1.05$  and  $q_2(0) = 0$ .

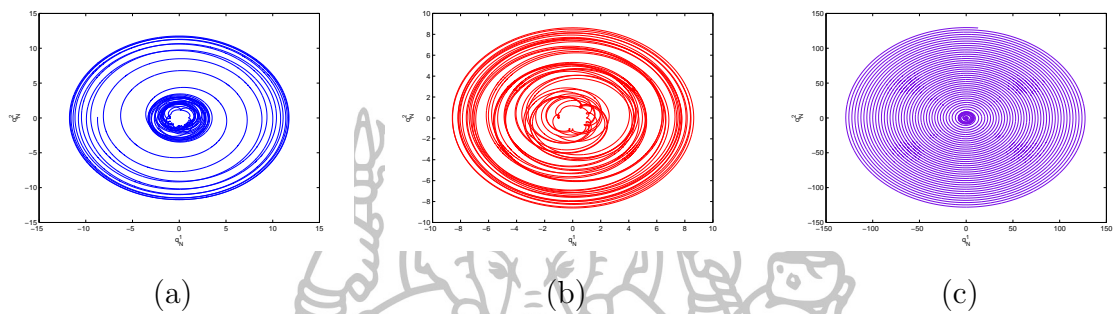


Figure 5.27: Phase plots of  $q_N^2$  versus  $q_N^1$  by (a) the Chebyshev-Gauss collocation method (b) the first-order symplectic method (c) the fourth-order Runge-Kutta method.

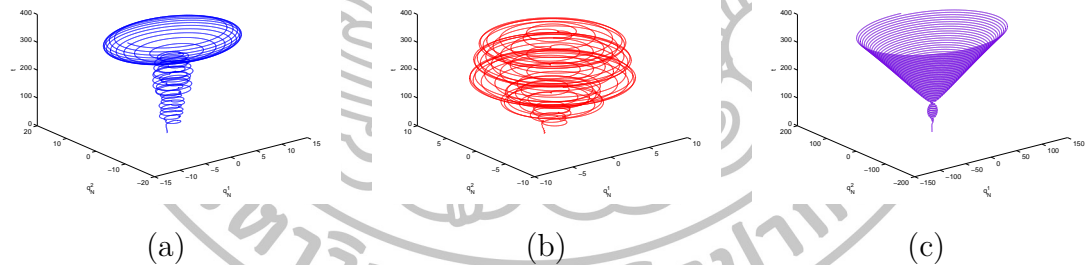


Figure 5.28: Phase plots of  $q_N^2$  versus  $q_N^1$  and  $t$  by (a) the Chebyshev-Gauss collocation method (b) the first-order symplectic method (c) the fourth-order Runge-Kutta method.

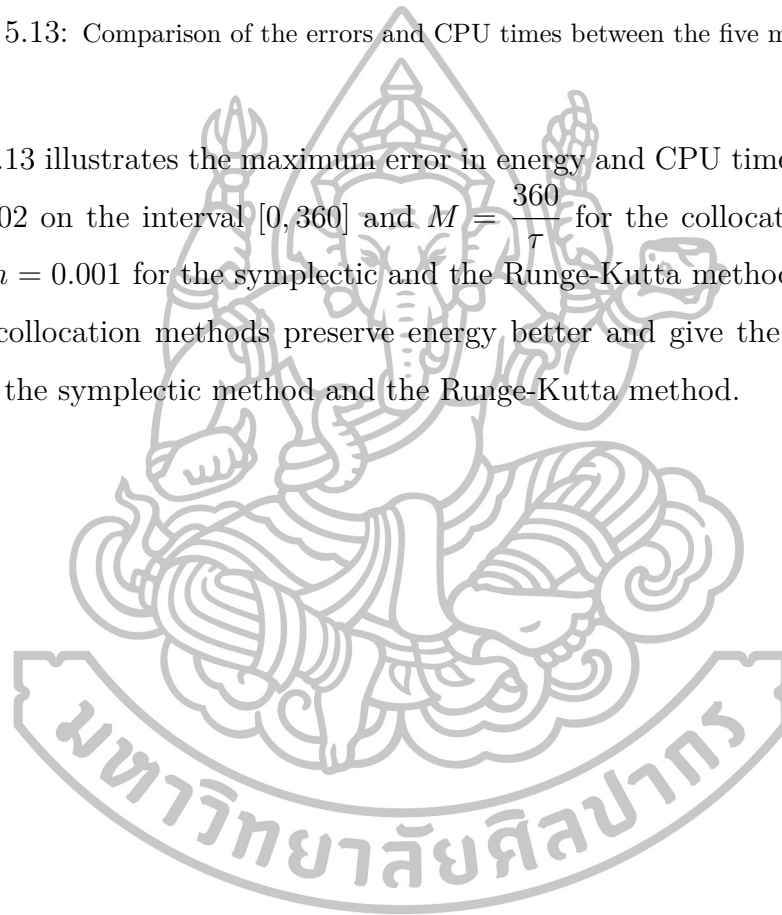
In Figure 5.27 and 5.28, we compare the phase plot of  $q_N^1$  and  $q_N^2$  of the Chebyshev-Gauss collocation method with the first-order symplectic method and the fourth-order Runge-Kutta method. We observe that the orbits from the Chebyshev-Gauss collocation method, the first-order symplectic method and the Runge-Kutta method spin out and diverges as  $t$  increases. The other two collocation methods also present the similar orbit to Figure 5.27(a), 5.28(a).



Method	Time (secs.)	Error in energy
CGC	319.861	1.65429e-7
LGC	294.403	1.766210e-8
CGC-Yang	141.078	1.65460e-7
Symp1	1344.604	8.08749e-3
RK4	1082.638	1.03653

Table 5.13: Comparison of the errors and CPU times between the five methods.

Table 5.13 illustrates the maximum error in energy and CPU times when  $N = 18$ ,  $\tau = 0.02$  on the interval  $[0, 360]$  and  $M = \frac{360}{\tau}$  for the collocation methods and when  $h = 0.001$  for the symplectic and the Runge-Kutta methods. From the table, the collocation methods preserve energy better and give the better CPU times than the symplectic method and the Runge-Kutta method.



# Chapter 6

## Conclusions

In this work, we proposed the Chebyshev–Gauss collocation method to solve to the initial value problems of ordinary differential equations. We constructed the algorithm for an ordinary differential equation as well as the system of ordinary differential equations in both single and multi-interval domain. The numerical results support the theoretical result discussed in Chapter 3. For a fixed  $T$ , the error drops rapidly as  $N$  increases. This behavior is expected since we increase the number of collocation points. We compare the results to show the order of convergence of  $\mathcal{O}(e^{-3.1N})$  and  $\mathcal{O}(N^{-4.33\sqrt{N}})$  in Figure 5 and 6 respectively. It shows that the method (3.21) possesses a spectral accuracy.

For a fixed  $\tau$  and  $N$ , with the scheme for a multi-interval domain, the error grows at a faster rate for a smaller  $t$  than a larger  $t$ . As  $t$  gets larger, the error increases due to the accumulation of errors from the subintervals. These errors may occur when we approximate the endpoint value of each subinterval and set it as the initial condition for the next subinterval. For the systems of differential equations, we have that the method (3.21) preserves both energy and the area. The CPU times for the method (3.21) are the best for the linear systems and are comparable to the Legendre–Gauss collocation method and the Chebyshev–Gauss spectral collocation method in [35] for nonlinear systems. One may improve the algorithm by designing the iterative methods for solving the implicit systems (3.21), especially when the coefficient matrix has a large condition number.

For the three-body problem, we presents a comparison of the collocation methods, the symplectic method and the Runge-Kutta method for the three-body prob-

lem. We choose appropriate sets of initial conditions to present the case of orbital behavior, chaotic behavior, the case when the solution converges to the stable point and the case when the solution converges to the unstable point.

For the case when the phase plots present an orbit (Example 5.3.1. and Example 5.3.4.), the collocation methods give a thinner loop than the fourth-order Runge-Kutta method and they preserve energy and CPU times much better than the symplectic and the fourth-order Runge-Kutta methods.

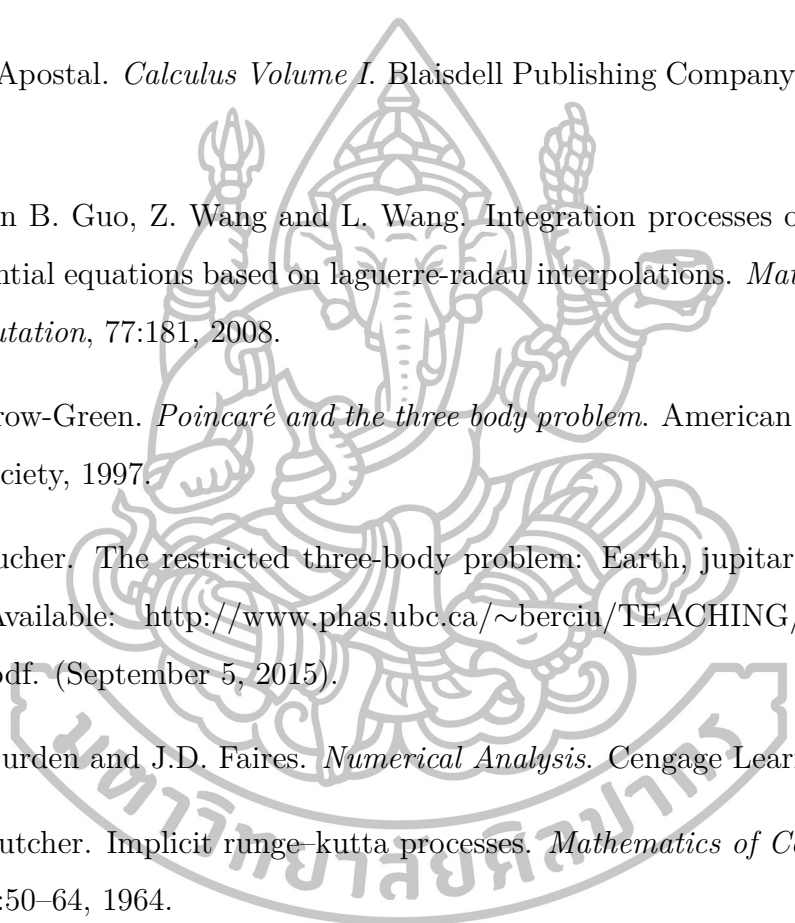
For the chaotic case (Example 5.3.2.), the collocation methods still give a better loop than the other two methods. However, the errors in energy for this case are almost of the same order. They do not preserve energy well.

For the case when the solution converges to the stable point (Example 5.3.3. and Example 5.3.5.), the collocation methods give a thinner loop than the fourth-order Runge-Kutta method and they preserve energy and CPU times much better than the symplectic and the fourth-order Runge-Kutta method.

For the case when the solution converges to the unstable point (Example 5.3.6. and Example 5.3.7.), the collocation methods give a thinner loop than the fourth-order Runge-Kutta method and they preserve energy and CPU times much better than the symplectic and the fourth-order Runge-Kutta method.



# References

- 
- [1] T. M. Apostol. *Calculus Volume I*. Blaisdell Publishing Company, New York, 1962.
- [2] H. Tian B. Guo, Z. Wang and L. Wang. Integration processes of ordinary differential equations based on laguerre-radau interpolations. *Mathematics of Computation*, 77:181, 2008.
- [3] J. Barrow-Green. *Poincaré and the three body problem*. American Mathematical Society, 1997.
- [4] K. Boucher. The restricted three-body problem: Earth, jupitar, sun. [Online] Available: [http://www.phas.ubc.ca/~berciu/TEACHING/PHYS349/](http://www.phas.ubc.ca/~berciu/TEACHING/PHYS349/karla.pdf) karla.pdf. (September 5, 2015).
- [5] R.L. Burden and J.D. Faires. *Numerical Analysis*. Cengage Learning, 2010.
- [6] J.C. Butcher. Implicit runge–kutta processes. *Mathematics of Computation*, 18(85):50–64, 1964.
- [7] J.C. Butcher. *The Numerical Analysis of Ordinary Differential Equations, Runge–Kutta and General Linear Methods*. John wiley & Sons, Chichester, 1987.
- [8] A. Quarteroni C. Canuto, M.Y. Hussaini and T.A. Zang. *Spectral Methods Fundamentals in Single Domains*. Springer-Verlag Berlin Heidelberg, 2006.
- [9] S.P. Norsett E. Hairer and G. Wanner. *Solving Ordinary Differential Equation I: Nonstiff Problems, Second Edition*. Springer-Verlag Berlin, 1993.

- [10] G. El-Baghdady and M.S. El-Azab. A new chebyshev spectral collocation method for solving a class of one-dimensional linear parabolic partial integro-differential equations. *British Journal of Mathematics & Computer Science*, 6(3):172–186, 2015.
- [11] B. Guo and Z. Wang. Integration based on laguerre-gauss interpolation. *Computer Methods in Applied Mechanics and Engineering*, 196:3726–3741, 2007.
- [12] B. Guo and Z. Wang. A spectral collocation method for solving initial value problems of first order ordinary differential equations. *Discrete and Continuous Dynamical Systems Series B*, 14:1029–1054, 2010.
- [13] B. Y. Guo and Z. Q. Wang. Jacobi approximations in non-uniformly jacobi-weighted sobolev spaces. *Journal of Approximation Theory*, 128:1–41, 2004.
- [14] B. Y. Guo and Z. Q. Wang. Legendre-gauss collocation methods for ordinary differential equations. *Advances In Computational Mathematics*, 30:249–280, 2009.
- [15] S. Gottlieb J. Hesthaven and D. Gottlieb. *Spectral methods for time-dependent problems*. Cambridge Monographs on Applied and Computational Mathematics, 2007.
- [16] T. Tang J. Shen and L. Wang. *Spectral methods algorithms analysis and applications*. Springer-Verlag Berlin Heidelberg, 2011.
- [17] F. Kang. On difference schemes and symplectic geometry. in: Proceedings of the 1984 beijing symposium on differential geometry and differential equations. *Science Press, Beijing*, pages 42–58, 1985.
- [18] N. Kanyamee and Z. Zhang. Comparison of a spectral collocation method and symplectic methods for hamiltonian systems. *International Journal of Numerical Analysis and Modeling*, 8(1):86–104, 2011.

- [19] D. A. Kopriva. *Implementing Spectral Methods for Partial Differential Equations: Algorithms for Scientists and Engineers*. Springer Science & Business Media, Netherlands, 2009.
- [20] J. D. Lambert. *Numerical Methods for Ordinary Differential Systems: The Initial Value Problem*. John Wiley & Sons, Chichester, 1991.
- [21] A. Lapshin. The three-body problem. [Online] Available: [http://www.mayr.informatik.tu-muenchen.de/konferenzen/Jass05/courses/2/Lapshin/Lapshin\\_paper.pdf](http://www.mayr.informatik.tu-muenchen.de/konferenzen/Jass05/courses/2/Lapshin/Lapshin_paper.pdf). (October 19, 2015).
- [22] J. Montaldi and T. Ratiu. *Geometric Mechanics and Symmetry: The Peyresq Lectures*. Cambridge University Press, Cambridge, 2005.
- [23] M. Nauenberg. The reception of Newton's Principia. [Online] Available: <http://www.arxiv.org/abs/1503.06861>. (October 12, 2015).
- [24] J. J. O'Connor and E. F. Robertson. Orbits and gravitation. [Online] Available: <http://www-history.mcs.st-and.ac.uk/HistTopics/Orbits.html>. (October 12, 2015).
- [25] S. Patty. Important inequalities for finite element analysis. [Online] Available: [http://www.math.tamu.edu/~srobertp/Courses/Math610\\_2015\\_Sp/Inequalities.pdf](http://www.math.tamu.edu/~srobertp/Courses/Math610_2015_Sp/Inequalities.pdf). (June 25, 2016).
- [26] B. Rink and T. Tuwankotta. Stability in hamiltonian system: Applications to the restricted three-body problem. [Online] Available: <http://www.few.vu.nl/brink/stability.pdf>. (September 9, 2015).
- [27] W. Rudin. *Principles of Mathematical Analysis 3rd ed.* International Student Edition, 1976.
- [28] D. Snyder. Gravity, part 2 : Newton, hooke, halley and the three body problem. [Online] Available: <http://umich.edu/~lowbrows/reflections/2006/dsnyder.17.html>. (October 12, 2015).

- [29] A. M. Stuart and A. R. Humphries. *Dynamical systems and Numerical Analysis*. Cambridge University Press, Cambridge, 1996.
- [30] A. Sugarbaker. Lagrange points and methods for observing extrasolar trojan planets. [Online] Available: <http://large.stanford.edu/courses/2007/ph210/sugarbaker1/>. (October 12, 2015).
- [31] M. J. Valtonen and H. Karttunen. *The three-body problem*. Cambridge University Press, United States of America by Cambridge University Press, New York, 2006.
- [32] H. Zhang W. Lu and S. Wang. Application of symplectic algebraic dynamics algorithm to circular restricted three-body problem. *Chinese Physics Letters*, 25(7):2342–2345, 2008.
- [33] Z. Wang and B. Guo. Legendre-gauss-radau collocation method for initial value problems of first order ordinary differential equations. *Journal of Scientific Computing*, 52:226–255, 2012.
- [34] Z. Wang and L. Wang. A legendre-gauss collocation methods for nonlinear delay differential equations. *Discrete and Continuous Dynamical Systems Series B*, 13(3):685–708, 2010.
- [35] X. Yang and Z. Wang. A chebyshev-gauss collocation methods for ordinary differential equations. *Computational Mathematics*, 33(1):59–85, 2015.

# Appendix A

## Appendix

### A.1 Chebyshev polynomials

The Chebyshev polynomials,  $\mathcal{T}_n(x)$ , are defined as the solution to the Sturm-Liouville problem with  $p(x) = \sqrt{1-x^2}$  and  $q(x) = 0$  [8, 16],

$$\left(\sqrt{1-x^2}\mathcal{T}'_n(x)\right)' + \frac{n^2}{\sqrt{1-x^2}}\mathcal{T}_n(x) = 0, \quad x \in [-1, 1]$$

or

$$(1-x^2)\mathcal{T}''_n(x) - x\mathcal{T}'_n(x) + n^2\mathcal{T}_n(x) = 0, \quad x \in [-1, 1].$$

An alternative representation of the Chebyshev polynomial of degree  $n$  is given by

$$\mathcal{T}_n(x) = \cos(n \arccos(x)).$$

where  $\mathcal{T}_n(x)$  is assumed bounded for  $x \in [-1, 1]$ .

The Chebyshev polynomials are given as  $\mathcal{T}_0(x) = 1$ ,  $\mathcal{T}_1(x) = x$ ,  $\mathcal{T}_2(x) = 2x^2-1$ ,  $\mathcal{T}_3(x) = 4x^3-3x$  and are orthogonal in  $L^2_{\omega^{-\frac{1}{2}}} \in [-1, 1]$  with  $\omega(x) = (1-x^2)$ ,

$$\int_{-1}^1 \mathcal{T}_n(x)\mathcal{T}_m(x)\omega^{-\frac{1}{2}}(x)dx = \frac{1}{2}\pi c_n\delta_{n,m}, \quad n \geq 0.$$

where  $c_0 = 2$ ,  $c_n = 1$  and  $\delta_{n,m}$  is the Kronecker symbol.

Some properties of Chebyshev polynomials are

$$\mathcal{T}_{n+1}(x) - 2x\mathcal{T}_n(x) + \mathcal{T}_{n-1}(x) = 0, \quad n \geq 1. \quad (\text{A.1})$$

For the shift Chebyshev polynomial on  $[0, T]$  with the transformation  $x = \frac{2t}{T} - 1$ ,  $x \in [0, T]$  and  $\frac{dx}{dt} = \frac{2}{T}$ . We defined the shifted Chebyshev polynomials  $\mathcal{T}_{T,n}(t)$  by

$$\mathcal{T}_{T,n}(t) = \mathcal{T}_n\left(\frac{2t}{T} - 1\right) = \cos\left(n \cos^{-1}\left(\frac{2t}{T} - 1\right)\right), \quad n = 0, 1, 2, \dots$$



Since

$$\begin{aligned}
 1 - x^2 &= (1 - x)(1 + x) \\
 &= \left(1 - \frac{2t}{T} + 1\right) \left(1 + \frac{2t}{T} - 1\right) \\
 &= \left(2 - \frac{2t}{T}\right) \left(\frac{2t}{T}\right) \\
 \therefore \sqrt{1 - x^2} &= \sqrt{\frac{4t}{T^2}(T - t)} = \frac{2}{T} \sqrt{t(T - t)}.
 \end{aligned}$$

Therefore,

$$\frac{1}{\sqrt{1 - x^2}} = \frac{T}{2} \frac{1}{\sqrt{t(T - t)}}.$$

Consider

$$\begin{aligned}
 \int_{-1}^1 \mathcal{T}_n(x) \mathcal{T}_m(x) \left(\frac{1}{\sqrt{1 - x^2}}\right) dx &= \int_0^T \mathcal{T}_n(t) \mathcal{T}_m(t) \left(\frac{T}{2} \frac{1}{\sqrt{t(T - t)}}\right) d\left(\frac{2t}{T} - 1\right) \\
 &= \int_0^T \mathcal{T}_n(t) \mathcal{T}_m(t) \left(\frac{T}{2} \frac{1}{\sqrt{t(T - t)}}\right) \frac{2}{T} dt \\
 \therefore \int_{-1}^1 \mathcal{T}_n(x) \mathcal{T}_m(x) \left(\frac{1}{\sqrt{1 - x^2}}\right) dx &= \int_0^T \mathcal{T}_n(t) \mathcal{T}_m(t) \left(\frac{1}{\sqrt{t(T - t)}}\right) dt. \quad (\text{A.2})
 \end{aligned}$$

So, the shifted Chebyshev polynomials are also orthogonal on the interval  $[0, T]$ ,

$$\int_0^T \mathcal{T}_{T,n}(t) \mathcal{T}_{T,m}(t) \omega^{-\frac{1}{2}}(t) dt = \frac{1}{2} \pi c_n \delta_{n,m}, \quad n \geq 0 \quad (\text{A.3})$$

where  $\omega(t) = t(T - t)$ ,  $c_0 = 2$ ,  $c_n = 1$  and  $\delta_{n,m}$  is the Kronecker symbol.

Some properties of Chebyshev polynomials on  $[0, T]$  are

$$\left(\mathcal{T}_{n+1}(x) - 2\left(\frac{2t}{T} - 1\right) \mathcal{T}_n(x) + \mathcal{T}_{n-1}(x)\right) = 0, \quad n \geq 1. \quad (\text{A.4})$$

## A.2 Cauchy-Schwarz Inequality

Let  $X$  be a Hilbert space, endowed with the inner product  $(u, v)$  and the associated norm  $\|u\|$ . The Cauchy-Schwarz inequality states that  $|(u, v)| \leq \|u\| \|v\|$  for all  $u, v \in X$ . Of particular importance in the analysis of numerical methods for partial differential equations is the Cauchy-Schwarz inequality in the weighted

Lebesgue spaces  $L^2\omega(\Omega)$ , where  $\Omega$  is a domain in  $\mathbb{R}^N$  and  $\omega = \omega(x)$  is a weight function. The previous inequality becomes [8] :

$$\left| \int_{\Omega} u(x)v(x)\omega(x)dx \right| \leq \left( \int_{\Omega} u^2(x)\omega(x)dx \right)^{1/2} \left( \int_{\Omega} v^2(x)\omega(x)dx \right)^{1/2}.$$

### A.3 Peter-Paul Inequality

Let  $a, b$  be nonnegative real numbers and  $p, q \in (0, \infty)$  such that  $\frac{1}{p} + \frac{1}{q} = 1$ . Then

$$ab \leq \frac{a^p}{p} + \frac{b^q}{q}.$$

For  $p = q = 2$ , we have

$$ab \leq \frac{a^2}{2} + \frac{b^2}{2} \tag{A.5}$$

which also gives rise to the so called Young's inequality and for an  $\epsilon > 0$ , we have the so called Peter-Paul Inequality [25],

$$ab \leq \frac{a^2}{2\epsilon} + \frac{\epsilon b^2}{2}. \tag{A.6}$$

### A.4 Properties of the integral

Since  $f(x) \leq g(x)$  and  $f(x)$  and  $g(x)$  are integrable on  $[a, b]$ , then [27]

$$\int_a^b f(x)dx \leq \int_a^b g(x)dx. \tag{A.7}$$

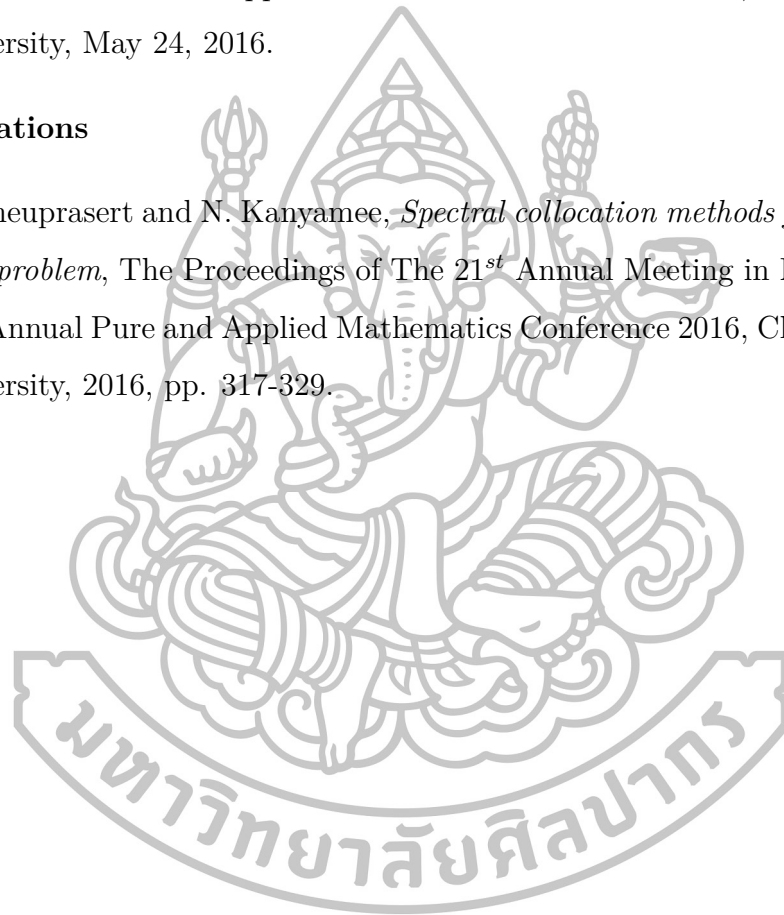
## Presentations and Publications

### Presentations

- K. Cheuprasert and N. Kanyamee, *Spectral collocation methods for the three-body problem*, The Proceedings of The 21<sup>st</sup> Annual Meeting in Mathematics and Annual Pure and Applied Mathematics Conference 2016, Chulalongkorn University, May 24, 2016.

### Publications

- K. Cheuprasert and N. Kanyamee, *Spectral collocation methods for the three-body problem*, The Proceedings of The 21<sup>st</sup> Annual Meeting in Mathematics and Annual Pure and Applied Mathematics Conference 2016, Chulalongkorn University, 2016, pp. 317-329.



## Curriculum Vitae

**Name** Miss Kanyakorn Cheuprasert

**Address** 2/30 Village No.7, Nongpaklong Sub-district,  
Mueang Nakhon Pathom District, Nakhon Pathom,  
73000.

**Date of Birth** 03 January 1991

**Education**

2009-2012 Bachelor of Science in Mathematics,  
(First Class Honors), Silpakorn University.

2013-2015 Master of Science in Mathematics,  
Silpakorn University.

**Scholarship** The Development and Promotion of Science  
and Technology Talented Project (DPST).

